CONTAMINANT TRANSPORT IN A FRACTURED CHALK AQUIFER AT SIGERSLEV, DENMARK, AS CHARACTERISED BY TRACER TECHNIQUES

Dissertation

zur

Erlangung des Doktorgrades (Dr. rer.nat.)

der

Mathematisch-Naturwissenschaftlichen Fakultät

der

Rheinischen Friedrich-Wilhelms-Universität Bonn

vorgelegt von

FATHY AHMED ABDALLA AHMED

aus Qena Ägypten

Bonn, Dezember 2004

Angefertigt mit Genehmigung der Mathematisch-Naturwissenschaftlichen Fakultät der Rheinischen Friedrich-Wilhelms-Universität Bonn

Ich versichere an Eides statt, dass ich diese Arbeit selbstständig ausgeführt habe und keine außer den angegebenen Hilfsmitteln verwendet habe.

Diese Dissertation ist auf dem Hochschulschriftenserver der ULB Bonn http://hss.ulb.uni-bonn.de/diss_online elektronisch publiziert.

1. Referent: Prof. Dr. Barbara Reichert
2. Referent: Prof. Dr. Jean Thein

Tag der Promotion: 02. February 2005

SUMMARY

Over the past three decades, the primary interest of hydrogeological investigations has shifted from problems of water supply to water quality issues. Contamination of aquifers is a growing and demanding problem. In the context of assessment studies for feasible radioactive waste disposal sites contaminant transport in fractured aquifers has received a great attention. Transport processes in fractured aquifer are characterised by a couple of transport mechanisms within the fracture and the neighbouring matrix.

In order to investigate the dominant transport mechanisms, various laboratory experiments with nitrate as a representative for agricultural contaminants compared to various hydrogeological tracers were performed in Danish chalk samples. The characteristics of the Danish chalk such as it's sorptive and diffusive properties were evaluated by batch and through-diffusion experiments.

The chalk exhibits linear sorption isotherms and low sorption capacities. This was expected due to the high purity of the Danish chalk with a low content of clay minerals and organic matter. Based on a series of through-diffusion experiments a chalk specific exponent m of 2.2 was derived for Archie's law. According to the results of batch and diffusion experiments, nitrate as well as the other used tracers showed a low retardation in the Danish chalk. To understand the possible transport mechanisms of tracers in a fractured chalk block, laboratory single- and multi-tracer tests were carried out in two blocks under defined boundary conditions. The breakthrough curves (BTC's) of the tracers are governed by sharp peaks due to advective transport and dispersive respectively diffusive transport processes in the tailing part of the BTC's. The simulation of the BTC's with the single fissure dispersion model could not reasonably fit the BTC's. A multi-channel SFDM with the superposition of BTC's of at least two different flow paths, resulted in an acceptable fit (by calculating the cumulative tracer breakthrough and recovery curves). Those simulations indicate the existence of flow channelling effects within the fracture. Comparing the BTC's of nitrate, uranin and lithium implied possible adsorption and/or degradation of nitrate within the fracture and the chalk matrix. The results showed that matrix diffusion process plays only a minor role in the determination of the fate of nitrate in the groundwater aquifers. The key factor controlling the fate of nitrate in the groundwater is the redox process. Reduction of nitrate is of particular importance for natural remediation process in the case of contaminated aquifers in agricultural areas.

Flow and transport behaviour of different solutes in a fractured chalk blocks were visualized and showed that flow and transport is concentrated in a few distinct channels. The description of the observed BTC`s with a multi-channel model is still a theoretical suggestion and needs more investigations to be confirmed. Those investigations include quantifying and measuring the fracture aperture with different techniques such as NMR and MRI.

KURZFASSUNG

Seit den letzten drei Jahrzehnten konzentriert sich das Interesse bei hydrogeologischen Untersuchungen zur Wasserversorgung auf die Sicherung der Wasserqualität. Die wachsende Gefährdung der Grundwasserleiter durch Kontamination stellt hierbei ein wichtiges Problem dar. Besondere Beachtung finden dabei die Prozesse des Schadstofftransports in geklüfteten und porösen Medien, darunter vor allem die Beurteilung von Deponien und Endlagern sowie der Wasserqualität in Kluftaquiferen.

Um die physikalischen Mechanismen beim Transport in der Kluft und der benachbarten Matrix zu untersuchen, wurden im Labor Diffusions- und Tracer-Experimente mit Nitrat (repräsentativ für eine Kontamination aus der Landwirtschaft) simultan mit verschiedenen hydrogeologischen Tracern durchgeführt. Anhand von Batch- und Diffusionsexperimenten wurden die Soprtions- und Diffusionseigenschaften der Dänischen Kreide bestimmt. Bedingt durch die hohe Reinheit der Dänischen Kreide und ihres geringen Gehaltes an Tonmineralen und organischem Material wurden bei den Batch-Tests lineare Sorptionsisothermen (Henry-Isothermen) mit geringer Sorptionskapazität ermittelt. Entsprechend dem Gesetz von Archie beträgt der Wert des Kreidespezifischen Exponenten m bei den Diffusionsexperimenten 2,2. Basierend auf diesem Exponenten kann die effektive Diffusion in abhangigkeit von der relativen Diffusivität und der Porosität der Kreideproben ermittelt werden. Die Ergebnisse aus den Batch- und Diffusionsexperimenten an der Dänischen Kreide zeigen sowohl bei Nitrat als auch bei den anderen verwendeten Tracern (Uranin, Pyranin Eosin, Chlorid und Lithium) eine geringe Retardation. Die Durchführung von Einzel- und Multitracer-Tests in zwei Kreideblöcken bei definierten Randbedingungen im Labor tragen zu einem besseren Verständnis der Transportmechanismen in Einzelklüften bei. Die Durchbruchskurven (Breakthrough curves = BTC’s) aus den Tracer-Tests zeigen scharfe Peaks mit einem deutlichen tailing, das auf Dispersion und Matrixdiffusion beruht. Da die Simulation der BTC’s mit einem eindimensionalen Dispersionsmodell keine gute Anpassung der Tracer-Konzentrationskurve ergibt, wurde ein Multichannel-Modell entwickelt um so eine akzeptable Übereinstimmung durch die Berechnung einer kumulativen Tracer-Kurve zu erreichen. Diese Simulationen zeigen deutlich, dass die BTC eine Überlagerung von mindestens zwei verschieden Fliesspfaden ist. Dies deutet eine mögliche Existenz von „flow channeling“-Effekten in der Kluft an.

Die Ergebnisse aus den Nitrate Tracer-Tests im Vergleich zu Uranin, Eosin und Lithium zeigen, dass eine Adsorption und Degradation von Nitrat in der Klüftung und in der Matrix stattfinden. Mit diesem Ergebnissen können das Fliess- und Transportverhalten der untersuchten Kluft eindeuting beschrieben werden. Eindeutig ist, dass das Fliess- und Transportfeld sehr unregelmäßig verteilt ist und sich auf wenige bestimmte Fliesskanäle. Die Beschreibung der beobachteten BTC’s mit dem einem Multi-Channel-Modell ist

ein theoretischer Ansatz, der noch weiteren Untersuchungen bedarf. Dazu gehören auch Methoden zur verbesserten Quantifizierung und Messung von Kluftöffnungen wie z.B. NMR- und MRI-Technologien. Der mögliche Effekt von Diffusion und Channeling in geklüfteten Medien bedarf ebenfalls weiterer Forschung.

ACKNOWLEDGEMENT

This research was carried out in the framework of the exchange grant by the Egyptian government and the hydrogeology group (Prof. Dr. Barbara Reichert), Geological Institute, University of Bonn, Germany. The research was focusing on the contaminant transport in fractured aquifers. I have received a great support during my research, therefore I would like to address my special thanks to the following persons:

I would like to express my deep and sincere appreciation to my research advisor Prof. Dr. Barbara Reichert for offering me the opportunity to carry out my research, for her guidance, helpful advice, support and supervision. I am indebted to her constant encouragement and fruitful and interesting discussions throughout this work. She has critically read this thesis and her valuable comments, corrections and suggestions are gratefully appreciated.

I would like to express my deep thanks to Prof. Dr. Jean Thein for his evaluation of my thesis.

I wish to express my deep gratitude to my colleagues of the hydrogeological group, Dr. Thorsten Faß, Tobias El-Fahem and Sebastien Cappy as well as especially to Dr. Kai Witthüser and Kerstin Kremer, for their cooperation, help and support during the work.

I am deeply indepted to the laboratory staff of the Geological Institute Mrs. Bettina Schulte-van Berkum, Mrs. Camilia Kurth and Mr. Rainer Schwarz for their continuous help during the laboratory work. In addition to all members of the Geological Institute for their generous encouragement during my stay in Bonn. To my friend Ateff Makluf (Institute of Geodesy, Bonn University) for his help during the tracer tests.

Sincere thanks are extended to Dr. J. Bloomfield, British Geological Survey for porosity measurements also to Dr. E. Nygaard, Geological Survey of Denmark and Greenland for his help during the field trip.

I would like to express my deep thanks to the Egyptian government for providing me with the PhD scholarship, to my colleagues and members of the Geology Department, Faculty of Science, South Valley University, Egypt for their continuous encouragement.

My special thanks and appreciations are also due to my mother, my sisters for their, heartily feelings and continuous prayers.

Lastly, very special thanks to my wife for her continuous encouragements and for providing me with an excellent environment and atmosphere for doing my research work. To my pretty daughters Maryam and Rawan, my son Ahmed for their lovely smiles that can relieve any kind of tiredness. To all of you, thank you very much.

TABLE OF CONTENTS

LIST OF FIGURES

LIST OF TABLES

NOTATION [LIST OF MAIN SYMBOLS]

Latin Symbols:

A	$[L^2]$	cross sectional area
C	$[ML^{-3}]$	measured solute concentration
^oC	[-]	degree centigrade
$C_{corr}(t)$	$[ML^{-3}]$	corrected concentration in the receiving cell B after time t
C_f	$[ML^{-3}]$	concentration within the fracture zone
$C_f(t)$	$[ML^{-3}]$	concentration within the fracture after time t
$C_i(t)$	$[ML^{-3}]$	concentration within the i-th flow path
$C_i(x,t)$	$[ML^{-3}]$	concentration within the i-th flow path at distance x
C_L	$[ML^{-3}]$	dissolved concentration
C_L^n	$[ML^{-3}]$	dissolved concentration with sorption exponent n
C_n	$[ML^{-3}]$	measured concentration in the receiving cell B after time t
C_0	$[ML^{-3}]$	initial concentration in the reservoir cell
C_p	$[ML^{-3}]$	concentration in the porous matrix
C_s	$[MM^{-1}]$	adsorbed concentration
C(t)	$[ML^{-3}]$	concentration in the receiving cell B after time t
C_w	$[ML^{-3}]$	dissolved concentration
C/C_0	$[ML^{-3}]$	relative concentration
C/M	$[ML^{-3}]$	normalised concentration
D_a	$[L^2T^{-1}]$	apparent diffusion coefficient
D_{hl}	$[L^2T^{-1}]$	longitudinal hydrodynamic dispersion coefficient
D_{ht}	$[L^2T^{-1}]$	transversal hydrodynamic dispersion coefficient
D_e	$[L^2T^{-1}]$	effective diffusion coefficient
D_i	$[L^2T^{-1}]$	dipersion coefficient for the i-th flow path
D_m	$[L^2T^{-1}]$	molecular diffusion coefficient
D_p	$[L^2T^{-1}]$	pore diffusion coefficient
D'	$[L^2T^{-1}]$	relative diffusivity
D/xv	$[L^2/T]$	disperion parameter
Eh	[-]	redox potential in solution
F	[-]	formation factor
J	$[ML^{-2}T^{-1}]$	mass flux of solute per unit area per unit time
K	$[LT^{-1}]$	hydraulic conductivity
K_B	$[L^2MT^{-3}]$	Boltzmann constant
K_d	$[L^3M^{-1}]$	distribution coefficient of solute within solid particles
K_{df}	[L]	distribution coefficient for the fracture surface
K_f	$[L^3M^{-1}]$	Freundlich distribution coefficient
K_{fr}	$[LT^{-1}]$	hydraulic conductivity of the fracture

K_{ij}	$[LT^{-1}]$	component of hydraulic conductivity
K_{OC}	[-]	organic carbon distribution coefficient
K_{OW}	[-]	octanol-water coefficient
M	[M]	injected tracer mass in the fracture
M_i	[M]	injected tracer mass in the i-th flow path
M_t	[M]	weight of dry chalk powder
Q	$[L^3T^{-1}]$	flow rate
Q_{fr}	$[L^3T^{-1}]$	flow rate through the fracture
Q_i	$[L^3T^{-1}]$	flow rate within the i-th flow path
Q^0	[-]	maximum sorptive capacity for the surface
R_d	[-]	retardation factor of matrix
R_f	[-]	retardation coefficient of fracture surface
R_i	[%]	partial tracer recovery of tracer
R_p	[-]	retardation coefficient of rock matrix
RR(t)	[%]	relative mass recovery of tracer
S_W	[-]	water solubility
T	$[^oC]$	temperature
T_m	[L]	effective hydrodynamic radius of the ion
$T_{½}$	[-]	half-life of radioactive isotopes or degraded contaminant
V	$[L^3]$	volume of solution in the receiving cell B
V_b	$[L^3]$	volume of solute concentration
V_f	$[L^3]$	volume of mobile water in the fracture
V_{nOut}	$[L^3]$	volume of taken sample [tracer or contaminant]
V_{nIn}	$[L^3]$	volume of daily sample from the receiving cell B
V_{max}	[L]	maximum flow velocity
$V`_a$	$[LT^{-1}]$	average solute velocity in the fracture
X	[L]	flow distance between entrance and observation point
a	[L]	diffusion parameter
a_i	[-]	diffusion parameter on the i-th flow path
a_w	$[L^{-1}]$	specific fracture surface
2b	[L]	fracture aperture
d	[L]	thickness of the chalk disc
f_{OC}	[-]	organic carbon content
g	$[LT^{-2}]$	acceleration of gravity
h	[L]	hydraulic head
k_{fr}	$[L^2]$	permeability of the fracture
l	[L]	shortest distance or path length of diffusion
l_e	[L]	effective path length of diffusion

m	[-]	cementation factor
n	[-]	total porosity
n_e	[-]	effective porosity
η	[-]	fracture porosity
q_i	$[L^3T^{-1}]$	Darcy's specific discharge
pe	[volt]	redox electron activity in solution
Pe	[-]	Peclet number
r_i	[-]	ratio of partial recovery to the total recovery
t_0	[T]	mean residence time for non-reactive tracer in the fracture
t_0'	[T]	mean residence time for reactive tracer in the fracture
t_{0i}	[T]	mean residence time in the i-th flow path
v_i	$[LT^{-1}]$	average velocity in the i-th flow path
$v_{x,y,z}$	$[LT^{-1}]$	average linear velocity components in x, y, z directions
v	[L]	water velocity within the fracture
w	[L]	fracture width perpendicular to the flow direction

Greek Symbols:

δ	[-]	constrictivity
$\delta(t)$	[-]	Dirac delta function
∂	[-]	partial derivative
$\partial C/\partial x$	$[ML^{-3}L^{-1}]$	concentration gradient (negative in the direction of diffusion)
$\partial h/\partial x$	[-]	hydraulic gradient in the flow direction x
μ	$[ML^{-1}T^{-1}]$	fluids viscosity
η	$[ML^{-1}T^{-1}]$	dynamic viscosity
λ	[-]	degradation rate
τ	[-]	tortuosity
ρ	$[ML^{-3}]$	fluid density
ρ_b	$[ML^{-3}]$	dry bulk mass density of rock material
α	[-]	rock capacity factor
α_l	[L]	longitudinal dynamic dispersivity
α_t	[L]	transverse dynamic dispersivity
ε	[-]	porosity
ε_d	[-]	storage porosity
ε_t	[-]	transport porosity
ζ	[-]	integration variable

Acronyms:

AAS	atomic absorbance spectrometry

AGW	artificial groundwater
BTC	breakthrough curve
CT	computer tomography
C-T	Cretaceous-Tertiary
EDTA	ethylenediaminetetraacetic acid
Eq.	equation
Eqs.	equations
EPM	equivalent porous medium
Fig.	figure
IC	Ion Chromatograph
MDM	multi-dispersion model
MRI	Magnetic Resonance Imaging
NMR	Nuclear Magnetic Resonance
PVC	polyvinyl chloride
SFDM	single fracture dispersion model
Tab.	table
WHO	world health organization
XRD	x-ray diffraction

1 INTRODUCTION

1.1 Statement of the problem

Groundwater is the main source of potable water in many parts of the world especially in semi-arid regions. Worldwide many rural communities and several large cities rely upon groundwater for domestic, industrial and agricultural uses, due to the lack of suitable surface water. For example in the Federal Republic of Germany 70 % of drinking water is taken from groundwater (Trauth and Xanthopoulos 1997).

Today's research efforts have shifted from problems of water supply to those of water quality, and one of the most challenging tasks (in characterising the groundwater pollution) is to predict how contaminants move through fractured aquifers. It is becoming difficult in many areas around the world to obtain a supply of potable groundwater for drinking or industrial purposes. This is mostly due to overuse and contamination as a result of extensive use of chemical and biological substances by agriculture, especially in aquifer recharge zones. Nitrate as the main form of nitrogen in aerated groundwater can readily be transported beneath the soil zone to groundwater due to its high water-solubility and mobility. It can easily pass through soil to the groundwater and is not prone to ion exchange (Macko and Ostrom 1994; Stumm and Morgan 1996).

Generally, nitrate pollution in superficial groundwater is a common problem throughout European, North American, Asian and African countries, therefore the problem is international in scope. Numerous international studies (e.g. Andersen and Kristiansen 1984; Howard 1984; van Beek et al. 1988; Hudak 2000; Thompson 2001; Kacaroglu and Gunay 1997; Zhang et al. 1996; Lagerstedt et al. 1994; Abdel-Dayem and Abdel-Ghani 1992) attest agricultural sources, especially inorganic fertilizer as the predominant source of nitrate in groundwater. Serious health implications are associated with increased nitrate concentrations in drinking water (Hornsby 1990; Blood et al. 1983; Barrett et al. 1998; Craun 1984). In agricultural areas movement of chemicals through agricultural soils has attracted a lot of attention due to concerns for the quality of groundwater, especially in fractured aquifers. Solute transport is increased by the presence of fractures and macro-pores, which can rapidly distribute pollution over vast areas. The spread of such contaminants in fractured aquifers by advective-dispersive transport within the fracture combined with matrix diffusion makes determination of sources in addition to control and remediation processes extremely difficult. The higher the matrix porosity, the higher the transport rate from the fracture to the matrix which implies that a large contaminant mass is likely to migrate into and be stored within the matrix. This large mass is bound to lengthen any remediation effort and reduce their effectiveness.

The heterogeneity and complexity of fractured media makes the quantification and the characterisation of groundwater flow and subsequent contaminant transport a challenging task. In such media, transport is described by combining advective-dispersive trans-

port, which is dominant in the fractures, with diffusive transport mechanisms, which are usually dominant in the rock matrix. The problem of transport in such media is primarily a problem of transport through double-porosity system (Bear et al. 1993; Grisak and Pickens 1980) which includes the porous matrix and the fracture network. These two components are hydraulically interconnected and cannot be treated separately.

Since the construction of the Aswan High Dam in 1968, Egyptian farmers often intensively applied nitrogenous fertilizers, manure and other chemicals with flush irrigation. Therefore contamination of groundwater with nitrate posses a serious threat to groundwater resources especially in the extensively irrigated regions such as the Nile Delta and the Nile Valley (Abdel-Dayem and Abdel-Ghani 1992; Shamrukh et al. 2001). In those areas nitrate-rich surface runoff from agricultural fields can easily percolate into the groundwater. Macro-pores as well as fractures enhance this problem due to their capacity to act as preferential flow paths. If the fractures or the macro-pores are near or even at the land surface irrigation water with agricultural chemicals may enter the groundwater and may travel long distances in short time with little dilution. Nitrate, as one of the dominant agricultural contaminants can accumulate in groundwater as long as the dissolved oxygen level in the aquifer remains sufficiently high. A reduction of nitrate can take place in case sufficient organic matter, pyrite and Fe(II)-silicates are available in the groundwater and the milieu conditions are suitable (Stumm and Morgan 1996). While the nitrate transformation in the microbial mediated redox processes are well know, the physical transport processes such as diffusion, dispersion and sorption of nitrate in porous fractured media, such as chalk aquifers, are poorly investigated. Therefore main research topic of this PhD-thesis, funded by the Egyptian government, was the determination of quantitative parameters for the nitrate transport processes in fractured porous aquifers. The PhD thesis is embedded in the ongoing research activities of the hydrogeology group (Prof. Dr. Barbara Reichert), Geological Institute, University of Bonn. Successfully finished research projects such as Fracflow (Contaminant Transport, Monitoring Technique and Remediation Strategies in Cross European Fractured Chalk; European Commission: ENV3-CT97-0441) and Fracflux form the basis of the research. In the context of those projects focus of the investigations were either field tracer tests combined with small scaled laboratory experiments (e.g. Witthüser 2001, Bansemer 2000) or numerical models to describe transport processes in fractured chalk (Gerik 2003). In this thesis, a physical model was designed to investigate the physical transport processes of nitrate transport in a single fracture bounded by a highly porous chalk matrix under defined boundary and initial conditions. Parallel laboratory batch and diffusion experiments were performed to characterise the chalk matrix properties in respect to its sorption and diffusion capacity. These results are useful to get a better understanding and quantitative description of the diffusive transport mechanisms in fractured media.

1.2 The objectives of the research

An evaluation of the long-term effects of nitrate as a representative for agricultural contaminants on groundwater quality in fractured aquifers requires a detailed knowledge of the possible transport mechanisms throughout the aquifer. The research presented here focuses on a quantitative understanding of transport processes of nitrate in a fractured chalk aquifer. The behaviour of nitrate was studied in comparison to various hydrological tracers such as lithium, chloride, pyranin, eosin and uranin. Taking into account the specific characteristics of fractured porous media emphasis was given to both fast advective-dispersive transport in the fractures and slow diffusive transport in the rock matrix.

The specific aims of the work are:

- Determination of the sorption capacity of the chalk matrix investigated for nitrate and for the various hydrological tracers such as uranin, eosin, pyranin and lithium (sorption isotherms).
- Characterisation of diffusion properties of the solutes within the chalk matrix (effective diffusion coefficients, rock capacity factors).
- Investigation of the transport behaviour of nitrate compared to various hydrologic tracers within a single fracture under defined boundary conditions in two fractured chalk blocks (Darcy and tracer tests).

2 NITRATE IN AQUIFERS

2.1 Nitrogen in an agrosystem and the nitrogen cycle

There are many chemical forms of nitrogen some inorganic and some organic, some gaseous and others soluble and others not. Nitrogen is cycled among these forms. Inorganic forms of nitrogen are released from organic forms by micro-organisms to form ammonium NH_4. Nitrate NO_3 is produced from ammonium in the presence of oxygen in a separate microbiological process called “nitrification” (CAST 1985; Ahmed et al. 1994). In the absence of free oxygen some micro-organisms are capable of using oxygen from nitrate and the nitrogen is transform into gaseous forms, including N_2 and nitrous oxide N_2O. This process is called “denitrification” (Appelo and Postma 1994). Ammonium may be volatilized as ammonia NH_3 gas if the pH is high and the material is not covered by soil (Hoff et al. 1981; Loehr et al. 1983).

2.2 Reduction of nitrate in aquifers

Nitrate introduced into groundwater by agricultural pollution can be expected to react with any available electron donors within the aquifer when it reaches the anoxic groundwater zone. Several electron donors found within the groundwater and in sediments can be involved in the denitrification reactions; for example organic matter, ferrous iron and sulfides of the pyrite (Postma et al. 1991; Agrawal et al. 1999; Jorgensen et al. 2004). Nitrate reduction mediated by microbial activities has been proved to effect aquifer geochemistry and the concentration of nitrate in groundwater (Wilson et al. 1986). Several studies have showed the presence and activities of aerobic and anaerobic bacteria in fractured chalk aquifers (Parker and James 1985; Fourmentraux-Chevron et al. 1998). Bacteria are associated with the surfaces of the fracture walls. Biofilms can be formed on these fracture walls given sufficient and continuous amounts of available organic matter since pore size will restrict colonization within the chalk matrix.

The reduction series of nitrate in groundwater can be written as:

$$NO_3^- \rightarrow NO_2^- \rightarrow N_{2(g)} \rightarrow NH_4^+ \qquad \textbf{(2-1)}$$

Intermediates between NO_2 and $N_2(g)$, such as NO(g) and $N_2O(g)$ are known to occur in aquifers, but rarely in significant amounts (Appelo and Postma 1994). The boundaries between NO_3 and N_2 and between N_2 and NH_4 are displayed in Fig. 2-1.

Reduction of nitrate by organic matter

Bacteria use the ions of nitrate as electron acceptor to oxidize organic matter to CO_2. If molecular nitrogen is the final product, the process is called denitrification, dissimilatory nitrate reduction (Obermann 1981; Appelo and Postma 1994; Fryar et al. 2000) or heterophic denitrification (Pauwels et al. 2000):

$$5CH_2O + 4NO_3^- + 4H^+ \rightarrow 2N_2 + 5CO_2 + 7H_2O \qquad \textbf{(2-2)}$$

Denitrification converts nitrate into inert molecular nitrogen, which is very important in the nutrient balance of lakes and rivers and provides a potential natural remediation mechanisms for removal of nitrate in anoxic groundwater (Moncaster et al. 2000).

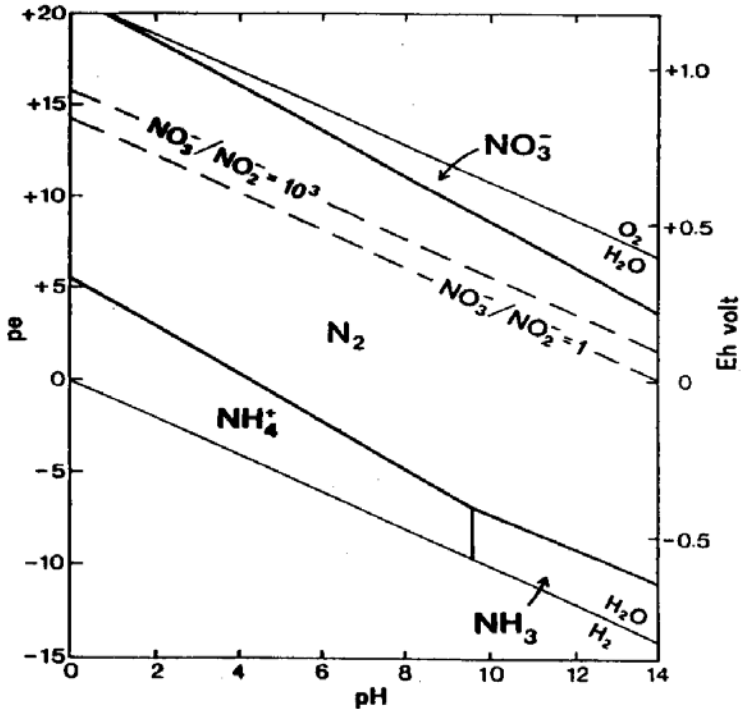

Fig. 2-1: Stability-field diagram based on Eh and pH for different nitrogen species at 25 °C (Appelo and Postma 1994). The diagram is valid under the conditions that pressure is 0.77 atom and the activities of dissolved species are 10^{-3}.

Nitrate reduction by ferrous iron Fe(II)

Nitrate can be reduced by Fe(II) (Appelo and Postma 1994):

$$10Fe^{2+} + 2NO_3^- + 14H_2O \rightarrow 10FeOOH + N_2 + 18H^+ \qquad \textbf{(2-3)}$$

Since the dissolved Fe^{2+} concentrations in groundwater rarely exceed 0.1 mg/L and nitrate loads are often large, it is clear that a source of Fe^{2+} in the sediments is required. In a study of nitrate contamination in agricultural areas, Postma et al. (1991) observed a sharp boundary between upper oxic and lower anoxic groundwater zones. Nitrate disappears at this boundary and dissolved Fe^{2+} remains below the boundary decreasing downward.

Nitrate reduction by the oxidation of pyrite

A number of studies showed that the NO_3 reduction can be coupled with pyrite oxidation (Kölle et al. 1983, 1985; Strebel et al. 1985; van Beek et al. 1988). This combined reaction is bacterially catalyzed. While the sulfide in pyrite is catalyzed by Thiobacillus denitrificans (Kölle et al. 1985, 1987), the Fe(II) subsequently is oxidized by nitrate with Gal-

lionella ferruginea (Gouy et al. 1984). Appelo and Postma (1994) demonstrated that the reduction of nitrate by the oxidation of pyrite involves the oxidation of both sulfide and Fe(II) and described this reaction with the following equations:

$$5FeS_2 + 14NO_3^- + 4H^+ \rightarrow 7N_2 + 5Fe^{2+} + 10SO_4^{2-} + 2H_2O \quad \textbf{(2-4)}$$

and

$$10Fe^{2+} + 2NO_3^- + 14H_2O \rightarrow 10FeOOH + N_2 + 18H^+ \quad \textbf{(2-5)}$$

Pauwels et al. (1997, 1998) carried out a small-scale tracer test to evaluate the denitrifying capacities of the aquifer due to the presence of pyrite in the Coet Dan basin, Brittany, France. Their results showed that the autotrophic denitrification process is very rapid. Several reasons may contribute to this high level of kinetics, including the solid-phase accumulation of metals introduced through anthropic pollution, which may act as a catalyst. As well as the elimination of sulfates through the precipitation of amorphous or crystallized sulfate phases such as jarosite.

Since the high nitrate concentrations (up to 1 mMol/L or more) introduced into the aquifers by fertilizers often exceeds the reducing capacity of dissolved species, reactions between reduced species dissolved in groundwater and nitrate are rarely quantitatively significant for nitrate reduction in aquifers. For substantial nitrate reduction in aquifers there must be an adequate reduction potential within the sediments provided by e.g. organic matter, pyrite and Fe(II)-silicates (Postma 1990).

2.3 The main health effect of nitrate on human and animals

Contamination of groundwater by nitrate is potentially an important environmental problem, in relation to the quality of water for human (Hornsby 1990) and animal (Blood et al. 1983) consumption. Infants under six months of age are susceptible to nitrate poisoning which is called methemoglobinemia or “blue baby syndrome“ thus the affected baby suffers oxygen deficiency (Craun 1984; CAST 1992). The effect of chronic exposure to high nitrate concentration by drinking water is the subject of considerable scientific debate. More information can be found in (Xu et al. 1992; Morales-Suarez-Varela et al. 1993; Barrett et al. 1998; CAST 1992; van Loon et al. 1998; McGeehin et al. 1993; Steindorf et al. 1994). The World Health Organization (WHO) guideline value for nitrate in water intended for human consumption is 50 mg/L as the upper limit of safe drinking water (WHO 1998b).

3 CONTAMINANT TRANSPORT IN FRACTURED AQUIFERS

3.1 Introduction

Contaminant and solute transport processes in fractured media became a major research topic in hydrogeology over the past three decades. This is due to the investigations for repository sites especially for radionuclides and the growing concern for the groundwater quality, (e.g. Lomize 1951; Louis 1969; Nuclear Waste Technical Review Board 1996; Jorgensen et al. 1998; Thein et al. 1997; Bear et al. 1993; Hsieh et al. 1993; Huyakorn and Pinder 1983; Sahimi 1993, 1995; Himmelsbach et al. 1998; Hines and Maddox 1985; Neretnieks 1991; Hakami and Larsson 1996; Ge 1997; Gavrilenko and Gueguen 1998). In double-porosity media such as fractured chalk aquifers, matrix diffusion processes, which influence both reactive and non-reactive solutes, rapidly attenuate concentrations as a contaminant is carried along the concentration gradient from the fractures into the rock matrix (Jardine et al. 1999). Within the fractures, there are some regions where water flows (channels) as well as regions where water is stagnant. Solutes may diffuse from water in channels into the stagnant water zones in between these channels as well as from the stagnant water into the rock matrix. Matrix diffusion provides accessibility to a large volume of voids and sorption sites for the solute, resulting in a large storage capacity of solutes within the matrix (Maloszewski and Zuber 1990). Small-scale tracer tests can be applied to determine flow paths, flow velocities and possible transport mechanisms within different type of aquifers. Many field experiments, laboratory and numerical studies were carried out to investigate the effects of matrix diffusion and channelling on contaminant transport (e.g Abelin et al. 1991; Tsang 1991; Tsang and Neretnieks 1998; Becker et al. 1999; Maloszewski et al. 1999; Bäumle et al. 2000; Bäumle 2003; Witthüser 2001; Witthüser et al. 2003; Grisak and Pickens 1980; Himmelsbach and Wendland 1998; Kasnavia et al. 1998; Xu et al. 1998; Reedy et al. 1996). In tracer tests the influence of the matrix diffusion can be proven by using multiple tracers having different molecular weight and hence different diffusion coefficients, resulting in different tailings of the breakthrough curves (BTC's) (Jardine et al. 1999; Becker and Shapiro 2000). Some authors (McKay et al. 1993; Becker et al. 1999) have used soluble and colloid tracers to examine the effects of matrix diffusion in consolidated and unconsolidated fractured media. A clear inspection and separation of the BTC's indicated that solutes diffused into the matrix while colloids were excluded based on their size. The late-time (tail) of the BTC is of particular importance to describe matrix diffusion, because the behaviour of the early-time (peak) is dominated by advection and dispersion. The slope of the tail contains information about the type of mass transfer (e.g. single-rate or multi-rate diffusion or first-order sorption) (Haggerty 2000).

Flow channelling is a widely recognised phenomenon in the fractured porous media and it has a substantial effect on solute transport in such media (Abelin et al. 1991; Tsang

and Neretnieks 1998, 2002; Tsang et al. 1988; Tsang 1993). A significant portion of the fracture has apertures that are quite small or even zero due to asperities. These restrictions cause the flow to channel and reduce the surface area of matrix blocks into which the solute will invade (Dykhuizen 1992). Solute transport in a fracture tends to seek easy pathways (channels) in the fracture plane (Fig. 3-1). These channels might transport a portion of the solute considerably faster than the average. Channels in the same fracture may not meet and mix their water over considerable distances, therefore solute transport can be considered separately for each channel.

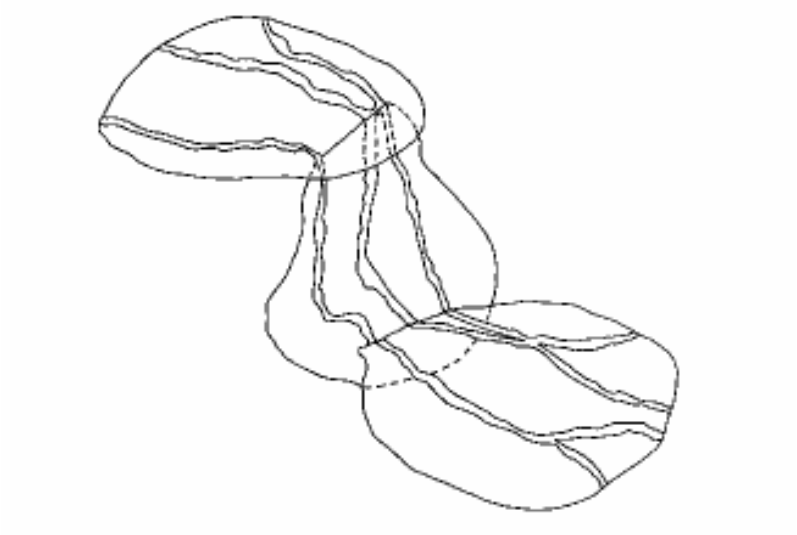

Fig. 3-1: The channelling concept within the fracture (Tsang 1993).

Stagnant water zones (which do not participate in the flow) may exist between those channels within the fracture. Solutes can be spread by diffusion from the flowing water in the channels into and out of those stagnant water zones. Experimental and theoretical work has shown, that flow channelling may be observed in either a single fracture or in a fracture network, and that it occurs on all scales, from centimetre to kilometre scale (Margolin et al. 1998; Moreno and Tsang. 1994; Tsang and Neretnieks 1998). In case of a single fracture, channelling is related to variations in the fracture aperture within the fracture plane where the flow is concentrated along the tortuous paths with the lowest hydraulic resistance (Bodin et al. 2003a; Tsang and Tsang 1989). However, there is no standard method to characterize and quantify channelling effects within the fracture. Rasmuson and Neretnieks (1986); Tsang and Tsang (1987) used an oversimplified approach by assuming that flow within the fracture may only occur in distinct parallel channels. Based on this assumption they were able to model and simulate specific features of the BTC's such as multiple-peaks. Tsang (1991) demonstrated that the rock surface available for surface sorption and diffusion might be only 10 or 20 % of the total fracture surface area due to channelling of the flow in the fracture plane. Other observations by Abelin et al. (1985) in three highly visible fractures in the Stripa deep (360 m) rock laboratory indicated that 5-20 % of the fracture widths carried more than 90 % of the flowing water.

Raven et al. (1988) studied fluid transport through parallel plates with irregular walls. The study revealed that, transport through rough fractures promoted the formation of zones along the edge of the fracture where the water is immobile. The fluids move through mobile zones, but the solutes can diffuse into immobile zones. The solutes would be stored in the immobile zone during the early part of solute transport and would be released from storage if the solute concentration in the mobile fluid would decrease (Fig. 3-2).

Pulse injection tracer tests conducted in fractured rocks showed BTC's with fast rise in concentration to reach an early peak and long tail into late time values. The most common explanation for this skewed BTC is that some of the tracer moves quickly through open channels resulting in an early peak, while the other portion is delayed by diffusion of tracer into the matrix and/or into stagnant water zones in the fracture resulting into a tail with low concentration.

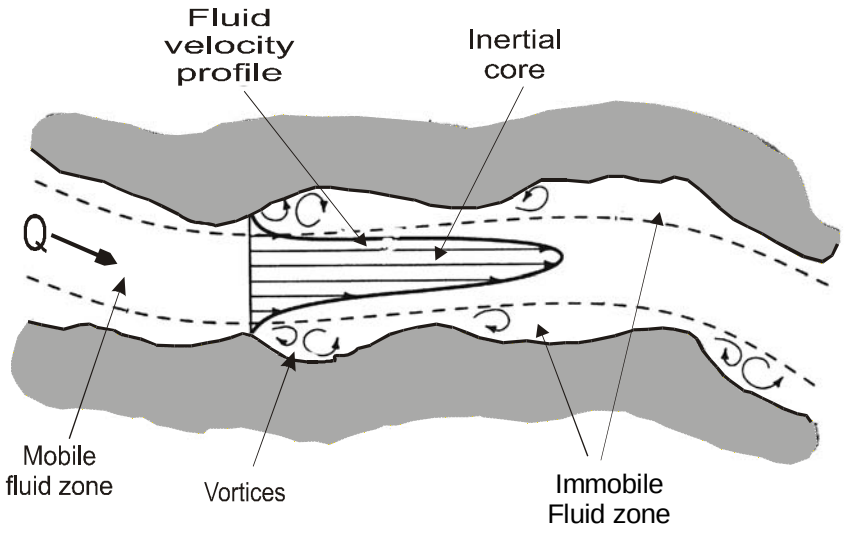

Fig. 3-2: Zones of mobile and immobile water in a natural fracture (Raven et al. 1988).

3.2 Transport processes in a single fracture

Mass transport processes in a single fractured can be summarised as follow (Fig. 3-3):

- Advection at the mean fluid velocity in the fracture. Advection in the matrix is negligible due to the high contrast of permeability between fracture and matrix.
- Hydrodynamic dispersion in the fracture due to variations of local fluid velocities with respect to the mean velocity.
- Molecular diffusion in the fracture plane and from the fracture into the matrix.
- Physico-chemical reactions between solute and the matrix and the fracture walls. These reactions cause retardation or slowing of apparent velocities.
- Biotic or microbial-mediated transformation.

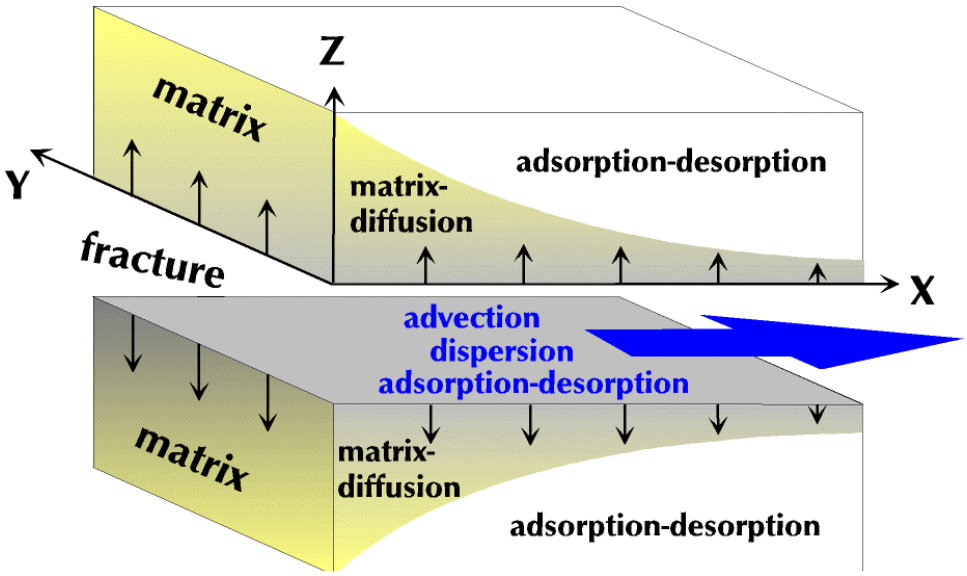

Fig. 3-3: Solute transport processes in fractured aquifers (Witthüser 2001).

The mathematical formulation of mass transport in fractured porous media is given in many textbooks (Bear et al. 1993; Lee and Farmer 1993; Sahimi 1993, 1995; Romm 1966) and articles (Becker and Shapiro 2000; Grisak and Pickens 1980; Maloszewski and Zuber 1985; Witthüser et al. 2003; Bodin et al. 2003a&b) and is briefly described here.

The solution of mass transport in fissured rocks with a porous matrix is governed by the following equations (3-1 and 3-2). It is assumed that there is no advection in the rock matrix, the matrix is completely homogenous and isotropic and it extends infinitely away from the fracture (Tang et al. 1981; Lever et al.1985):

The solute transport in a fracture is:

$$\underbrace{R_f \frac{\partial C_f}{\partial t}}_{\text{Retardation}} + \underbrace{\bar{v}_a \frac{\partial C_f}{\partial x_i}}_{\text{Advection}} - \underbrace{D_{h_{ij}} \frac{\partial^2 C_f}{\partial x_i^2}}_{\text{Dispersion}} - \underbrace{\frac{2D_e}{b} \cdot \frac{\partial C_p}{\partial z}\bigg|_{z=\pm b/2}}_{\text{Diffusion}} + \underbrace{R_f C_f}_{\text{Decay}} = 0 \qquad \textbf{(3-1)}$$

Solute transport in the rock matrix is described by:

$$\underbrace{R_p \frac{\partial C_p}{\partial t}}_{\text{Retardation}} - \underbrace{\frac{D_e}{\varepsilon} \frac{\partial^2 C_p}{\partial z^2}}_{\text{Diffusion}} + \underbrace{R_p C_p}_{\text{Decay}} = 0 \qquad \textbf{(3-2)}$$

R_f retardation coefficient of fracture surface [-]
R_p retardation coefficient of rock matrix [-]
C_f concentration in the mobile (fracture) zone [ML^{-3}]
C_p concentration in the immobile (matrix) zone [ML^{-3}]
$\bar{v}_a$ average solute velocity in the fracture [LT^{-1}]
D_h hydrodynamic dispersion coefficient [L^2T^{-1}]

D_e effective diffusion coefficient [L^2T^{-1}]
λ decay or degradation constant [-]
i,j spatial coordinate direction x and z [-]
x spatial coordinate taken to be positive in the direction of flow in the fracture [-]
z direction of transport in the matrix perpendicular to the fracture [-]
ε matrix porosity [-]

3.2.1 Advection

Darcy's law for an uncompressible fluid is written as (Derouane and Dassargues 1998):

$$q_i = K_{ij} \frac{\partial h}{\partial x_i} \qquad \textbf{(3-3)}$$

q_i Darcy's specific discharge [L^3T^{-1}]
K_{ij} component of hydraulic conductivity [LT^{-1}]
$\partial h/\partial x_i$ hydraulic gradient in the flow direction x [-]

The phase average velocity v_i is expressed by:

$$v_i = -\frac{q_i}{n_e} \qquad \textbf{(3-4)}$$

From Eqs. (3-3) and (3-4):

$$v_i = -\frac{\partial h}{\partial x_i} \cdot \frac{K_{ij}}{n_e} \qquad \textbf{(3-5)}$$

Where n_e is the effective porosity and $n_e < n$ (n is the total porosity).

The most fundamental and widespread model describing fracture flow is the cubic law, where the flow in a fracture is treated as linear laminar flow between two parallel smooth plates (Eq. 3-7). The cubic law seems to be valid in fractures with rough surfaces if the changes in fracture aperture along the flow direction are only minor (Moreno et al. 1988). In general the fractures in natural formations can hardly mimic parallel plates. Other authors have suggested that a variable rather than a constant aperture results in flow channelling into preferential flow paths along the zones of the largest interconnected apertures (Tsang and Tsang 1989; Tsang et al. 1991). The fracture hydraulic conductivity K_{fr} for the parallel plate model is proportional to the square of the fracture aperture (Witherspoon et al. 1980; Nicholl et al. 1999):

$$K_{fr} = \frac{\rho \cdot g}{12\mu}(2b)^2 \qquad \textbf{(3-6)}$$

From Eq. (3-6) the permeability in the fracture is $k_{fr} = (2b)^2/12$, where $K_{fr} = k_{fr}(\rho g/\mu)$. The volumetric flow rate Q_{fr} for viscous incompressible fluids is given by the cubic law, which states that, for a given head gradient flow through a fracture is proportional to the cube

of the fracture aperture. Combining Darcy law with fracture hydraulic conductivity K_{fr} (Eq. 3-6) gives the cubic law (Romm 1966; Lee and Farmer 1993; Nicholl et al. 1999):

$$Q_{fr} = \frac{\rho \cdot g \cdot w}{12\mu} \cdot (2b)^3 \cdot \frac{\partial h}{\partial x} \qquad \textbf{(3-7)}$$

Q_{fr} volumetric fluid flow rate in the fracture [L^3T^{-1}]
g acceleration of gravity [MT^{-2}]
ρ fluid density [ML^{-3}]
$\partial h / \partial x$ hydraulic gradient in the flow direction x [-]
2b fracture aperture [L]
w width of the fracture perpendicular to the flow direction [L]
μ fluid absolute viscosity [L^2T^{-1}]
A cross sectional area A = w 2b [L^2]

3.2.2 Hydrodynamic dispersion

In groundwater, the hydrodynamic dispersion as an important aquifer characteristic describes the mechanical D_d and diffusive D_m mixing of the solute. It may act to dilute the solutes, spreading them both vertically and horizontally as they travel down gradient. The hydrodynamic dispersion coefficient D_h represents the processes of mechanical dispersion due to the variation of the fluid velocity across the fracture as well as the diffusive dispersion along the fracture (Fig. 3-3). The dispersion is expressed as a function of the standard deviation of the mean residence time distribution. For non-reactive solutes the water flow rate and the matrix porosity determine the residence time. In case of reactive solutes diffusion and sorption properties of the rock-matrix are important for the determination of dispersion (Moreno et al. 1997).

For one-dimensional flow hydrodynamic dispersion is defined as (Bear 1972):

$$D_{hl} = \alpha_l \cdot v_x + D_m \qquad \textbf{(3-8)}$$

$$D_{ht} = \alpha_t \cdot v_x + D_m \qquad \textbf{(3-9)}$$

D_{hl} longitudinal hydrodynamic dispersion coefficient [L^2T^{-1}]
D_{ht} transverse hydrodynamic dispersion coefficient [L^2T^{-1}]
α_l, α_t longitudinal, transversal dispersivity [L]

The dispersivity within a single fracture is usually small and dependent on the aperture, roughness and type and frequency of bridging materials within the fracture (Grisak and Pickens 1980). Dispersivity in a fractured medium (Fig. 3-4) is a scale dependent and increases with the scale of measurement. This is due to the heterogeneous nature of the aquifer materials and can be summarized in the words channelling or uneven distribution (Gelhar 1987; Neretnieks 1985). Flow channelling within the fracture is widely recognised to have a large effect on dispersion (Berkowitz 2002; Moreno and Tsang 1994). Velocity variations in the fluid in a flow channel and velocity variations between

the different flow channels in the porous media might be responsible for this effect (Abelin et al. 1991). Some investigations carried by Neretnieks (1983) in a stratified media, where there are parallel unconnected strata with different transmissivity. The result showed that the dispersion coefficient should increase with distance and matrix diffusion can have a dominating influence on the spreading of solute when the accessed stagnant water volume is large in comparison to the mobile water.

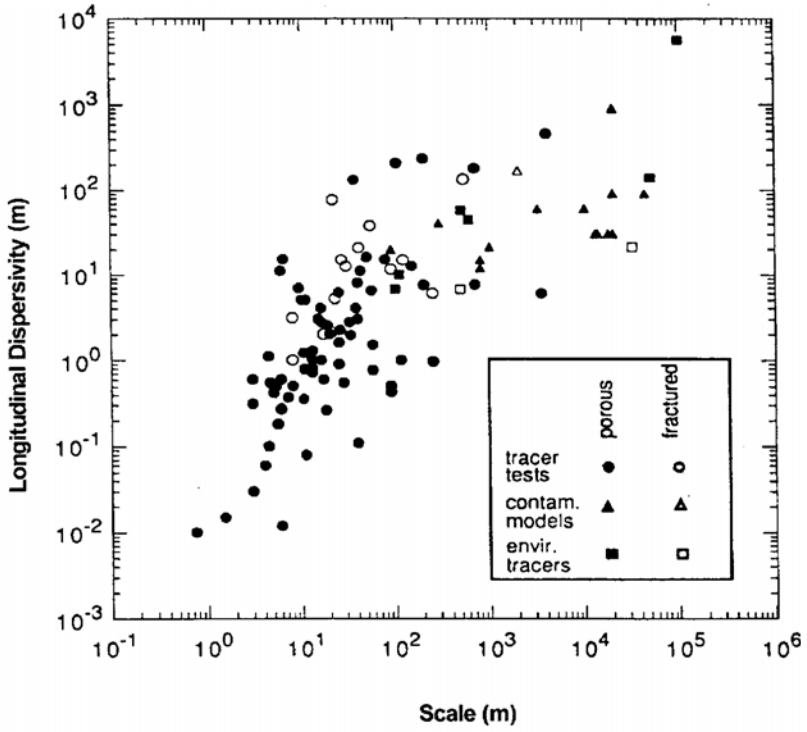

Fig. 3-4: Longitudinal dispersivities as a function of scale of observation from different tracer tests and different aquifer materials (Gelhar et al. 1992).

3.2.3 Diffusion

Matrix diffusion is a transport mechanism by which solutes are transferred from the water-flowing portions of permeable media (fractures) to the non-flowing portions (matrix), and vice versa due to the concentration gradients (Fig. 3-3).

The concept of molecular diffusion is recognized for the first time by Foster (1975) in England, who described the effects of molecular diffusion on contaminant behaviour in fractured rock. Foster used this mechanism in a simple mechanical model to account for the attenuation of tritium at shallow depth in fractured chalk. Most of the following diffusion studies deal with the safety assessment of geological disposal of high-level radioactive waste in low porosity crystalline rocks (Neretnieks 1980, 1985; Lever and Bradbury 1985; Skagius and Neretnieks 1986; Kozaki et al.1999, 2001; Xu et al. 2001). The inner surfaces in the rock matrix are many times (thousands or more) larger than the surfaces of the fractures. Diffusion from the fractures into the porous matrix as a physical retardation mechanism constitutes an attenuation mechanism that can be highly effective in removing contaminant mass from the primary flow channels thereby

retarding the advance of the contaminant in the system (Gersak and Pickens 1981; Neretneiks 1980; Tang et al. 1981; Sudicky and Frind 1982, 1984). The total effects of matrix diffusion will be larger in flow paths which have a larger exposed rock surface from which the dissolved solutes may diffuse into the matrix (Abelin et al. 1991). This causes an apparent retardation with respect to solutes that do not enter the matrix. Sorption sites can be reached by the solute through diffusion, which causes further retardation. Another effect of matrix diffusion is tailing on breakthrough curves where solutes take a long time to come out of the matrix because concentration gradients are very small (Maloszewski and Zuber 1993; Tsang 1995; Carrera et al. 1998*).* Unfortunately, there is very little data in literature regarding the diffusion of nitrate especially in fractured aquifers. Most scientific works have been carried out using a chloride ion, which can be considered as an easily detectable analogous anion to nitrate (Hill 1984; Gooddy et al. 1996; Kozaki et al. 2001).

Polak et al. (2003) studied tracer diffusion from a fracture into and within a chalk matrix using computer tomography (CT) system as a non-destructive imaging technique. This technique employs x-rays and mathematical reconstruction algorithms to view a cross-sectional slice of an object. The study suggested that the variations in relative concentration (C/C_0) show two distinct concentration patterns: a sharp concentration decrease within a thin layer adjacent to the matrix-fracture interface (transition layer), followed by a diffusion-type concentration decrease along the rest of the matrix.

Various tracer tests (e.g. Becker and Shapiro 2000; Einsiedl et al. 2000) proved that the tailing effect of breakthrough curves is not always a result of matrix diffusion processes. Becker and Shapiro (2000) showed in tracer tests in a fractured crystalline rock that tracers of varying diffusion produced identical late time breakthrough. This result implies that the tailing was not caused by any purely diffusive transport mechanism rather this tailing resulted from hydrodynamic transport mechanisms such as advection or hydrodynamic dispersion due to highly heterogeneous spatial and temporal nature of transport in fractured rock. Gooddy et al. (1996) adopted a simple and rapid approach in which standard (2.5 cm) diameter cylindrical chalk cores with different porosities and permeabilities are used to determine the diffusion coefficient of chloride. Apparent diffusion coefficients were found to correlate best with gas permeability also reasonable correlations exist also with the formation factor and the porosity. Young et al. (1976) illustrated that nitrate profiles in the unsaturated zone of chalk aquifer could be a consequence of nitrate diffusion from the fractures into the porous matrix. Oakes (1977) assumed that only 15 % of the surface input of nitrates and tritium travelled with the infiltrating water to the water table. and did not interact with the matrix pore water. Most of the nitrate and tritium have remained shallow because of solute storage in the unfractured chalk matrix.

Diffusion in water

Diffusion is a 1-D process induced by the random thermal motion or Brownian motion. It describes the movement of both ionic and molecular species dissolved in the water along a concentration gradient. Diffusion obeys Fick's laws and is described by a diffusion coefficient which depends on the tracer and the scale. Fick's first law in one-dimension (x-direction) describes the diffusive flux (J) of a solute in solutions directly to the concentration gradient under steady state conditions:

$$J = -D_m \frac{\partial C}{\partial x} \qquad \textbf{(3-10)}$$

J mass flux of solute per unit area per unit time [$ML^{-2}T^{-1}$]
D_m diffusion coefficient in free solution (molecular or self-diffusion coef.) [L^2T^{-1}]
$\partial C/\partial x$ concentration gradient (negative in the direction of diffusion) [$ML^{-3}L^{-1}$]

Molecular diffusion strongly depends on the frictional force between molecules, hence the dynamic viscosity of the solution. Because the dynamic viscosity is dependent on the temperature, diffusion processes show strong temperature dependence. Aqueous diffusion coefficients for spherical molecules or colloids that are very much larger than the water molecules can be calculated from Stokes-Einstein-equation. This equation states the relation between the molecular diffusion coefficient and the solution viscosity (Atkins 1986):

$$D_m = \frac{K_B T}{6\pi T_m \eta} \qquad \textbf{(3-11)}$$

K_B Boltzmann constant [L^2MT^{-3}]
T_m effective hydrodynamic radius of the ion [L]
η dynamic viscosity [$ML^{-1}T^{-1}$]

Changes in concentration with time (unsteady state) are described by a linear partial differential equation of second order referred as Fick's 2nd law of diffusion in one (x)-dimensions:

$$\frac{\partial C}{\partial t} = D_m \frac{\partial^2 C}{\partial x^2} \qquad \textbf{(3-12)}$$

Diffusion in porous media

Because the matrix will partially delay and impede the solute flux, diffusion in porous media cannot proceed as fast as in free water due to (Drever 1997):

- The transport porosity ε_t, describing that part of the cross section of the sediment, which is occupied by solution.
- The tortuosity factor τ, which is purely a geometric parameter accounting for the increased distance of transport. It is usually expressed as the square of the ratio of

the effective path length l_e to the shortest distance l. Hence $l_e > l$ for porous media, τ is always greater than 1 (Epstein 1989):

$$\tau = \left(\frac{l_e}{l}\right)^2 \succ 1 \qquad \textbf{(3-13)}$$

At the small scale (few connected pores), the pore diffusion coefficient D_p includes the resistance to diffusion from the pore geometry δ/τ^2. Compared to Eq. (3-10), the one dimensional diffusive flux in a porous media in a steady state due to the concentration gradient is described by Fick's 1st Law:

$$J = -D_e \frac{\partial C_p}{\partial x} = -D_m \varepsilon_t \frac{\delta}{\tau^2} \frac{\partial C_p}{\partial x} = D_p \varepsilon_t \frac{\partial C_p}{\partial x} = D_m D' \frac{\partial C_p}{\partial x} \qquad \textbf{(3-14)}$$

D_e effective diffusion coefficient $[L^2T^{-1}]$
δ/τ^2 geometric factor [-]
D_p pore diffusion coefficient $[L^2T^{-1}]$
ε_t transport porosity [-]
D' relative diffusivity [-]

Where δ is constrictivity of pores which describes the cross-section variation in pore space and depends on pore and diffusing component sizes. The total porosity ε is made up of transport porosity or effective porosity ε_t and storage porosity ε_d as follows:

$$\varepsilon = \varepsilon_t + \varepsilon_d \qquad \textbf{(3-15)}$$

The transport porosity ε_t describes those pores that are connected and used for transport in x-direction. The storage porosity ε_d refers to pores that have a dead end. Hence the storage porosity does not contribute to the transport process itself, but it can affect the capacity to hold the contaminants, it is neglected in the transport equations.

At large scale (rock matrix), the effective diffusion coefficient D_e includes the effects of porosity through a formation factor F (Eqs. 3-16 and 3-19). From Eqs. (3-14) and (3-15) the effective diffusion coefficient will be:

$$D_e = D_m \varepsilon_t \frac{\delta}{\tau^2} = D_p \varepsilon_t \qquad \textbf{(3-16)}$$

The change in concentration of an adsorbing solute in the porous media under transient conditions is described by Fick's 2nd law:

$$\left(\varepsilon + \rho K_d\right) \frac{\partial C_p}{\partial t} = D_p \varepsilon_t \frac{\partial^2 C_p}{\partial x^2} \qquad \textbf{(3-17)}$$

ρ density $[ML^{-3}]$

K_d distribution coefficient (for non-absorbable solute = 0) [L^3M^{-1}]

From Eq. (3-17) the rock capacity factor α measuring the capacity of the porous matrix to transport and store the diffusing solute is given as:

$$\alpha = \varepsilon + \rho K_d \qquad \textbf{(3-18)}$$

If the diffusing component is non-adsorbed α will equal the total matrix porosity (Skagius and Neretnieks 1986). The determined effective diffusion coefficient is used to calculate the relative diffusivity D' (formation factor F) and the exponent m of Archie's law (cementation factor or Archie exponent) (Archie 1942; Klingenberg 1951; Boving and Grathwohl 2001):

$$D' = F = \frac{D_e}{D_m} = \varepsilon^m \qquad \textbf{(3-19)}$$

D' relative diffusivity [L^2T^{-1}]

F formation factor [-]

m cementation factor related to the type of rock [-]

According to Archie's law the relative diffusivity D' depends only on the diffusive properties of the rock samples and is considered to be independent of temperature, sorption capacities of the porous media and the properties of the solute. Archie's law enables us to establish a reasonable relation for the investigated varieties of rock samples. This relation can be used for the prediction of diffusion coefficient for any kind of tracer or contaminant, thus avoiding time-consuming diffusion experiments.

From the above mentioned equations the following relation between the different types of diffusion coefficients can be obtained:

$$D_m > D_p > D_e > D_a \qquad \textbf{(3-20)}$$

More information about the matrix diffusion can be found in Day 1977; Gersak et al. 1980; Wellings and Bell 1980; Tang et al. 1981; Neretneiks et al.1982; Sudicky and Frind 1982; Feenstra et al. 1984; Lever et al. 1985; Maloszewski and Zuber 1985,1991, 1993; Raven et al. 1988; Moreno et al. 1988; Shackelford 1991; Haggerty and Gorelick 1995; Ohlsson and Neretnieks 1995; Gooddy et al.1996; Carrera et al. 1998; Grathwohl 1998; Steger 1998; Kozaki et al. 1998; Kozaki et al. 1999; Lapcevic et al. 1999; Maloszewski and Zuber. 1991; Maloszewski et al. 1999; Bansemer 2000; FRACFLOW 2000; Witthüser et al. 2000; Kozai et al. 2001; Kozaki et al. 2001; Shapiro 2001; Tsang and Tsang 2001; Xu et al. 2001; Bondin et al. 2003 a&b.

3.2.4 Sorption

Soils and aquifers contain abundant material, especially colloidal-sized particles (< 2 μm) such as clays, organic matter, iron and aluminium oxides and hydroxides which are

able to sorb chemicals from water. Sorption processes can be subdivided into three main types (Weber et al. 1991):

- Electrostatic interactions between negative charged mineral and cationic species in water.
- Chemical interactions between the solute and the grain surfaces.
- Electromagnetic interactions or Van der Wall's forces.

Diffusion and sorption reactions play an important role in the slowdown and retardation of solutes in the aquifers (Fig. 3-3). Sorption mainly occurs at the surfaces of the fractures when groundwater flow is fast. With increasing residence times, sorption occurs within the matrix due to the available exchange surfaces in the matrix. Sorption reactions are generally considered as instantaneous and reversible processes.

Anions such as phosphate are adsorbed by clay particles only in acid solution where phosphate is either adsorbed or precipitated, and does not move freely through aquifers (Ryden and Pratt 1980; CAST 1985; Jardine et al. 1988). Anions such as bicarbonate, sulfate and nitrate are too large to be effectively adsorbed (Fetter 1994).

Nitrate is highly water-soluble, mobile and not prone to ion exchange or sorption on the soil and aquifer particles during its transport through aquifers (Hem 1985; Jardine et al. 1988; Fetter 1994; Macko and Ostrom 1994; Mueller et al. 1995; Stumm and Morgan 1996; CAST 1985). Other workers such as Stagnitti et al. (2000) studied the breakthrough curves for chloride, nitrate and phosphate to predict the fate of nutrients in soil and estimate the possible risk of groundwater pollution. They found a retardation factor of 1.06 and a reaction rate of 0.035/day for nitrate, indicating a small adsorption but significant reaction rate.

A number of factors control the interaction of contaminants with aquifer solid particles. These factors include chemical and physical characteristics of the contaminant (sorbate), composition of the surface of the solid (sorbent) and the fluid media encompassing both. The most common used technique to characterize sorption properties of the rock is the batch test. The main aim is to determine the sorption coefficient K_d by obtaining an equilibrium condition between a solution of known initial concentration and crushed rock. The amount adsorbed onto the solid can be calculated as the difference in mass of the solute in solution before the test and in solution at equilibrium. A graphical plot (Fig. 3-5) of adsorbed contaminant concentrations C_s fixed on solid surface as a function of contaminant concentrations C_L in the liquid phase is known as an adsorption isotherm and it is expressed as:

$$C_s = f(C_L) \qquad \textbf{(3-21)}$$

The sorption isotherms can be linear, concave, convex or a complex combination of all of these shapes. The most common sorption isotherms are Henry, Freundlich and Langmuir sorption isotherms (Domenico and Schwartz 1990) (Fig. 3-5).

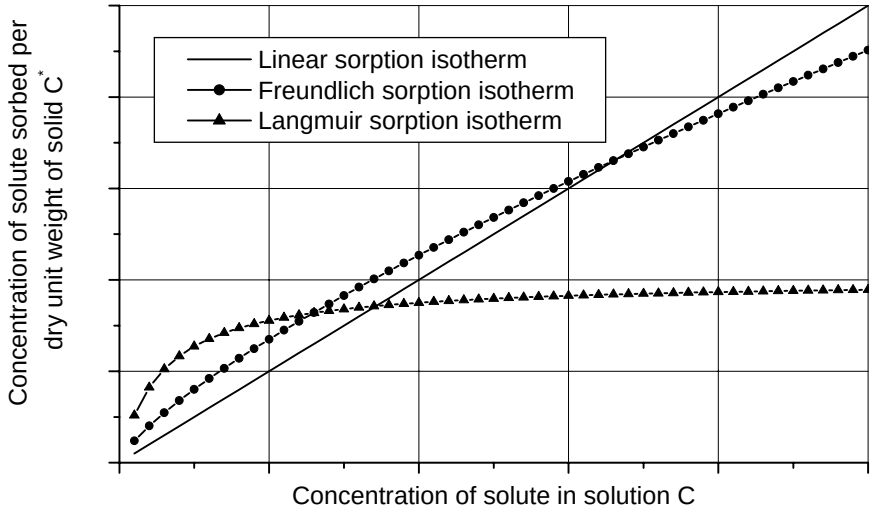

Fig. 3-5: Equilibrium sorption isotherms.

Linear or Henry sorption isotherm

Linear sorption isotherm (Fig. 3-5) is the simplest sorption isotherm where K_d is independent of concentration:

$$C_s = K_d C_L \qquad \textbf{(3-22)}$$

C_s adsorbed concentration measured as mass of contaminant per mass of dry matrix material [MM^{-1}]

C_L dissolved concentration measured as mass of contaminant per volume of solution [ML^{-3}]

K_d matrix distribution coefficient [L^3M^{-1}]

The distribution coefficient K_d can be used to compute the retardation coefficient of fracture surface R_f (Eq. 3-1) and retardation coefficient of rock matrix R_p (Eq. 3-2). According to Henry sorption isotherm R_f and R_p can be calculated as (Freeze and Cherry 1979; Thorbjarnarson and Mackay 1997):

$$R_f = 1 + a_w K_{d_f} = 1 + \frac{2K_{d_f}}{2b} \qquad \textbf{(3-23)}$$

$$R_p = 1 + \frac{\rho K_d}{\varepsilon} = \frac{\alpha}{\varepsilon} \qquad \textbf{(3-24)}$$

K_{d_f} distribution coefficient for the fracture surface [L]

a_w specific fracture surface [L^{-1}]

ρ_b dry bulk density of the dry matrix material [ML^{-3}]

For non-reactive solutes such as deuterium and chloride the K_d equals zero and R_p one (Maloszewski and Zuber 1990; Shackelford 1991; Kozaki et al. 1999; Maloszewski et al. 1999). Reactive solutes such as NO_3 and NH_4 (Pauwels et al. 1997) will travel at a slower rate than groundwater due to adsorption.

Freundlich sorption isotherm

The Freundlich isotherm (Fig. 3-5) a non linear sorption isotherm (Domenico and Schwartz 1990) is described as followed:

$$C_s = K_f C_L^n \quad \textbf{(3-25)}$$

$$\log C_s = b \log C_L + \log K_f \quad \textbf{(3-26)}$$

n sorption exponent (constant, usually ranging between 0.7 - 1.2) [-]
K_f Freundlich K_d [L^3M^{-1}]

In a plot of C_s versus C_L on the log-log paper, the slope of the curve is a straight line. In the case of n = 1 the relationship is linear and the K_f equals the K_d (Cherry et al. 1984):

$$\frac{\Delta C_s}{\Delta C_L} = K_d \quad \textbf{(3-27)}$$

Langmuir sorption isotherm

The Langmuir isotherm (Fig. 3-5) can be described as (Domenico and Schwartz 1990):

$$C_s = \frac{Q^o K C_L}{1 + K C_L} \quad \textbf{(3-28)}$$

Q^0 maximum sorptive capacity for the surface [-]
K distribution coefficient [L^3M^{-1}]

The organic carbon partition coefficients K_{OC} can be estimated using several well known correlations such as K_{OC}-K_{OW} (octanol-water coefficient) (Karickhoff et al. 1979; Karickhoff 1981; Lyman et al. 1990) or K_{OC}-S_W (water solubility) (Karickhoff et al. 1979; Means et al. 1980). Those correlations are applicable as long as the organic carbon content f_{OC} in the aquifer is sufficient to neglect sorption on inorganic surfaces ($f_{OC} > 0.1$ % Karickhoff et al. 1979). In those cases it is possible to estimate the distribution coefficients of hydrophobic organic compounds based on the f_{OC} of the aquifer and the K_{OC} of the compound (Kenaga 1980):

$$K_{OC} = \frac{K_d}{f_{OC}} \quad \textbf{(3-29)}$$

K_{OC} organic carbon partition coefficients [-]
f_{OC} organic carbon content [-]

The K_{OC}-concept is useful in determining the mobility of organic chemicals. It assumes that structure and composition of organic matter has no impact on the K_{OC} values. Oxidation of organic matter may result in a significant decrease of the K_{OC} values, therefore structure and composition of organic matter cannot be neglected in the predication of organic carbon partition coefficients (Grathwohl 1990).

3.2.5 Decay

Decay reactions of the contaminants that are relatively slow in comparison to the average travel time are able to induce a decrease over time in the solute mass. The reactions of the first-order kinetics due to radioactive decay or biodegradation follow the relationship (Spitz and Moreno 1996):

$$\frac{\partial C}{\partial t} = -\lambda \qquad \textbf{(3-30)}$$

Where λ is the rate coefficient of biodegradation or decay and is defined by (Tang et al. 1981; Sudicky and Frind 1984):

$$\lambda = \frac{\ln 2}{T_{1/2}} \qquad \textbf{(3-31)}$$

$T_{½}$ is the half-life of the radioactive isotopes or the degraded contaminant [-]

3.3 Mathematical modelling of transport in the fractured media

The mathematical modelling of contaminant transport in the fractured media is developed by following either a continuous or a discrete approach (Bodin et al. 2003b). In the continuous approach, the real fractured medium is replaced by equivalent porous medium (EPM) where the key parameters are the equivalent permeability and the dispersion tensors. The discrete approach takes into account the transport mechanisms in each fracture; therefore it is more logical than the continuous approach (Bodin et al. 2003b). To apply the discreet approach, transport parameters for each fracture have to be determined by carrying out laboratory and field tracer tests.

3.3.1 Analytical models of contaminant transport in fractured media

Analytical solutions are derived from the fundamental partial differential equations for solute transport. Formulating the contaminant transport problem in terms of equations (Eqs. 3-1 and 3-2) and boundary conditions (Eqs. 3-32 to 3-37) is the first step to obtain an analytical solution to solute transport problems. The initial conditions describe the values of the variable at the time equal to zero. Boundary conditions specify the interaction between the area of interest and its surrounding environment.

Step or constant input

The first analytical solution for the problem of contaminant transport along a single discrete fracture in a porous rock matrix was developed by (Grisack and Pickens 1981).

The model accounts for diffusive flux of solutes into the matrix and neglected dispersion within the fracture for one dimensional convergent flow experiments. Tang et al. (1981) found an analytical solution for a single discrete fracture taking into account advection and dispersion within the fracture and diffusion into the matrix.

Instantaneous or Dirac input

According to the experimental set-up the Single Fracture Dispersion Model (SFDM, Maloszewski and Zuber 1990) was used to describe the observed BTC`s. The model takes advective-dispersive transport in the fracture coupled with diffusive transport in the porous rock-matrix into account. In short-term tracer tests, the mean transit time of water and tracer is sufficiently short. Therefore the tracer has no time to diffuse into the matrix deep enough to reach the adjacent fractures. For an instantaneous injection (Dirac delta function $\delta(t)$) of tracer into the fracture, the following boundary and initial conditions are used (Maloszewski and Zuber 1993):

For Eq. (3-1) the boundary and initial conditions are:

$$C_f(x,0) = 0 \qquad \textbf{(3-32)}$$

$$C_f(0,t) = (M/Q)\delta(t) \qquad \textbf{(3-33)}$$

$$C_f(\infty,t) = 0 \qquad \textbf{(3-34)}$$

For Eq. (3-2) the boundary and initial conditions are:

$$C_p(z,x,0) = 0 \qquad \textbf{(3-35)}$$

$$C_p(b,x,t) = C_f(x,t) \qquad \textbf{(3-36)}$$

$$C_p(\infty,x,t) = 0 \qquad \textbf{(3-37)}$$

M mass or activity of tracer instantaneously injected into the fracture [M]
Q volumetric flow rate through the fracture [L^3T^{-1}]
$\delta(t)$ Dirac delta function [-]

Eqs. (3-32) and (3-35) are initial conditions, and state that at all points x and z at time t = 0, the concentration is zero within the flow domain ($C_p = C_f = 0$). The second boundary condition Eq. (3-33) states that, at x = 0, for all time t, the concentration is maintained at C_0 and defines the tracer concentration as the so-called flux concentration. Eq. (3-34) states that, when the flow system is infinitely long, the tracer concentrations at $x = \infty$ from the injection point is zero for all time t. Eq. (3-36) characterizes the coupling of the porous matrix to the fracture and concentration balance between fracture and matrix at $z = \pm b/2$. The SFDM model for an instantaneous injection (Dirac delta function) of tracer into the fracture using the boundary and initial conditions (Eqs. 3-32 to 3-37) (Maloszewski and Zuber 1990) is given by:

$$C_f(t) = \frac{aM\sqrt{Pe \cdot t_o}}{2\pi Q} \int_0^t \exp\left[-\frac{Pe(t_o - \xi)^2}{4\xi t_o} - \frac{a^2\xi^2}{t-\xi} \right] \frac{d\xi}{\sqrt{\xi(t-\xi)^3}} \quad \textbf{(3-38)}$$

$C_f(t)$ concentration measured at a given distance x [ML^{-3}]
Pe Peclet number [-]
a parameter describing matrix diffusion [L]
ζ integration variable [-]
t_0 mean residence time of water and/or non-reactive tracer within the fracture [T]

In case of breakthrough curves with low recovery rates, several assumptions are necessary to apply the SFDM. Assuming that the transversal dispersion is neglected, a transversal dispersion term $g(\alpha_t)$ is included in the SFDM as (Witthüser et al. 2003):

$$C_f(t) = \frac{aM\sqrt{Pe \cdot t_o}}{2\pi Q} \int_0^t \exp\left[-\frac{Pe(t_o - \xi)^2}{4\xi t_o} - \frac{a^2\xi^2}{t-\xi} \right] \frac{d\xi}{\sqrt{\xi(t-\xi)^3}} g(\alpha_t) \quad \textbf{(3-39)}$$

At the time t_{max}, the maximum concentration C_{max} can be given by:

$$C_f(t_{max}) = \frac{aM\sqrt{Pe \cdot t_o}}{2\pi Q} \int_0^{t_{max}} \exp\left[-\frac{Pe(t_o - \xi)^2}{4\xi t_o} - \frac{a^2\xi^2}{t-\xi} \right] \frac{d\xi}{\sqrt{\xi(t-\xi)^3}} g(\alpha_t) = c_{max} \quad \textbf{(3-40)}$$

By dividing Eqs. (3-39) and (3-40) the dispersion term $g(\alpha_t)$ as well as M and Q are eliminated:

$$C_f(t) = c_{max} \frac{\int_0^t \exp\left[-\frac{Pe(t_o - \xi)^2}{4\xi t_o} - \frac{a^2\xi^2}{t-\xi} \right] \frac{d\xi}{\sqrt{\xi(t-\xi)^3}}}{\int_0^{t_{max}} \exp\left[-\frac{Pe(t_o - \xi)^2}{4\xi t_o} - \frac{a^2\xi^2}{t-\xi} \right] \frac{d\xi}{\sqrt{\xi(t-\xi)^3}}} \quad \textbf{(3-41)}$$

Eq. (3-41) enables to calculate the transport parameters for the tracer tests with low recovery rates. To fit the simulated concentrations (Eqs. 3-38 and 3-41) with the observed concentrations, three fit parameters have to be determined:

The diffusion parameter a:

$$a = \frac{\varepsilon\sqrt{D_p}}{2b} \quad \textbf{(3-42)}$$

The mean transit time of water and/or non-reactive tracer t_0:

$$t_0 = \frac{X}{v} = \frac{V_f}{Q} \quad \textbf{(3-43)}$$

The Peclet number Pe as a measure of the relative importance of advection to hydrodynamic dispersions:

$$Pe = \frac{vX}{D_{h_l}} = \frac{vX}{D_m + \alpha_l v} \qquad \textbf{(3-44)}$$

X flow distance between entrance and observation point (fracture length) [L]

V_f volume of mobile water in the fracture [L^3]

In the case of a reactive tracer the adsorption retardation factors R_f (for the fracture surface) and R_p (for the rock-matrix) are taken into account in the equations of the fitting parameters. In such a case the fitting parameters of the model can be found by simultaneous injection of non-reactive and reactive tracers. For reactive tracer with linear sorption (R_f>1, R_p>1), the mean residence time t_0' and diffusion parameter a are given by (Maloszewski 1994):

$$t_0' = t_0 R_f \qquad \textbf{(3-45)}$$

$$a = \frac{\varepsilon\sqrt{D_p R_p}}{2bR_f} \qquad \textbf{(3-46)}$$

R_f retardation coefficient of fracture surface [-]

R_p retardation coefficient of rock matrix [-]

The retardation factor of the fracture R_f can be determined by comparing t_0' with t_0 for non-reactive tracer, whereas R_p can be found by comparison of a parameter for reactive tracer (Eq. 3-46) with a parameter for non-reactive tracer (Eq. 3-42). By knowing the distance X between the injection and the observation point, the fitting parameters Pe and t_0 can be used to calculate the longitudinal dispersivity α_l and the mean water velocity v within the fracture (Eqs. 3-43 and 3-44). If the pore diffusion coefficient D_p and the porosity ε are known from e.g. laboratory measurements, Eq. 3-42 can be used to estimate the fracture aperture 2b. The pore diffusion coefficient D_p can be estimated using the value of the fracture aperture obtained from the Darcy experiments (Eq. 3-42).

The effective diffusion coefficient D_e of the applied tracer is then given by:

$$D_e = \varepsilon_t D_p \qquad \textbf{(3-47)}$$

Since we do not know the transport porosity ε_t we assume that all pores of the matrix contribute to the diffusive transport ($\varepsilon=\varepsilon_t$) for all our calculations. If the matrix porosity and diffusion coefficient are measured on a rock sample, the fracture aperture can be calculated from a tracer test using Eq. (3-42).

The tracer mass recovery is calculated by integration the BTC multiplied by the flow rate. To improve the recovery rate the cumulative amount of tracer that reaches the sampling point as a function of time is calculated.

The relative mass recovery RR(t) as a function of time is calculated as:

$$RR(t) = \frac{Q}{M}\int_0^t C_f(t)dt \qquad \textbf{(3-48)}$$

Tracer curves with several peaks can not be described only by single dispersion model. In consequences, the concept of multi-flow or multi-dispersion model MDM developed for interpreting tracer experiments in karstified rock are used (Maloszewiski et al. 1992). The model (Fig. 3-6) assumes that the whole mass of tracer M instantaneously injected into the system at t = 0 is transported in several flow paths N, which meet in the outflow of the system, where a complete mixing of the flow paths is assumed. This means the tracer mass M_i entering each flow path is proportional to the volumetric flow rate Q_i through that flow path. Each i-th flow path has its own diffusion parameter a_i, mean residence time t_{0i}, dispersion parameter Pe_i and the flow rate Q_i. Some flow paths may originate and end somewhere within the fracture and independently from that, the model parameters are always calculated for flow paths which originate in the injection point and end in the sampling point (Fig. 3-6). Therefore the model has to be considered as a rough approximation of the reality. The model also assumes that possible diffusion of tracer from the mobile water into the stagnant water within the matrix and/or the non active parts of the karstic system is neglected due to the high water velocity within the different flow paths.

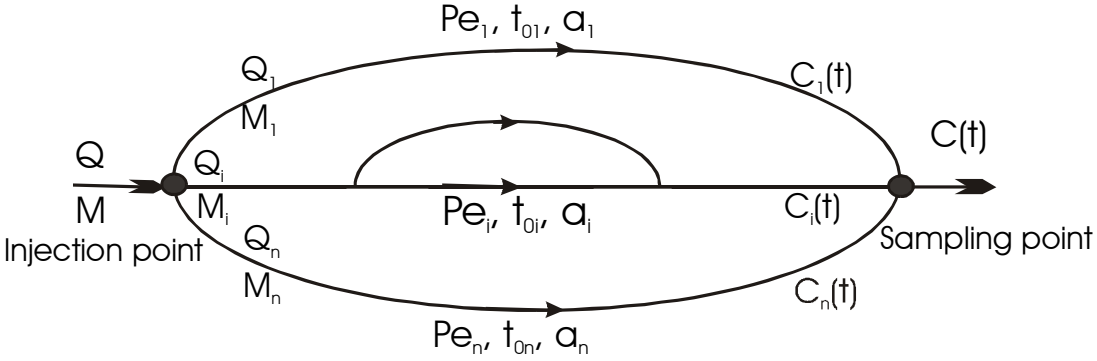

Fig. 3-6: Conceptual model of the flow channelling within the fracture.

Taking into account all the above mentioned assumptions for each flow path the transport of non-reactive tracer can be governed by this equation:

$$D_i \frac{\partial^2 C_i}{\partial x^2} + v_i \frac{\partial C_i}{\partial x} = \frac{\partial C_i}{\partial t} \qquad \textbf{(3-49)}$$

D_i dispersion coefficient for the i-th flow path [L^2T^{-1}]

$C_i(x,t)$ tracer concentration in water for the i-th flow path [ML^{-3}]

v_i mean flow velocity of water for the i-th flow path [LT^{-1}]

For an instantaneous input described by Dirac function Maloszewiski et al. (1992) developed an analytical solution of the partial differential Eq. (3-49) as follow:

$$C_i(t) = \frac{M_i}{Q} \frac{1}{t_{0i}\sqrt{4\pi(P_{Di})(t/t_{0i})^3}} . \exp\left[- \frac{(1 - t/t_{0i})^2}{4(P_{Di})(t/t_{0i})} \right] \quad \textbf{(3-50)}$$

$C_i(t)$ tracer concentration within the i-th flow path [ML^{-3}]

M_i mass or activity of tracer instantaneously injected into i-th flow path [M]

P_{Di} dispersion parameter $(D/xv)_i$ on the i-th flow path [L^2T^{-1}]

The total output concentration C(t) is the superposition of the partial concentrations $C_i(t)$:

$$C(t) = \sum_{i=1}^{N} C_i(t) \quad \textbf{(3-51)}$$

The partial tracer recoveries R_i observed at the end of each i-th flow path are calculated using Q and $C_i(t)$:

$$R_i = Q\int_0^{\infty} C_i(t) = M_i \quad \textbf{(3-52)}$$

Theoretically, the sum of all partial recovers (cumulative tracer curve) is equal to the total recovery and to the mass of tracer injected:

$$R = \sum_{i=1}^{N} R_i = M \quad \textbf{(3-53)}$$

The ratio of i-th recovery R_i to the total recovery R observed at the sampling point produce the portion of tracer r_i transported through the i-th flow path:

$$r_i = \frac{R_i}{R} = \frac{Q_i}{Q} \quad \textbf{(3-54)}$$

R_i residual recovery observed at the end of each i-th flow path [%]

Q_i volumetric flow rate in i-th flow path [L^3T^{-1}]

i channel within the fracture [-]

4 CHALK AND CHALK AQUIFERS

4.1 Geneses of chalk in Europe

The chalk is primarily a pelagic sediment of accumulation rather than mechanical deposition. It is a rock composed mainly of skeletal calcite of the phylum Haptophyta with minor amounts (< 10 %) of other biogenic fragments (Mortimore 1990). Therefore it is extremely pure limestone. Chalk was deposited over large areas of NW Europe during the Cretaceous Period as pelagic sediment (deep-sea ooze) and through a series of diagenetic processes the sediment became lithified.

In the North Sea the chalk attains a maximum thickness of 2000 m in the Viking Graben and Central Trough, but 300 - 350 m is more usual on the flanks and in the areas where it crops out. The considerable thickness of chalk in the Central Trough is due to redeposition following sliding, slumping and the formation of debris flow and turbidity. Tectonic movements initiated large scale displacement of unstable chalk down the flanks of the trough to accumulate in the trough itself as complex allochthonous sequences. Burial and subsequent uplift of the lithified sediments caused fractures to form (Downing et al. 1993).

Fig. 4-1: Chalk distribution in Europe (FRACFLOW 2000).

4.2 Mineralogy

Chalk is an extremely soft and pure limestone consisting mainly of calcium carbonate with small portions of other constituents (Tab. 4-1). Clay minerals mainly include the smectite group usually in the form of Ca-montmorillonite. The mica group is less important and chlorite is rare. In the white-chalk facies such as in English and Danish chalk, the clay content is typically less than 2 % (Hancock 1993). Quartz occurs as clay and

silt-grade particles and as pseudomorphs after foraminifera throughout the chalk. Most of the original biogenic silica has undergone a series of diagenetic changes to become concentrated into chert-nodules called flints (Hancock 1993).

Tab. 4-1: Components of white chalk (96-99% low-magnesian calcite (Hancock 1993)).

Type of components	Description	%
Biogenic	- Haptophyta (coccolith-bearing algae)	80-92
	- Foraminifera (benthic in most stages)	5-10
	- Inoceramid bivalves-commonly 2 %	0-5
	- Bryozoa	0-5
Inorganic	- Clay minerals (Ca-montmorillonite usually dominant and clay grade muscovite)	1-4
	- Silica minerals (+flints, clay grade quartz and cristobalite)	1-2

4.3 Hydrogeology

The chalk with its depositional, diagenetic and tectonic setting is a typical dual-porosity or double-porosity aquifer (Fig. 4-2), with one porosity due to the matrix pores (30-40 %) and the other due to the fractures (probably $<$ 1 %). In these aquifers the chalk-matrix pores provide the storage capacity and the fractures provide the permeable pathways for water and solutes transport. However, in the reality the chalk is a multi-porosity aquifer with a range of fracture apertures and matrix pore sizes. It forms one of the major aquifers in NW Europe.

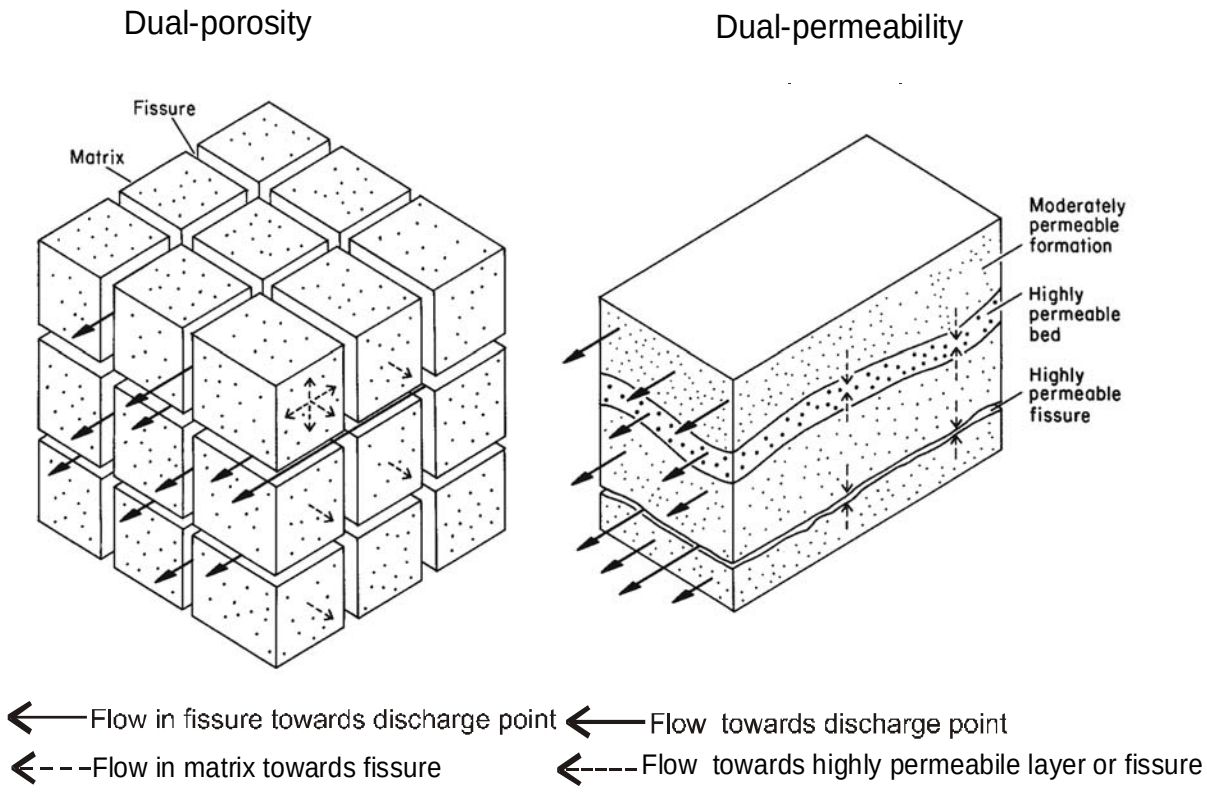

Fig. 4-2: An idealized dual-porosity and dual-permeability aquifer (Price et al. 1993).

The most important property of the chalk, that makes it an excellent groundwater aquifer, is its well developed fracture system. The same property makes it vulnerable to pollution from different sources. Gooddy et al. (1996) differentiated between three components of porosity and permeability in chalk. The first porosity-permeability component is the high intergranular porosity (25-40 %) with low intergranular permeability as a result of small pore throat sizes. The second is contributed by joints or fractures, this component has low porosity (0.1-1 %), but can increase hydraulic conductivity by two or three orders of magnitude if joints are relatively closely spaced and open. The third component is due to the enlargement of the fractures by solution, it can increase the chalk transmissivity up to 1000 m^2/d. The typical hydrogeological properties of the chalk are given in Tab. 4-2.

Tab. 4-2: The general properties of the chalk aquifers (Price et al. 1993).

- Porosity of the matrix (%)	30-40
- Porosity of the fractures (%)	0.01
- Permeability of the matrix (m/s)	10^{-9}-10^{-8}
- Permeability of the fissured chalk (m/s)	10^{-5}-10^{-3}

Chalk is generally a permeable formation. Consequently, it displays low or moderate hydraulic gradients. The actual mechanism of recharging in the chalk aquifers is subjected to annoying discussions: whether recharging takes place through the matrix or via the fissures depending on the relative magnitude of the infiltration rate and the hydraulic conductivity of the chalk matrix. In the saturated zone the hydraulic conductivity of the matrix makes a negligible contribution to the transmissivity of the aquifers. The overall effects of diagenesis on chalk porosity and permeability are shown in Fig. 4-3.

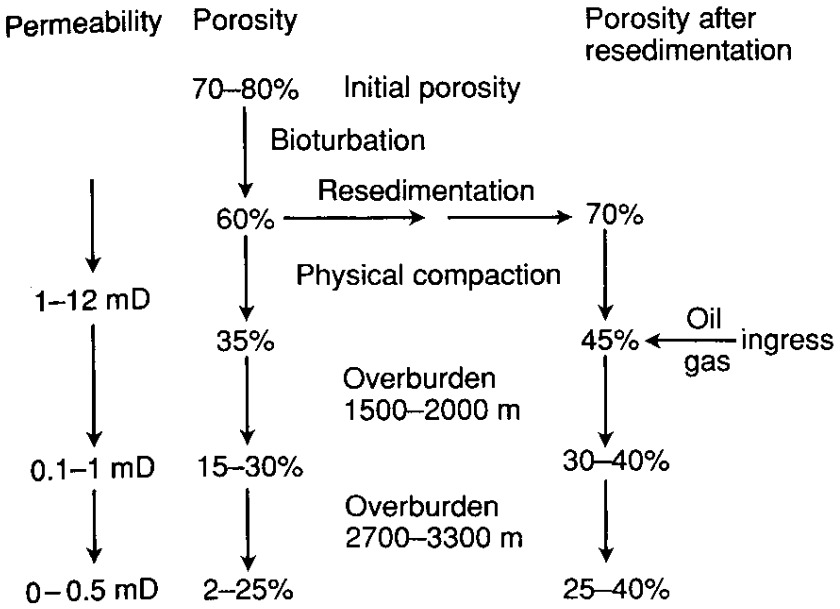

Fig. 4-3: Changes of porosity and permeability in chalk with increasing diagenesis and the advantage of resedimentation (Hancock 1993).

As clearly shown in Fig. 4-3, early diagenesis and an overburden of 250 m reduced the porosity to 35-50 % with a matrix permeability around 1-12 mD. An increase of overburden to 1000 m gives only a slight further reduction of porosity around 30-40 %. With 1500-2000 m overburden the porosity falls to 15-30 % and the permeability to 0.1-1 mD (Hancock 1993). The overall effects of diagenesis process on chalk are to harden the chalk and reducing the porosity and permeability of the chalk. When the chalk is deeply buried, as in North Sea oilfields, fractures may increase the permeability of the rock to a value of the order 100 m/d. At lower depths on shore, a combination of factors such as dissolution, stress release as overburden is removed and weathering can lead to significant enlargement of these fractures. This enlargement is responsible for the majority of the high transmissivities that characterize much of the chalk aquifer at outcrop or beneath thin overburden in North-West Europe (Price et al. 1993). Furthermore the primary fissure component, although important, can not account for the high transmissivity values that make the chalk such a productive aquifer (Price 1987). Price et al. (1982) reported that the high transmissivity value is due to the enlargement process of the primary fissure components by solution (secondary fissures).

5 TEST SITE SIGERSLEV

The chalk samples were obtained from the test site “Sigerslev quarry” an active chalk quarry run by Faxe Kridt A/S. The quarry is located just behind the Stevns sea cliff on the Danish island of Zealand (Sjaelland), about 60 km south of Copenhagen, Denmark (Fig. 5-1).

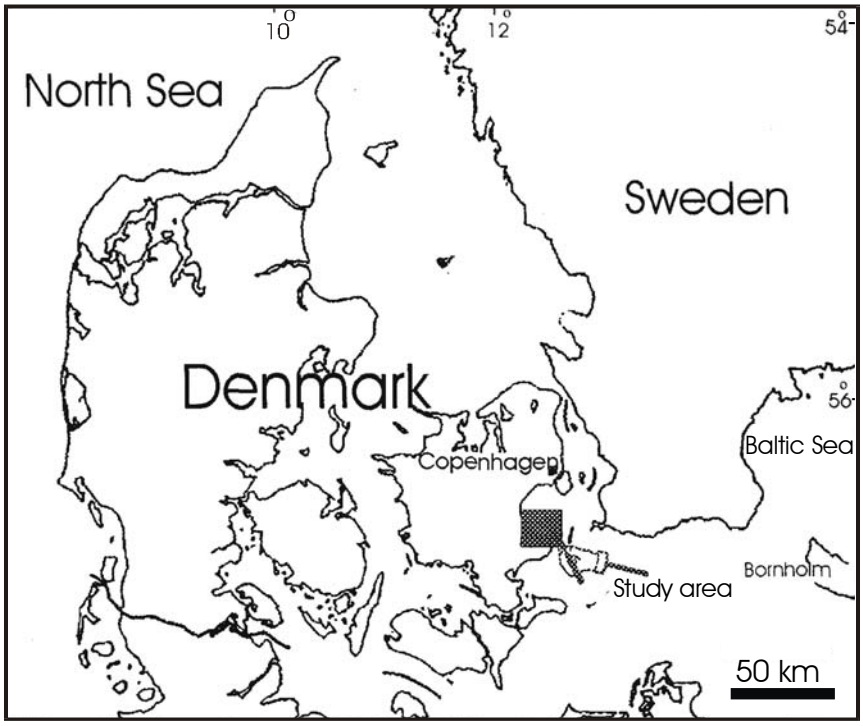

Fig. 5-1: Location map of the study area Sigerslev, Denmark (Frykman 1994).

5.1 Geology

The study area consists from the top to the bottom of the following geological units (Frykmann 1994; Skjernaa 1998): Glacial deposits of melt water, silt, sand, gravel and minor clay and clayey till of Quaternary age (1-20 m thick) into clayey till as the most widespread surface deposit. Chalk (> 500 m thick) and limestone (~40 m thick) are of Upper Cretaceous and Tertiary age.

The lowermost formation to be seen in the outcrop in eastern Seeland is the chalk, which is Uppermost Maastrichtian age. The thickness of the chalk is up to 2000 m in the Northern Seeland (Knudsen 1996), it represents sedimentations from several stages.

The stratigraphy of the Danish chalk is well displayed at Stevns Klint. Soft and friable chalk of Late Maastrichtian Age is overlain by a relatively hard limestone of Danian Age (bryozoan limestone). The bryozoan limestone is marine sediment consisting mainly of coccolithes and about 20-45 % bryozoans. The limestone also includes flint (approx. 20 %) in the form of discontinuous layers (Skjernaa 1998). The interrelationship between the transition beds is complicated and they include a thin (approx. 15 cm) dark clay bed,

called Fish clay. It was formed in a shallow cold sea, basically without life, after the sudden change of the climate. The fish clay layer is recognized as the geological borderline between Cretaceous (chalk) and Tertiary (bryozoan limestone) period (C-T boundary).

The chalk contains flint in the form of irregular lenses concentrated at certain levels in the chalk constituting approximately 5 % of the rock. Its content of clay minerals is generally less than 0.5 %. The chalk reaches a maximum thickness of approx. 1800 m in the Danish sub-basin (Stenestad 1972).

5.2 Tectonic setting and fracturing

The chalk in the Stevns area is exposed due to a gentle, large scale Cenozoic uplift. Glacially induced deformation occurs locally in the uppermost part of the chalk where large scale faulting is not an important element in the deformation pattern but subvertical joints and horizontal cleavage surfaces are very prominent in the area (Frykman 2001). There are several sets of vertical fractures, however, the dominant strike directions are given in Tab. 5-1 (FRACFLOW 1999).

Tab. 5-1: Average spacing of the different sets of fractures in the Sigerslev quarry (FRACFLOW 1999).

Fractures set	Average spacing
Horizontal	0.4 m
Vertical; strike 25^{o}	3.6 m
Vertical; strike 65^{o}	6.0 m
Vertical; strike 145^{o}	3.2 m
Vertical; strike 175^{o}	4.2 m

Chalk in the Sigerslev quarry is gently folded with axes trending NW-SE. Fracturing occurs principally in the top 20-50 m (FRACFLOW 2001). The dominating structural element is the Fennoscandian Border Zone (Fig. 5-2) extending from the Skagerak Sea (north of Jutland) through Scania (Baartman and Christensen 1975).

A range of fracture parameters have been collected such as fracture orientation, size, spacing and length distributions as well as observations on fracture termination style, mineralisation and the presence or absence of clay drapes. Three orthogonal or conjugate fracture sets oriented with respect to bedding were characterised. Fig. 5-3 shows an example of some of the fracture orientation data for both single and multi-layer fractures. The orientation of the multi-layer vertical fractures is predominantly to the north or north-east compared with the single and intra-layer fractures that have a preferred north-west orientation.

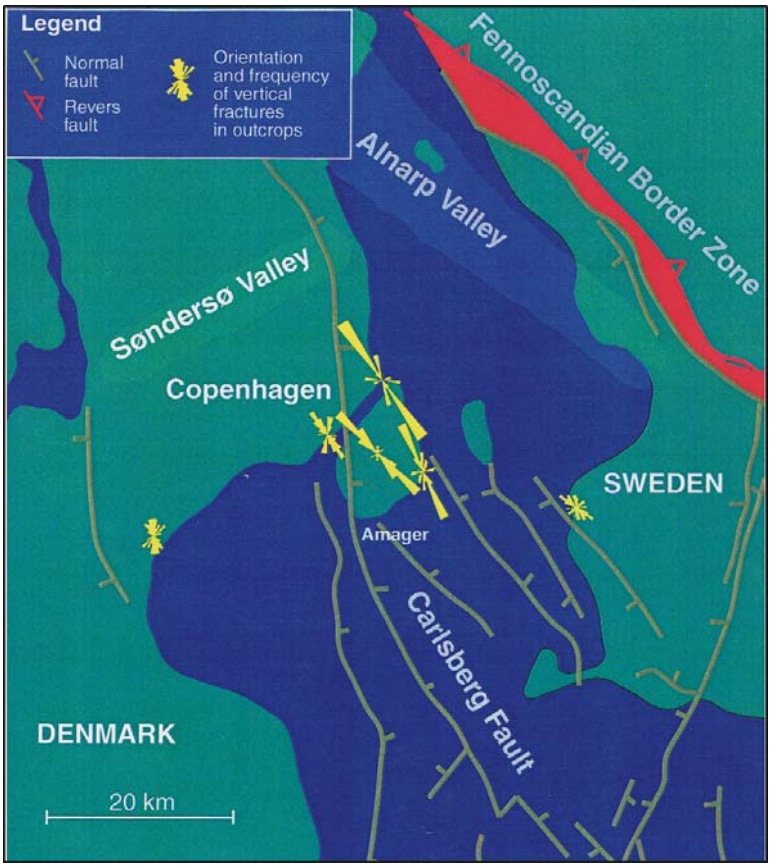

Fig. 5-2: Structural map of the area with fractures orientations (Jakobsen and Klitten 1998).

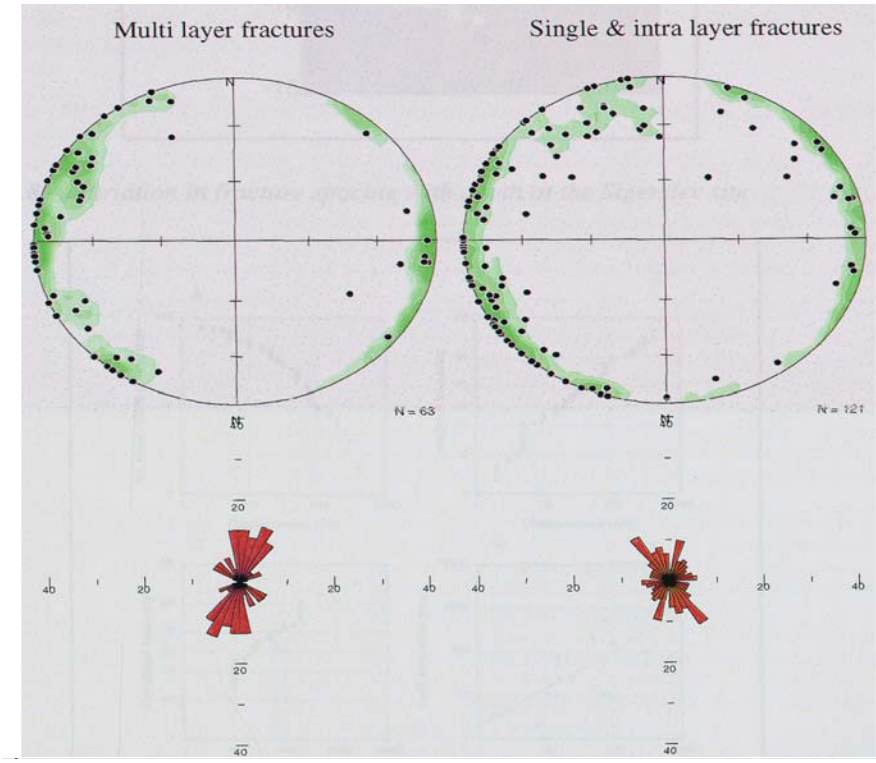

Fig. 5-3: Fracture orientation data for single and multi-layer fractures at the Sigerslev area (FRACFLOW 2001).

Fractures with coatings of ferric iron or manganese have almost exclusively the direction of 30°, suggesting that groundwater also flows in the system of vertical fractures in this direction (FRACFLOW 1998). Horizontal fractures are the main hydraulically active conduits (Fig. 5-4). The horizontal fractures of the bedding planes are larger than the verticals with higher connectivity, and are more hydraulically active of the intersection with the vertical stained fractures (FRACFLOW 1999).

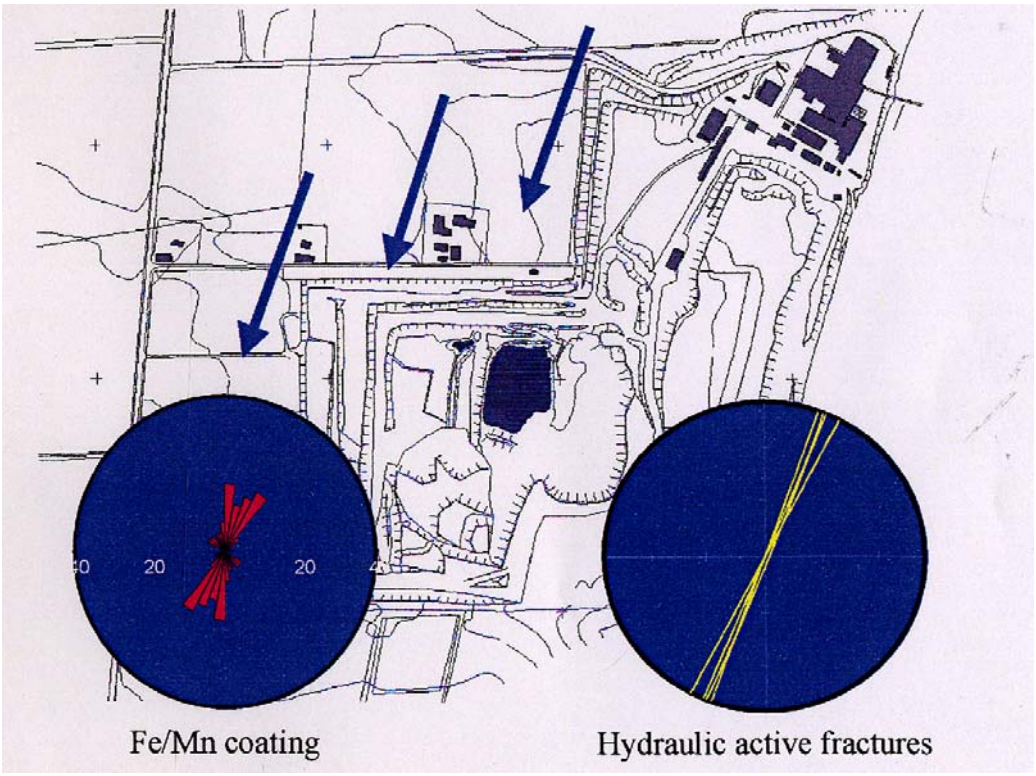

Fig. 5-4: Groundwater flow pattern in the Sigerslev quarry (FRACFLOW 1999).

5.3 Mineralogy

It is well known that the mineralogical content of chalk such as organic carbon and clay minerals has a great influence upon the magnitude and extant of transport and retardation mechanisms. The mineralogical composition of the Danish chalk was determined by x-ray diffraction (XRD) analysis of some bulk chalk samples. XRD analysis was carried out using D8 Advance (Bruker axs) with Cu α radiation to make the XRD scans. The samples showed high concentrations of calcite, and small concentrations of quartz and clay minerals.

Geochemical analysis (carried out using a Siemens SRS 303 x-ray fluorescence spectrophotometry XRF) of major and trace element oxides for the same selected samples showed that the chalk samples contained higher CaO contents (53.2 %) as confirmed by the XRD result in the form of high calcite contents. The mineralogical composition of the Danish chalk is given in Tab. 5-2 (Witthüser et al. 2003).

Tab. 5-2: Mineralogical composition (Weight %) of chalk samples from the test field Sigerslev quarry (Witthüser et al. 2003):

Calcite	Quartz	Illite	Apatite	Hematite	Rutile	TOC (f_{CO})
98.13	0.82	0.47	0.59	0.06	0.01	0.033

It is obvious from Tab. 5-2 that Danish chalk is characterised by low fractions of organic carbon contents with a mean f_{OC} of 0.033 %. This low value of organic carbon suggests a low sorption capacity for contaminants in the chalk.

5.4 Hydrogeology

The area under investigation is characterized by humid climate with annual precipitation around 650 mm/a, of which 280 mm/a serve as groundwater recharge (FRACFLOW 2001). In Denmark, except for the Bornholm Island, the chalk represents the oldest freshwater aquifer. The salinity of pore-water in the chalk aquifers increases with depth in the lower part of the aquifers and in coastal zones with decreasing distance from the shoreline (Nygaard 1993). Due to the low matrix permeability the suitability of the chalk as an aquifer almost depends on the presence of permeable fractures.

In general two aquifers can be distinguished. An upper, main aquifer is built from bryozooan limestone and mostly confined by a section of variable beds of glacial drift. The bryozooan limestones have a thickness of 40 m with matrix porosities between 33-46 % and a matrix (gas) permeability of approx. 6-22 m/d (Frykman 1994). A lower aquifer developed in the Maastrichtian chalk. It is confined in areas away from coastal exposure. Transmissvity and storage coefficient of the chalk aquifer is $6*10^{-4}$ m^2/s and $2*10^{-5}$ m^2/s respectively (Wichmann 1995). Due to the small pore-throats sizes (approx.1 µm) of the chalk matrix, its permeability is typically very low (8.32 m/d to 8.55 m/d). Matrix porosity ranges from a few % in flint layers to about 50 % for the chalk matrix itself. The hydraulic conductivity of the fractures is estimated to be 0.11-0.33 m/d (FRACFLOW 2001). More information about the geology, tectonics and hydrogeology of Stevens/Sigerslev can be found in Nygaard 1993; Fredericia et al. 1998; Frykman 1994, 2001; Wichmann 1995; Bansemer 2000; Blum 2000; FRACFLOW 2000, 2001; Witthüser 2001 and Gerik 2003.

6 LABORATORY EXPERIMENTS

This section describes the methodical approach selected to get the necessary information on the transport behaviour within fractured porous media. After an overview on the tracers used the various laboratory experimental procedures as well as details regarding the data evaluation is presented.

The diffusive transport process of nitrate, chloride, lithium, uranin, eosin and pyranin was investigated in Danish chalk by carrying out through-diffusion experiments. In batch experiments, nitrate, lithium, uranin, eosin and pyranin were used to determine the distribution coefficients and retardation factors in the Danish chalk matrix. In order to investigate the physical mechanisms that determine the transport into the fracture and the neighbouring matrix tracer tests with nitrate and various hydrogeological tracers such as lithium, eosin and uranin were carried out using two fractured Danish chalk blocks.

6.1 Contaminants and tracers used in the experiments

As reference for agricultural contaminants nitrate was chosen. Its transport behaviour was compared with several hydrological tracers used in groundwater tracing experiments, such as chloride, lithium, uranin, eosin and pyranin.

Nitrate was used as reactive tracer in a shaly aquifer (Pauwels et al. 1997), in agricultural soil (Stagnitti et al. 2000) and also in agricultural soil within the unsaturated zone of British chalk (Foster and Bath 1983). Nitrate also has been used as a non-reactive tracer to investigate solute transport in undisturbed soil columns (Jardine et al. 1988).

Uranin, eosin, chloride and lithium are often chosen as non-reactive or quasi-ideal tracers to study the water movement (Bäumle et al. 2000; Höhn et al. 1994; Käss 1998; Fetter 1994). But, uranin, eosin and lithium showed significant retardation due to the sorption process in a porous aquifer (Reichert 1991; Reichert and Hötzl 1992). Comparable retardations for uranin and eosin are reported for tracing experiments in fractured aquifers (Maloszewski et al. 1991).

In order to investigate the diffusive and sorptive characteristics of both the hydrological tracers selected and nitrate a variety of techniques and analytical methods were applied, including Atomic Absorption Spectrometry (AAS), Ion Chromatography (IC) and Spectrofluorophotometery. The detection limits for the contaminants and tracers are given in Tab. 6-1.

Tab. 6-1: **Detection limits of the used contaminants and tracers.**

Tracer/contaminant	Detection limit	Tracer/contaminant	Detection limit
Nitrate	0.500 mg/L	Eosin	0.020 μg/L
Chloride	0.200 mg/L	Uranin	0.049 μg/L
Lithium	0.020 mg/L	Pyranin	0.080 μg/L

The concentrations of nitrate NO_3 and chloride Cl were determined using a SHIMADZU HIC-6A Ion Chromatography (IC). This system includes the separator column Shim-pack IC-A1 and a conductometer as a detector (CDD6A). The IC system is defined as an automatic chemical-physical separation and detection of anions. The method is based on a combination of an anion-exchange columns and a suppressor unit which allows the conductometric determination of separated species (Gjerde and Fritz 1987). Lithium samples were analyzed using AAS with a detection limit of approximately 0.02 mg/L.

Identification and quantification of the fluorescent dyes were carried out with the Spectrofluorophotometer SHIMADZU RF-5301PC. In order to receive the highest fluorescence signal the water samples were buffered to the appropriate ph-value. For uranin (see below) a pH of 11.5 was used. This value was adjusted by adding a few drops of EDTA-tetra sodium salt. Pyranin shows the highest intensity in environment. Hence eosin is less influence by the pH-value no buffering is necessary.

6.1.1 Nitrate

Nitrate is the most common form of inorganic nitrogen and usually enters the groundwater from various point and non-point sources such as sewage, industry, animal waste and fertilizers. The main anthropogenic sources for nitrate are the extensive application of mineral and organic fertilizers. In strongly oxidizing groundwater nitrate is the stable form of nitrogen and it moves with no transformation and a little or no retardation (Freeze and Cherry 1979).

Nitrate can be used as a reactive tracer in many cases, for example where uranin will probably fail due to acidic conditions (Pauwels et al. 1997; Canter 1997; Joung 1983; Foster and Bath 1983). On the other side Job and Zötl (1969) reported a tracing experiment with an injection of 20 kg of sodium nitrate where nitrate was detected after a flow path of 320 m. Certainly, nitrate may have high background concentrations in groundwater, especially in agricultural areas. But nitrate may also be subjected to reduction in the presence of any reducing agent such as organic matter, ferrous iron or pyrite. Nitrate does not form insoluble minerals that precipitate nor is it adsorbed significantly under aquifer conditions. The upper limit of nitrate for safe drinking water for human consumption is 50 mg/L (WHO 1998b).

6.1.2 Chloride

Tracing with salts (mainly inorganic compounds) which dissociate in aqueous solutions into cations and anions can give good results in groundwater contamination studies. Chloride as a conservative tracer does not react with the soil and/or native groundwater, does not participate in redox reactions, is not adsorbed onto mineral or organic surfaces, and does not undergo biological or radioactive decay (Fetter 1994). Chloride is added to the subsurface via industrial discharges, sewage, animal wastes and road salt-

ing. The fertilizer industry produces potassium chloride (Potash-fertilizer) in different grades up to 95 % KCl. Sodium chloride NaCl was often used as a conservative salt tracer, which is very easily dissolved in water (358.5 g/L at 20°C) and dissociates as Na and Cl ions. Potassium chloride has many advantages comparable to NaCl, due to the lower background levels of potassium in groundwater, but potassium has a greater tendency to ion exchange (Käss 1998).

6.1.3 Lithium

The lithium cation has a small ionic radius. Therefore it is a cation with the least tendency to ion exchange. In spite of its low tendency to ionic exchange, some adsorption losses during the underground passage have to be expected (Käss 1998). Lithium chloride is widely used as a tracer due to its cheap price, and its good solubility in water, e.g. 832 g/L at 20°C and even 984 g/L at 60°C (Ullmann 1988). The toxic effects of lithium upon warm-blooded animals are very small (Käss 1998).

6.1.4 Fluorescent dyes

An overview on the physical and chemical characteristics of the widely used hydrological dye tracers uranin, eosin and pyranin is given in Tab. 6-2.

Tab. 6-2: Overview on the dye tracers uranin, eosin and pyranin, commonly used in groundwater tracer tests (after Reichert 1991).

Name	**Uranin**	**Eosin**	**Pyranin**
Chemical Composition	$C_{20}H_{10}O_5Na_2$	$C_{20}H_6Br_4O_5Na_2$	$C_{16}H_7O_{10}S_3Na_3$
Color index[1)]	45 350	45 380	54 040
Molecular weight [g/mol]	376.28	691.88	524.39
Peak $\lambda_{Ex}/\lambda_{EM}$ [nm]	492 / 513	515 / 535	460 / 512 [2)] 407 / 512 [3)]
Detection limit [ppb] [4)]	0.002	0,01	0,008
Water solubility [g/L]	600	300	178
Sorption tendency	very low except acid environment	low	low
Photochemical instability	high	very high	high
occurrence of microbial decay	rare under special conditions	rare under special conditions	none

1) Color-Index of the Society of Dyers and Colorists (1975), Bradford/UK
2) pH ≥ 10
3) pH ≤ 4.5
4) tracer detection in clean water using spectrofluorimetric instrumentation

Uranin

Uranin is the most intensive fluorescing substance and it is the first choice for groundwater tracing due to its low detection limit (Tab. 6-2). The maximal fluorescence is reached at pH > 8.50. At neutral solution (pH = 7.00) the fluorescence intensity is only 80 %. Under acidic conditions (pH < 7.00) uranin changes into the cation which is sorptive and lipophilic (Käss 1992*)*. Uranin usually is used in tracer experiments as a conservative or reference dye tracer because it has a low sorption rates (Tab. 6-2) (Behrens and Teichmann 1988). Mikulla et al. (1997) carried out batch and column tests using uranin in undisturbed soil with high content of organic carbon (31.2 %). The result showed a clear retardation for uranin (K_d 10.2) due to sorption process.

Pyranin

Pyranin is a fluorescence tracer with a low sorption tendency. Pyranin is well-suited for tracing in acidic underground where uranin is not. Pyranin measurement depends on the pH value of the solution (Tab. 6-2). To adjust the pH value for the samples at 4.5 a few drops from buffer were added (acetic acid 5.5 molar ≅ 31.5 mL with sodium acetate 4.5 molar ≅ 36.9 g).

Eosin

Eosin is non toxic therefore it is often used in cosmetic products. Compared to uranin, eosin has a slightly more sorptive tendency and its fluorescence is not pH dependent (Käss 1998). Compared with uranin and pyranin it has a high polarity, therefore it has a higher affinity to sorption on solid surfaces (Reichert 1991). To avoid photo decay of the fluorescence tracers brown bottles have been used for sampling.

6.2 Batch experiments

6.2.1 Experimental method

The sorption behaviour of nitrate, lithium, uranin, eosin and pyranin (sorbate) in Danish chalk (sorbent) were studied by means of batch tests. The chalk samples were pulverized to a particle size of < 0.2 mm. This size was selected in order to prevent a diffusion limited sorption and to reach equilibrium by making the external surface area to be much larger than the internal surface area (Xu and Wörman 1999). Following O'Connor and Conolly (1980), who reported that the distribution coefficients decrease with increasing solute concentration in batch tests, a powder : solution ratio of 1 : 4 (2.5 g chalk powder to 10 mL tracer solution) was chosen. This ratio yielded reproducible distribution coefficients. The initial concentrations vary between 0.01 and 10 mg/L for the organic dye tracers (eosin, uranin and pyranin), between 1 and 50 mg/L for lithium, and between 1 and 250 mg/L for nitrate (compare Tab. 7-2). Each sorption isotherm involved four to eight interim points. The suspensions (chalk powder and tracer solution) were filled in vials and shaken at a constant room temperature (20 ± 2°C) for about 72

hours. Uranin, eosin and pyranin were stirred in darkness to avoid a photochemical decay of the tracers. After the shaking process the suspensions were separated into their dissolved and particulate components by centrifugation (3000 cycle/min) for 45 min. For measuring reasons, the samples were filtered with a 0.2 μm membrane filter before analysis.

The amount adsorbed by the chalk powder C_s can be calculated as the difference in mass of the solute in solution before the test C_o and in solution at equilibrium C_L. The graphical plot of adsorbed concentration C_s as a function of dissolved concentration C_L gives the adsorption isotherm.

$$C_s = \frac{(C_o - C_L)V_b}{m_t} \qquad \textbf{(6-1)}$$

V_b volume of solute solution (10 mL) [L^3]
m_t weight of dry chalk powder (2.5 g) [M]

6.3 Through-diffusion experiments

6.3.1 Sample preparation

Laboratory diffusion experiments were conducted using flat, 10 mm thick chalk discs. The discs were carefully cleaned with deionized water and inspected for heterogeneities and cracks. The chalk discs were placed in a desiccator and maintained in a vacuum for a week followed by submerging the discs in degassed and deionized water for at least two weeks. In the case of ionic tracers, isotonic solutions are used for discs saturation and also for the receiving cell to ovoid the osmotically driven fluxes (Bradbury and Green 1985).

6.3.2 Experimental set up

The experimental set up is in principle the same that has been used previously by Feenstra et al. (1984). The chalk discs were mounted into the diffusion cell devices (Fig. 6-1 and 6-2) made of Plexiglas, steel or PVC. The mounted chalk disc was sandwiched between the reservoir and the receiving cell with an O-ring providing a watertight seal. Screws held both cells together. The diffusive flux from the reservoir cell (A) filled with the contaminant or the tracer solution, into the receiving cell (B), filled to the same level with degassed and deionized water or isotonic salt solution, is observed. The diffusion of contaminants or tracers through the chalk sample resulted in an increase in their concentrations in reservoir cell (B). Fig. 6-3 shows a conceptual model for the laboratory diffusion tests. The diffusion experiments were carried out at room temperature (20 ± 1^oC).

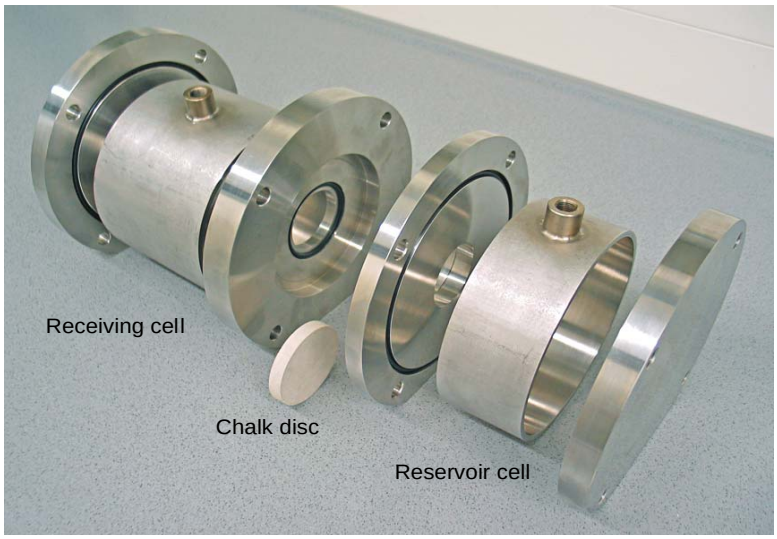

Fig. 6-1: Diffusion cell components (cell components and chalk sample).

Fig. 6-2: Stainless steel diffusion cell (build up cell).

In general daily samples of 10 mL (±0.02 mL) were taken from reservoir cell (B) during the duration of an experiment. Nitrate, chloride and lithium samples were stored in 30 mL PVC bottles in the refrigerator (5°C) to prevent any chemical reaction or microbial degradation before the analyses. The samples for the fluorescent tracers (uranin, eosin and pyranin) were stored in brown glass bottles in a dark place to avoid photochemical decay. Each time a sample was taken from the measuring cell, 10 mL of deionized water or isotonic salt solution was added to the receiving cell B to keep the head in the cell constant, thus preventing advective transport through the chalk disc.

To eliminate the effect of dilution of the concentration in the receiving cell, the corrected concentration was calculated as follows:

$$C_{corr}(t) = \frac{\sum_{n=1}^{t-1} C_n \cdot V_{nOut}}{V + \sum_{n=1}^{t-1} (V_{nOut} - V_{nIn})} \quad \textbf{(6-2)}$$

$C_{corr}(t)$ corrected concentration in the receiving cell (B) after time t [ML^{-3}]
C_n measured concentration in the receiving cell (B) after time t [ML^{-3}]
V_{nOut} volume of the daily taken sample [L^3]
V_{nIn} volume of the daily given sample (deionized water or isotonic solution) [L^3]

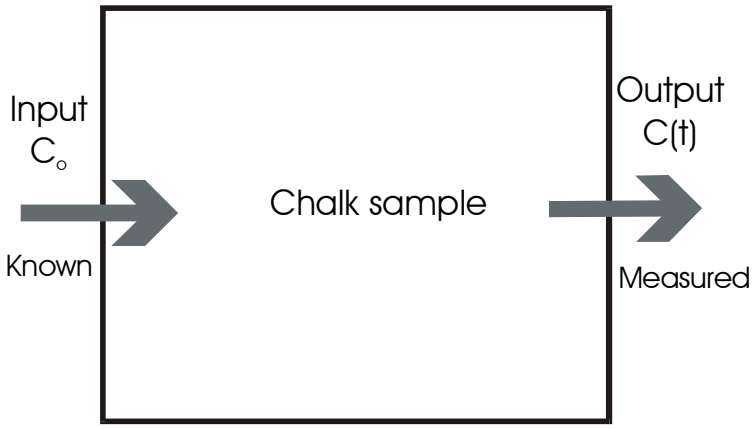

Fig. 6-3: Conceptual model for the laboratory diffusion test.

6.3.3 Mathematical description

An analytical solution of Fick's 2nd Law (Eq. 3-17) for a porous slab ($C_{(0 \le x \le d)} = 0$; t = 0) is used to describe the observed change in concentration in the receiving cell B (Carslaw and Jaeger 1959):

$$C(t) = \frac{AdC_0}{V}\left(\frac{D_e t}{d^2} - \frac{\alpha}{6} - \frac{2\alpha}{\pi^2}\sum_{n=1}^{\infty}\frac{(-1)^n}{n^2}\exp\left[-\frac{D_e n^2 \pi^2 t}{\alpha d^2}\right]\right) \quad \textbf{(6-3)}$$

C(t) measured concentration in the receiving cell B after time t [ML^{-3}]
C_0 initial concentration in the reservoir cell at t = 0 [ML^{-3}]
α rock capacity factor [-]
V volume of solution in the receiving cell B [L^3]
A cross-sectional area of the chalk disc (diffusive area) [L^2]
d thickness of the chalk disc (≈1cm) [L]
t time [T]

The two fit parameters of Eq. 6-3, the effective diffusion coefficient D_e and rock capacity factor α were initialized with values determined from the linear part (steady-state-diffusion region) of the experimental concentration-time curve (Fig. 7-3).

At large time ($t \rightarrow \infty$) the exponential term is negligible and a linear relationship is obtained between concentration and time. The asymptotic solution for the region of steady-state diffusion of the experimental curve (Lever et al. 1985) is:

$$C(t) = \frac{AdC_o}{V}\left(D_e \frac{t}{d^2} - \frac{\alpha}{6}\right) = \underbrace{\frac{AC_oD_e}{Vd}}_{a} \cdot t - \underbrace{\frac{\alpha AdC_o}{6V}}_{b} = a \cdot t + b \qquad \textbf{(6-4)}$$

The effective diffusion coefficient and rock capacity factor can be calculated according to Eq. (6-4) from the slope a and the intercept with the ordinate b respectively of the linear part of the concentration-time curve as follows:

$$D_e = \frac{aVd}{AC_o} \qquad \textbf{(6-5)}$$

$$\alpha = -\frac{bV6}{AdC_o} \qquad \textbf{(6-6)}$$

a slope of the linear part of the concentration-time curve [$ML^{-3}T$]

b intersection of the linear part with the ordinate (negative value) [ML^{-3}]

Hill (1984) demonstrated that the diffusion coefficient of the anions (nitrate, chloride and sulfate) and water were unaffected by orientation of the chalk sample (vertical or horizontal).

6.4 Tracer experiments

6.4.1 Principle of groundwater tracing

Tracing techniques in groundwater are recognized as a common tool to evaluate the subsurface flow directions, velocity, mass transport mechanisms or sources of contamination and aquifer characteristics. It involves the introduction of non-toxic tracers into the subsurface via injection points and receiving the tracer via sampling points. The appropriate tracer substances for groundwater tracing should be low in purchase cost, ease of use (injection, sampling and analysis), exhibit a relatively conservative behaviour with good detection limits in the groundwater and no or very low toxicity. Several groundwater flow velocities can be determined from a tracer breakthrough curve (BTC). The maximum flow velocity V_{max} is defined by the flow distance and the time of the first arrival of the tracer T_{max} and the dominant effective flow velocity is determined from the time of tracer maximum concentration T_{max}. The BTC's are normally used to estimate the effective porosity and the longitudinal dispersivity. The effective porosity n_e is the ratio of the volume of mobile water $V_{mobile\ water}$ to the volume of the rock V_{Rock}:

$$n_e = \frac{V_{mobilewater}}{V_{rock}} \qquad \textbf{(6-7)}$$

Where the volume of mobile water is defined by the product of the mean transit time t_0 and the discharge Q:

$$V_{mobilewater} = t_0 \cdot Q \quad \textbf{(6-8)}$$

The longitudinal dispersivity α_l of solute is the mixing process associated with the variations of the flow velocities within the fracture. From Eq. (3-43) the longitudinal dispersivity is:

$$\alpha_l = \frac{x}{Pe} \quad \textbf{(6-9)}$$

6.4.2 Preparation of the chalk blocks

The laboratory tracer tests were conducted in two artificially fractured chalk blocks A and B to provide information about the possible transport mechanisms of solutes in a single fracture. The two chalk blocks were isolated on new terrace in the Sigerslev quarry, Denmark (December 2001) and fitted into a metal boxes for transport. In the laboratory the blocks were dismantled and cut into approximately rectangular shapes. This procedure ensured a relatively fresh and undisturbed chalk matrix block. The dimensions of blocks are for A is 17 x 15 x 14 cm³ and for B 32 x 29 x 23 cm³. The matrix porosities are experimentally measured using mercury injection as 45 % for A and 48 % for B (Dr. J. Bloomfield, British Geological Survey). The bulk densities of the two blocks vary between 1.4771 g/mL for block A and 1.4748 g/mL for block B. An artificial fracture with rough surfaces was created in the middle of each block by sawing a small slit around the block surfaces and fracturing it with a wedge and hammer. The two pieces of the each block were put together, resembling its natural set-up, and sealed from its sides with resin (Biresin S10). Small tubes were placed into the fracture to inject and extract water and tracer (Fig. 6-7). The blocks were saturated by injecting degassed artificial groundwater, similar to the natural groundwater of the test site (Tab. 6-3) into the fracture and applying a vacuum via the tubes on the sides of the blocks. To ensure a homogeneous sub pressure in the matrix, 6 mm deep slits were cut into the sides of the blocks and covered on the top prior its sealing, thus building a kind of drainage system linked to the tubes (Fig. 6-4). The saturation process was gravimetrically controlled and reached stationary conditions asymptotically after about eight weeks. Taking into account the matrix porosity, the volumes of the block and the injected water, an almost complete saturation (94 and 96 vol.-%) of the chalk matrix block A, and B respectively was achieved.

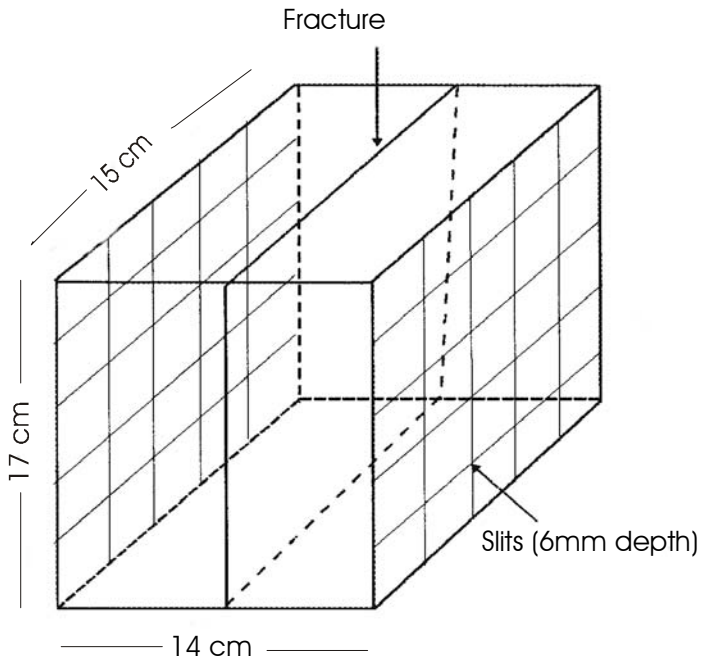

Fig. 6-4: Sketch of the block with slits on both sides, block A.

From the saturation curve of the fractured chalk block B (Fig. 6-5) abrupt change in the saturation behaviour was observed in the first two days after that the saturation process was going smoothly until the complete saturation was achieved.

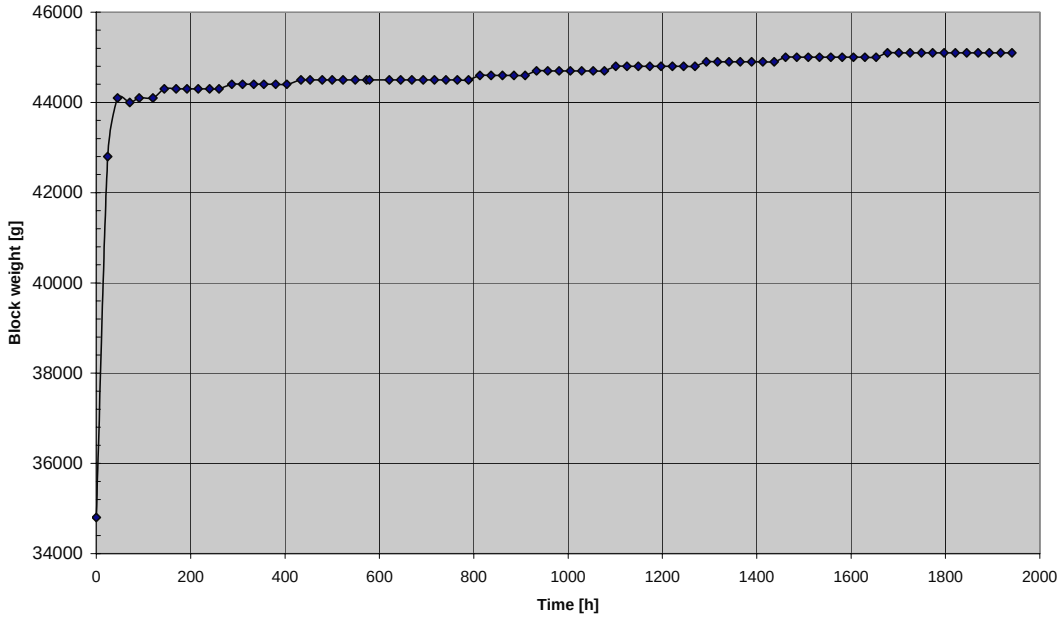

Fig. 6-5: Saturation curve, block B.

After the saturation process of both blocks several Darcy experiments were performed to determine the main hydraulic properties of the fracture (Fig. 6.6) using the cubic law (Chapter 3 Eq. 3-7).

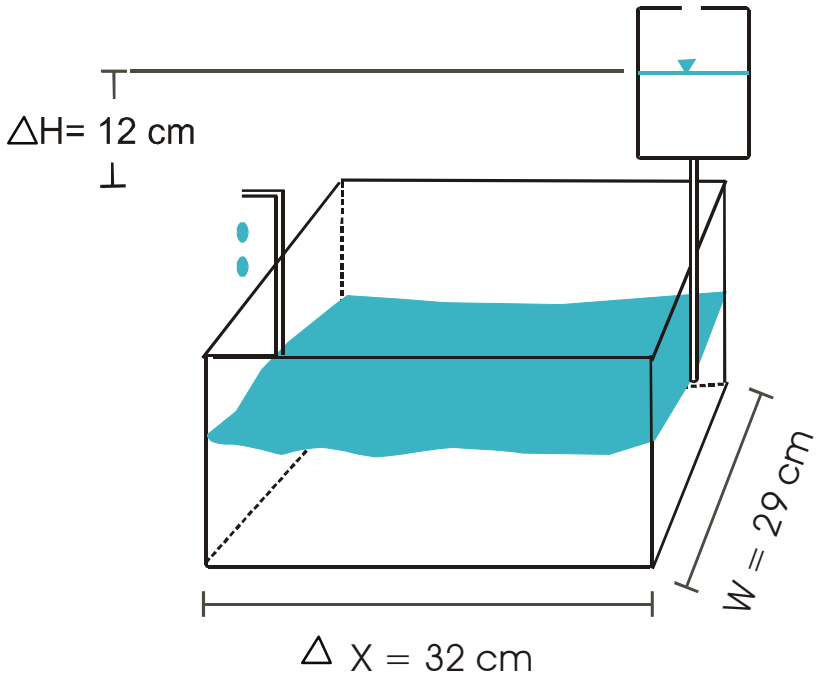

Fig. 6-6: Set up of the Darcy experiments, block B.

Tab. 6-3 : Chemical composition of natural (personal communication Dr. E. Nygaard 2002) and artificial groundwater.

Chemical parameter	Natural groundwater	Artificial groundwater
Na^+ [mg/L]	725	725
Ca^{2+} [mg/L]	158	155
Mg^{2+} [mg/L]	104	100
K^+ [mg/L]	34	34
SO_4^{2-} [mg/L]	205	192
Cl^- [mg/L]	1385	1386
HCO_3^- [mg/L]	317	317
NO_3^- [mg/L]	22	-
F^- [mg/L]	1.2	-
NH_4^+ [mg/L]	0.05	-
NO_2^- [mg/L]	0.03	-
H_2S [mg/L]	0.05	-
PH [-]	7.25	7.69
EC [S/cm]	610	499

6.4.3 Experimental set up

A four-channel peristaltic pump (Ismatec IP 30) was used to maintain a constant flow field from the bottom to the top of the vertical fracture during experiment. The tracer so-

lutions were always injected as a short pulse with a plastic syringe into the bottom of the fracture (Fig. 6-7) under a steady-state flow field.

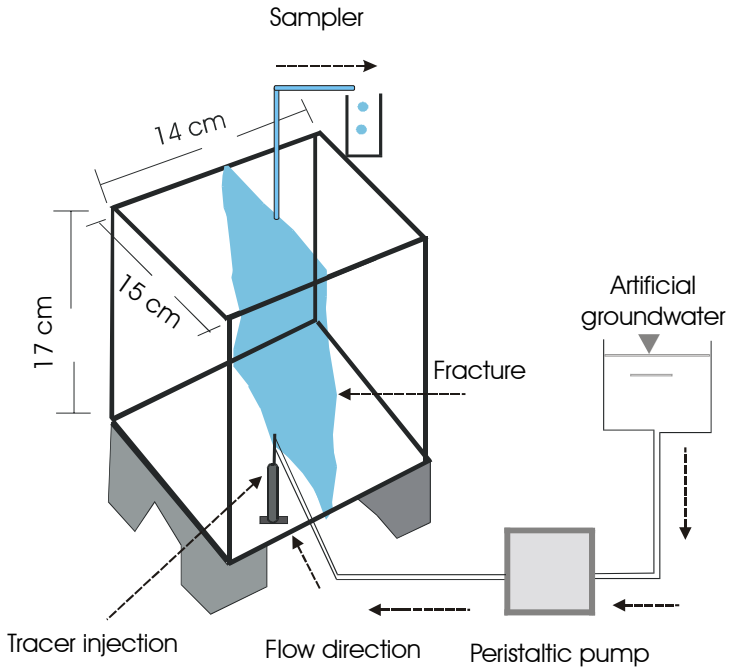

Fig. 6-7: Set up of the single fracture tracer test performed in a fractured chalk block A.

Five single- and two multi-tracer tests were performed in the fractured chalk block A, and two single- and one multi-tracer tests were performed in the fractured chalk block B, After each tracer test, the block has been flushed with deionised water for three weeks. An overview including the used tracers, flow distances (X), injected masses (M) and flow rates (Q) of the single- and multi-tracer tests are given in Tab. 6-4.

Tab. 6-4: Summary of single- and multi-tracer tests performed into the fractured chalk blocks A and B.

Test No.	Tracer	x [m]	M [mg]	Q [L/s]	Fig. No.
1	Nitrate	0.17	29	1.58 E-5	7-6 to 7-8
2	Nitrate	0.17	58	1.00 E-5	7-9
3	Nitrate	0.17	45	9.00 E-6	7-10
4	Nitrate	0.17	60	8.17 E-6	7-11
5	Uranin	0.17	2.20 E-2	9.00 E-6	7-13
6	Uranin	0.32	1.00 E-2	1.00 E-5	7-14 to 7-16
7	Uranin	0.32	1.27 E-2	1.08 E-5	7-17
8	[1]Nitrate/eosin	0.17	34/1.0 E-2	8.7E-6	7-18 & 7-19
9	[2]Nitrate/uranin/ lithium	0.17	31.5/1.7E-2/ 0.3	9 E-6	7-20 to 7-22
10	[3]Uranin/lithium	0.32	2.2E-2/0.19	1.67 E-5	7-23 & 7-24

[1,2,3] multi-tracer tests.

7 RESULTS

In this chapter the results of the various laboratory experiments described in the previous chapter will be presented and thoroughly discussed. Emphasis will be put on the observations of contaminant transport into the fracture and the neighbouring chalk-matrix as a function of the fracture and the matrix characteristics.

Contaminant transport parameters were experimentally determined in the Danish chalk using nitrate as a classical agricultural contaminant and chloride, lithium, pyranin, eosin and uranin as hydrological tracers. The parameters obtained and the respective methods in this work used to obtain them are summarized in Tab. 7-1.

Tab. 7-1: Laboratory measured transport parameters.

Parameter	Abbreviation	Unit	Method of measurement
effective diffusion coefficient	D_e	[m^2/s]	diffusion & tracer test
rock capacity factor	α	[-]	diffusion test
relative diffusivity	D'	[m^2/s]	diffusion test
distribution coefficient between solid and liquid phase	K_d	[-]	batch & diffusion test
retardation factor of the fracture surface	R_f	[-]	batch & multi-tracer test
retardation factor of the rock matrix	R_p	[-]	batch & multi-tracer test
flow velocity within the fracture	v	[m/s]	tracer test
longitudinal dynamic dispersivity	α_l	[m]	tracer test
transversal dispersivity	D_{hij}	[m^2/s]	tracer test
fracture aperture	2b	[µm]	Darcy & tracer test
flow rate within the fracture	Q	[l/s]	Darcy test
fracture hydraulic conductivity	K_{fr}	[m/s]	Darcy test
fracture permeability	k_{fr}	[m/s]	Darcy test
matrix porosity	ε	[-]	mercury porosimetry

7.1 Batch experiments

As described earlier the equilibrium sorption capacities of the substances under investigation were determined using ratios of 2.5 g chalk powder to 10 mL tracer solution after an equilibration time of 72 hours. After the centrifugation and the filtration by 0.2 µm cellulose membrane filter the samples were directly analyzed. Each experiment was repeated three times. The initial concentrations used in the batch experiments are given in Tab. 7-2.

Tab. 7-2: Contaminants and tracers concentrations used in the batch experiments.

Contaminant / tracer	Initial concentrations (mg/L)							
Nitrate	1	10	25	50	100	150	200	250
Eosin	0.01	0.1	0.5	1	5	7	10	-
Uranin	-	-	0.1	1	5	7	10	-
Pyranin	-	-	-	1	5	7	10	-
Lithium	-	-	1	5	7	10	25	50

In all batch experiments linear sorption isotherms were observed and therefore described with Henry isotherms (Fig. 7-1 and 7-2). An overview of the determined distribution coefficients (K_d) together with the respective correlation coefficients (R^2) is given in Table 7-3. As expected from the high purity and low contents of clay minerals, organic carbon and iron oxides of the Danish chalk (compare Tab. 5-2), all substances tested show low sorption capacities with K_d values between 0.0019 and 0.003 L/g. The correlation coefficients R^2, given in Tab. 7-3, proof the excellent fit of the experimental isotherms with the Henry model.

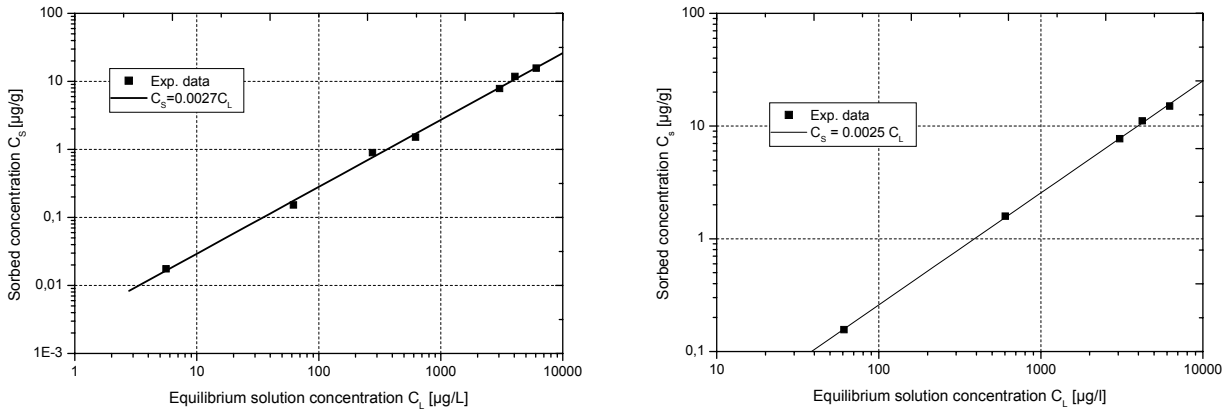

Fig. 7-1: Sorption isotherms for eosin (left side) and uranin (right side) both fitted with the Henry model (symbols are the measured values; the solid lines represent the least squares fit).

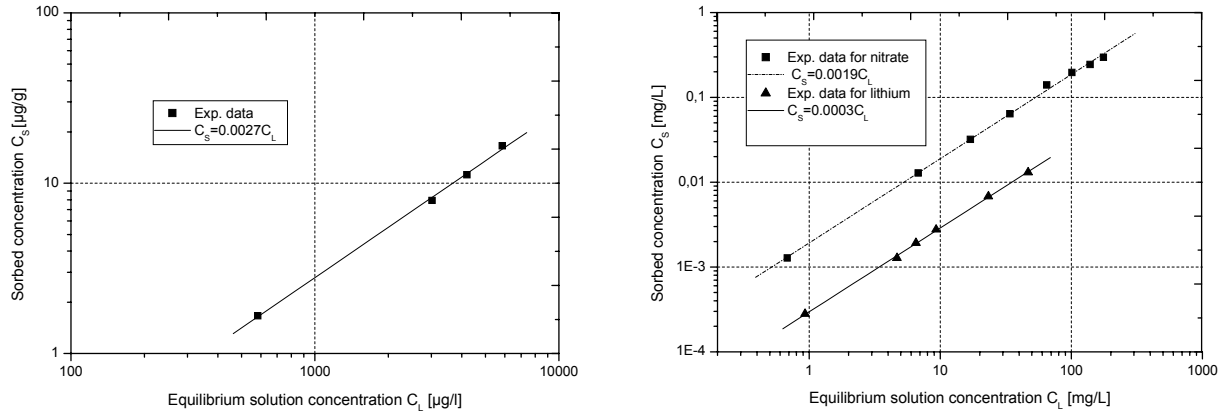

Fig. 7-2: Sorption isotherms for pyranin (left side) and nitrate together with lithium (right side) fitted with Henry model (symbols are the measured values; the solid and dashed lines represent the least squares fit).

Tab. 7-3: Distribution coefficient K_d and correlation coefficient R^2 for nitrate, lithium, uranin, pyranin and eosin in Danish chalk.

	Henry-Modell	
Tracer	K_d [L/g]	Correlation Coefficient R^2
Nitrate	0.0019	0.99926
Eosin	0.0027	0.99902
Uranin	0.0025	0.99985
Pyranin	0.0027	0.99928
Lithium	0.0030	0.99969

In respect to the hydrological tracer uranin, eosin, pyranin and lithium the results of this work agree well with the previous work performed in Bonn in chalk (Witthüser 2001; 2003; Bansmer 2000). For the determined low sorption capacities for nitrate good agreement with reported values is given, too. Stagnitti et al. (2000) showed that adsorption and reaction of nitrate with soil particles are possible. But, their determined values for the retardation factor and reaction rate with 1.06 and 0.035/day respectively, indicate a comparable low retardation combined with a significant reaction rate. Other studies (e.g. Canter 1997; Foster and Bath 1983) showed that nitrate also is susceptible to reduction, fixation and mineralization in various chemical forms. In general nitrate is expected a highly mobile and not effected by ion exchange mechanism or sorption on soil and/or aquifer particles during its transport through aquifers (Hem 1985; Jardine et al. 1988; Fetter 1994; Macko and Ostrom 1994; Mueller et al. 1995; Stumm and Morgan 1996; Cast 1985).

7.2 Diffusion experiments

The effective diffusion coefficients as determined in the laboratory experiments are products of the free diffusion coefficients of the different solutes in water and the tortuosity factor as well as the porosity of the chalk discs. The effective diffusion coefficients

are generally one or more orders of magnitude smaller than the respective molecular diffusion coefficients in water. The tests were conducted on chalk discs of approx. 1cm thickness to determine the effective diffusion coefficients D_e and rock capacity factors α according to Eq. (6-4). The graphs of the diffusion experiments (compare Fig. 7-3) appear similar in shape, but differ in slope. The pre-steady state region is characterized by a slow increase in the tracer concentration. The steady state is achieved when the diffusive transport of the tracers becomes constant and the concentration in the receiving cell increases linearly with time. The effective diffusion coefficients D_e and rock capacity factors α were determined from the slope of the linear part of the breakthrough curve and then estimated with the least square method (Bradbury and Green 1985).

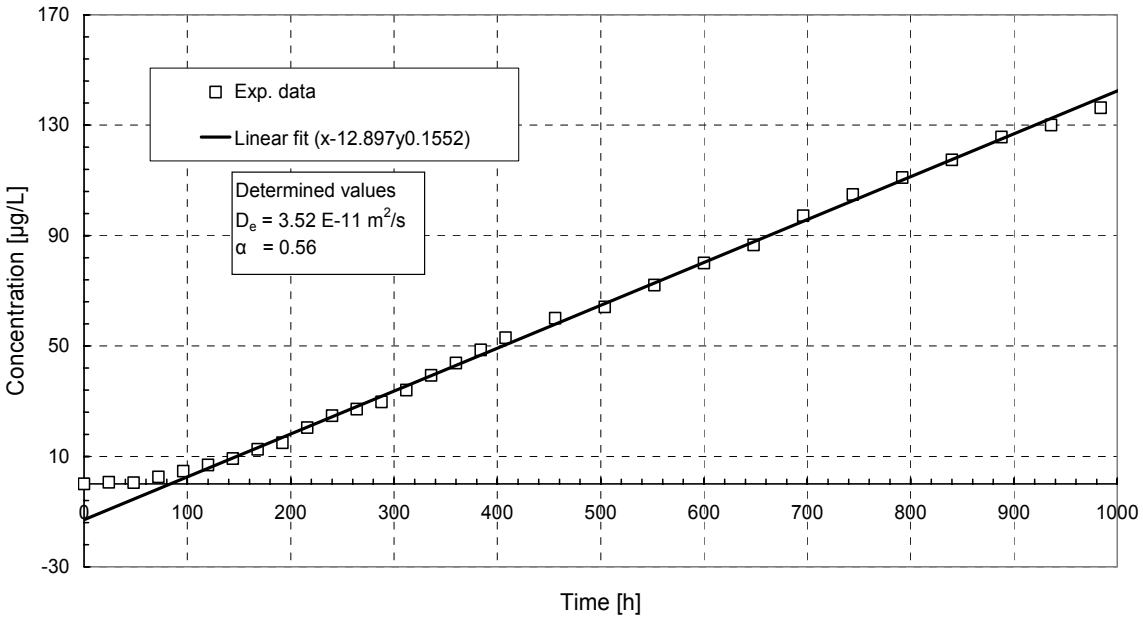

Fig. 7-3: Example of a breakthrough curve of uranin in diffusion cell experiments.

7.2.1 Molecular diffusion coefficient

Molecular diffusion coefficients D_m in free water range for most of the major ions from 1 E-9 to 2 E-9 m^2/s at 25 ^oC (Robinson and Stokes 1959). The literature values of D_m for the used contaminants and tracers are given in Tab. 7-4.

Tab. 7-4: Molecular diffusion coefficients of the investigated contaminants and tracers in free water at 25 ^oC.

Contaminant / tracer	D_m [m^2/s]	Reference
Nitrate	1.92 E-9	Parsons (1959)
Chloride	2.03 E-9	Parsons (1959)
Lithium	1.03 E-9	Li and Gregory (1974)
Uranin	4.51 E-10	Witthüser (2001)
Pyranin	4.11 E-10	Witthüser (2001)
Eosin	3.87 E-10	Witthüser (2001)

7.2.2 Estimation of effective diffusion coefficient

The estimated effective diffusion coefficient of any solute depends on the diffusive properties of the rock samples (relative diffusivities) as well as on the molecular diffusivities of the solute itself. The determined effective diffusion coefficients D_e together with the rock capacity factors α of the used contaminants and tracers are given in Tab. 7-5. Effective diffusion coefficients and rock capacity factors were determined from the concentrations versus time plot by a linear correlation of the experimental data (Fig. 7-3). The experimental determined effective diffusion coefficients of nitrate and various artificial tracers such as chloride, lithium, uranin, pyranin and eosin ranged between 2.75 E-11 m^2/s to 5.46 E-10 m^2/s.

It is obvious, that the effective diffusion coefficients for nitrate, chloride and lithium are nearly similar and higher than those for uranin, pyranin and eosin. The results from multi-tracer experiments showed significant decrease of the effective diffusion coefficients of the tracers compared to those obtained from single tracer experiments. These smaller values of the effective diffusion coefficients might be explained by the interactions between the ionic tracers.

In general the calculated values provide a basis to compare the diffusive transport behaviour of the tracers in chalk aquifers in the absence of any hydraulic head. Results of the diffusion experiments (Tab. 7-5) showed that repeated experiments yielded similar values for the effective diffusion coefficients and rock capacity factors. Generally, the obtained values of the effective diffusion coefficients and rock capacity factors are reasonably comparable with literature values for chalk (Hell 1984; Grathwohl 1988; Witthüser 2001; Witthüser et al. 2000, 2003; Bansemer 2000). The observed variations of the effective diffusion coefficients have to be explained by both the variations in molecular diffusion coefficients and in the porosity values for the chalk. The results indicate a sorptive behaviour for nitrate and the other tracers within the chalk matrix ($\alpha > \varepsilon$). Assuming linear sorption isotherms (compare section 7.1), the determined rock capacity factors can be used to calculate the distribution coefficient (Eq. 3-18). Those coefficients were several times higher than those obtained from the performed batch experiments (see Tab. 7-3 and 7-5).

Tab. 7-5: Effective diffusivities D_e, rock capacity factors α, porosities ε and relative diffusivities D' in Danish chalk (single- and multi-tracer experiments).

Tracer	D_e [m^2/s]	α [-]	ε [%]	D' [-]
Nitrate	3.26 E-10	0.68	41.55	0.17
Nitrate	4.16 E-10	0.71	48.00	0.21
Nitrate	4.81 E-10	0.69	40.86	0.25
Nitrate	4.38 E-10	0.50	42.77	0.22
Nitrate	4.81 E-10	0.56	42.20	0.25
Nitrate	5.46 E-10	0.47	48.30	0.28
Chloride	3.93 E-10	0.60	43.68	0.20
Lithium	2.32 E-10	0.56	49.50	0.23
Uranin	9.75 E-11	0.59	47.80	0.22
Uranin	8.02 E-11	0.54	47.60	0.18
Uranin	7.32 E-11	0.58	47.80	0.16
Uranin	6.90 E-11	0.55	33.80	0.15
Pyranin	9.47 E-11	0.49	47.60	0.23
Pyranin	1.08 E-10	0.49	41.00	0.26
Pyranin	1.01 E-10	0.50	41.80	0.24
Pyranin	1.06 E-10	0.55	47.60	0.25
Eosin	1.11 E-10	0.654	47.00	0.33
Eosin	8.99 E-11	0.54	45.83	0.27
[1]Nitrate	2.12 E-10	0.61	43.68	0.11
[1]Uranin	4.40 E-11	0.69	43.68	0.10
[2]Nitrate	1.81 E-10	0.48	43.00	0.09
[2]Eosin	2.90 E-11	0.52	43.00	0.09
[3]Nitrate	2.11 E-10	0.53	43.68	0.11
[3]Eosin	2.75 E-11	0.63	43.68	0.083
[4]Nitrate	1.92 E-10	0.487	41.80	0.10
[4]Uranin	3.51 E-11	0.53	41.8	0.08
[5]Nitrate	1.54 E-10	0.56	40.80	0.08
[5]Chloride	2.58 E-10	0.55	40.80	0.13
[5]Lithium	1.76 E-10	0.52	40.80	0.17
[5]Uranin	3.51 E-11	0.55	40.80	0.08
[6]Nitrate	2.15 E-10	0.53	43.00	0.11
[6]Chloride	2.78 E-10	0.513	43.00	0.14
[6]Lithium	2.55 E-10	0.53	43.00	0.25
[7]Nitrate	2.52 E-10	0.54	43.70	0.13
[7]Chloride	2.18 E-10	0.49	43.70	0.11
[7]Uranin	4.54 E-11	0.56	43.70	0.10

[1,2,3,4,5,6,7] multi-tracer diffusion experiments 1-7.

7.2.3 Relative diffusivity

Effective diffusion coefficients depend on the nature and properties of both solute and rock. The effect of molecular diffusivity of a solute on the estimated effective diffusivity can be removed by dividing the effective diffusivity and the molecular diffusivity of the used substance. The resulting relative diffusivities D' depend only on the diffusion properties of the chalk samples (Grathwohl 1998). Those are mainly controlled by the total porosity and only to a negligible extent by the mean pore-throat sizes or the pore-throat size distributions. Therefore, it's possible to estimate the relative diffusivities as a function of the total porosities of the rock samples. There are several possible correlations between relative diffusivities and rock porosities. Among of these relations, Archie's law (Eq. 3-19) empirically relates porosity ε and relative diffusivity D' by the cementation factor m. From this relation (Fig 7-4) a good correlation between relative diffusivity and measured porosity for Danish chalk can be given. The Danish chalk specific exponent m of (Archie's law) is 2.2. Consequently a reasonable and good prediction of the effective diffusion coefficients or the relative diffusivities in the chalk samples for any contaminant or tracer can be made using Archie's law:

$$D_e = D_m \varepsilon^{2.2} \Rightarrow D' = \varepsilon^{2.2} \quad \textbf{(7-1)}$$

In the multi-tracer diffusion experiments significant decreased relative diffusivities respectively higher cementation factor m of tracers compared to those predicted from Archie's law are observed (Tab. 7-5 and Fig. 7-4). This decrease of relative diffusivities might be due to interactions between the ionic tracers itself. The resulting m-value of Archie's law for the multi-tracer experiments is 2.6.

$$D' = \varepsilon^{2.6} \quad \textbf{(7-2)}$$

Witthüser et al. 2003 have carried out through-diffusion experiments with Danish chalk from the same test site. Their results showed that the values of the neutral deuterium tracer in the multi-tracer experiments obey Archie's law. While the relative diffusivities from the ionic tracers such as lithium, uranin, pyranin, eosin and sodium naphthionate deviate considerably from the expected value from Archie's law. The ionic tracers showed higher relative diffusivities of the anionic tracers and lower values for the cation lithium, than those predicted from Archie's law. These deviations from Archie's law result from the interactions between the ionic tracers where deuterium confirms the applicability of Archie's law.

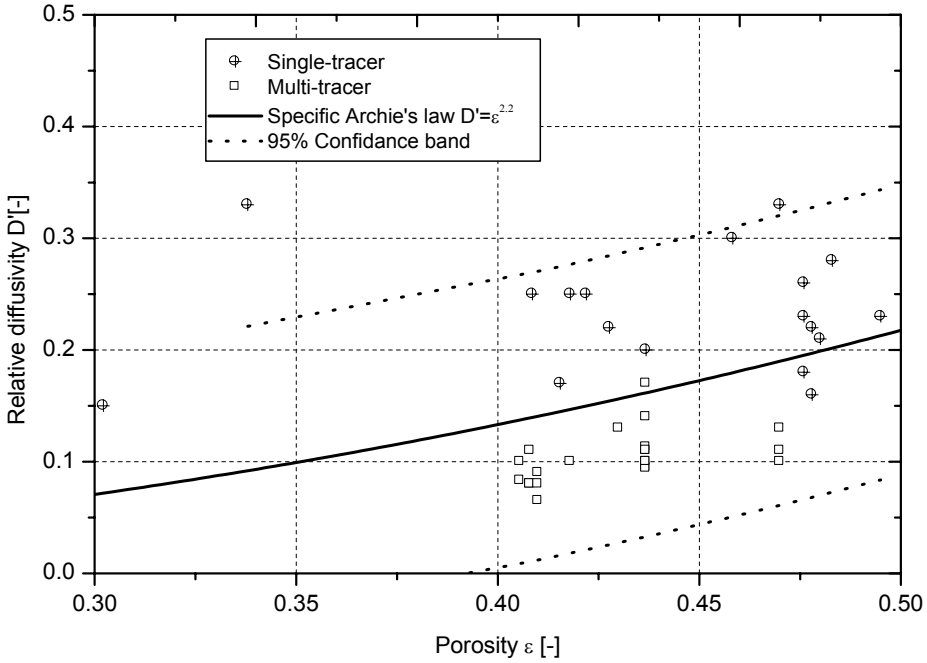

Fig. 7-4: Correlation between porosities and relative diffusivities for Danish chalk and fitted Archie's law.

Using diffusion data reported in the literature (Hill 1984; Grathwohl 1998; Witthüser 2001; Witthüser 2003 P.C.) along with the experimental data reported here, a good correlation between relative diffusivity D' and measured porosity ε for Danish and English chalk can be given with a chalk specific exponent m of 2.2 in the Archie's law for any contaminant or tracer in Danish and English chalk (Fig 7-5):

$$D' = \varepsilon^{2.2} \qquad \textbf{(7-3)}$$

In this way most of the data points are grouped around the regression line thus indicating that the above correlation is justified (Fig 7-4 and 7-5). Most of the samples fall into the 95% confidence band for the prediction of relative diffusivities according to Archie's law (Fig 7-4). Consequently this correlation appears to be a simple way to determine the effective diffusion coefficients for any kind of solute, thus avoiding time-consuming diffusion experiments.

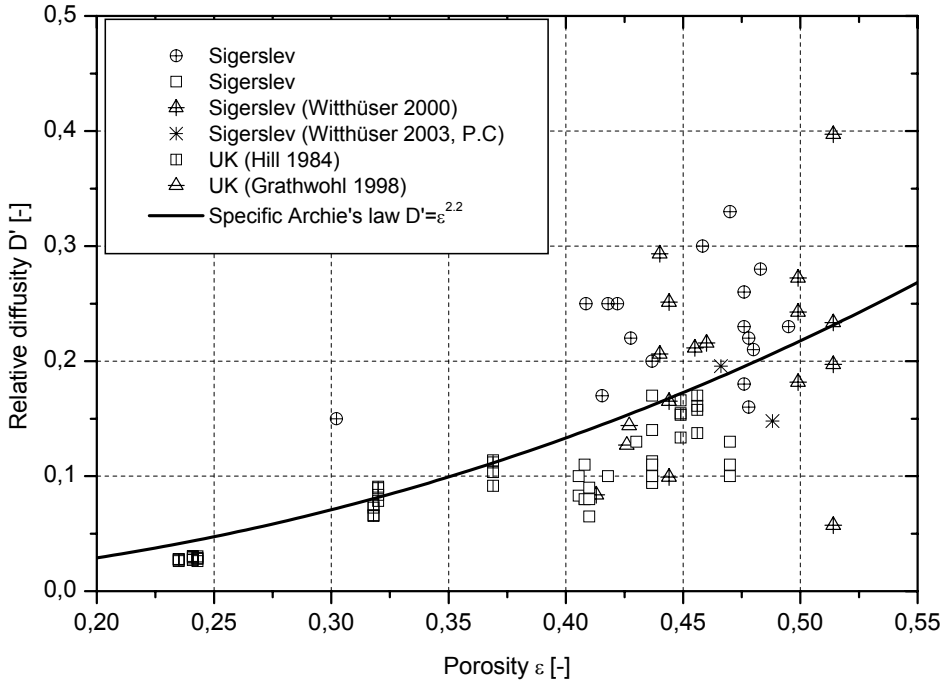

Fig. 7-5: Correlation between porosities and relative diffusivities for Danish and English chalk and fitted Archie's law (own and literature values).

The calculated values of the Archie's exponent m for uncracked English chalk samples are between 2.1 and 2.6 (Hill 1984) and for several sedimentary rock samples are between 1.8 and 2.4 (Grathwohl 1998). In general and comparing to the reported values of Archie's exponent m in the literature (Fig. 7-5) Archie's exponent m for the Maastrichtian cahlk is in the range of the reported values.

7.3 Tracer experiments

Goal of the laboratory tracer tests was to characterise transport processes in a single fracture within a highly porous chalk matrix. The results are very useful to understand the possible transport mechanisms of nitrate and various tracers in fractured chalk aquifers. The tests were conducted under steady-state conditions using pulse injections of tracers into the fractures within two fractured chalk blocks (A and B). All BTC's display fast rises in concentrations to reach early peaks followed by long tailings. The proper way to compare the different BTC's obtained in a single or multi-tracer experiment is to normalize all the observed concentrations by the total mass of tracer injected (C/M) (Maloszewski and Zuber 1990). The recovery rate is calculated in percent of injected mass. The inverse modelling of the experimental data using the Single Fracture Dispersion Model (SFDM) (Maloszewski and Zuber 1985, 1990) allows the determination of several transport parameters such as fracture aperture, dispersivity, and velocity. Hence the SFDM was not able to describe the breakthrough sufficiently, a new model was applied based on the concept of a multi-channel SFDM (Maloszewski et al. 1992) developed for interpreting tracer experiments in karstified aquifers.

7.3.1 Hydraulic properties of the blocks

In order to define the hydraulic characteristics of the artificial fracture several Darcy experiments were performed in both blocks. The main hydraulic properties of the fracture are the volumetric flow rate within the fracture, the fracture hydraulic conductivity, the fracture permeability and the fracture aperture. The results from the Darcy experiments are given in Tab. 7-6.

Tab. 7-6: Fracture hydraulic parameters determined from the Darcy experiments.

Parameter			Block A	Block B
flow rate within the fracture	Q	[m^3/s]	7.0 E-7	9.0 E-7
fracture hydraulic conductivity	K_f	[m/s]	2.8 E-2	3.6 E-2
fracture permeability	k_f	[m/s]	3.2 E-9	4.2 E-9
fracture aperture	2b	[µm]	197	225

The most difficult parameter to quantify and measure in the laboratory is the fracture aperture (e.g. Wang and Narasimhan 1988). The determined aperture values are highly sensitive to the chosen sample size (Witherspoon et al. 1979). With the assumption that the measured hydraulic gradient is correct, rough approximation of the mean fracture aperture can be calculated using the cubic law (Chapter 3 Eq. 3-7). Due to the above limitations as well as the channelling flow and the nature of the solute itself, differences between the obtained values from the hydraulic test and the tracer tests might be occurred. The resulting fracture apertures from the Darcy experiments are 197 µm for block A and 225 µm for block B.

7.3.2 Single-tracer tests with nitrate in the fractured chalk block A

Four single-tracer tests with nitrate were performed in the fractured chalk block A (Fig. 7-6 to 7-11). As expected from the highly porous chalk matrix, the BTC's show distinct tailing effects. The time of the first arrival of nitrate varies between 600 and 1800 seconds, peak concentration times vary between 1200 and 2700 seconds respectively after injection. From the inspection of the BTC's of nitrate (Fig. 7-6 to 7-10), and their deviations from the fitted SFDM, the existence of a second flow path within the fracture was assumed. Interpretation of these deviations can be based on the assumption that the BTC's are characterised by several additional peaks. These types of BTC's can be fairly described by the concept of multi-channel model (Maloszewski et al. 1992). The concept was developed for the modelling of BTC's in karstified aquifers. Because of the high number of unknowns, the determination of all parameters form the BTC with multi-channel SFDM cannot be done automatically (Maloszewski et al. 1992).

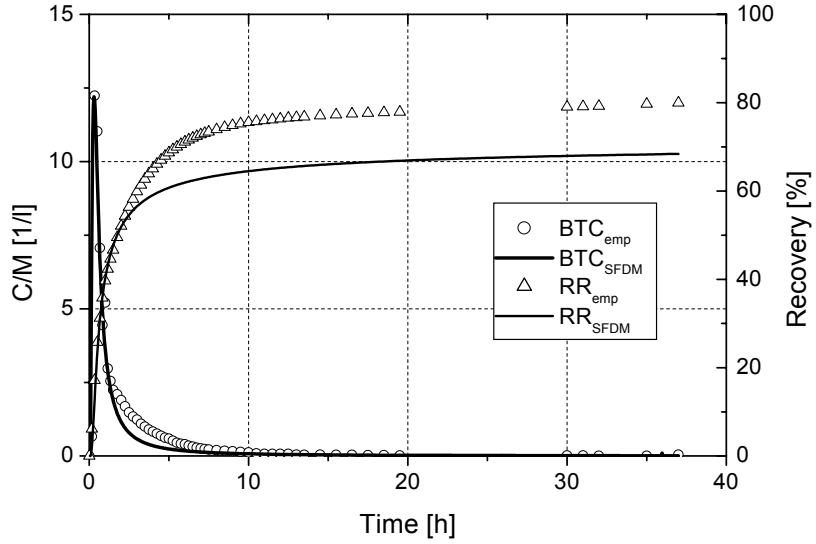

Fig. 7-6: Nitrate test 1, block A: experimental breakthrough and recovery curves and fitted SFDM.

Pre-requisite of the simulation processes with the multi-channel SFDM is the dividing of the experimental BTC's into several partial curves (the so-called residual breakthrough curves Fig. 7-7). This approach starts with looking for a best fit to the concentration measured at the initial part of the curve. This first peak represents the first flow channel. In the next step the theoretical curves (BTC residual) has to subtracted from the whole experimental curve, the next remaining peak has to be fitted, his theoretical BTC has to be subtracted. The whole procedure has to be repeated till the background concentration or zero concentration is reached.

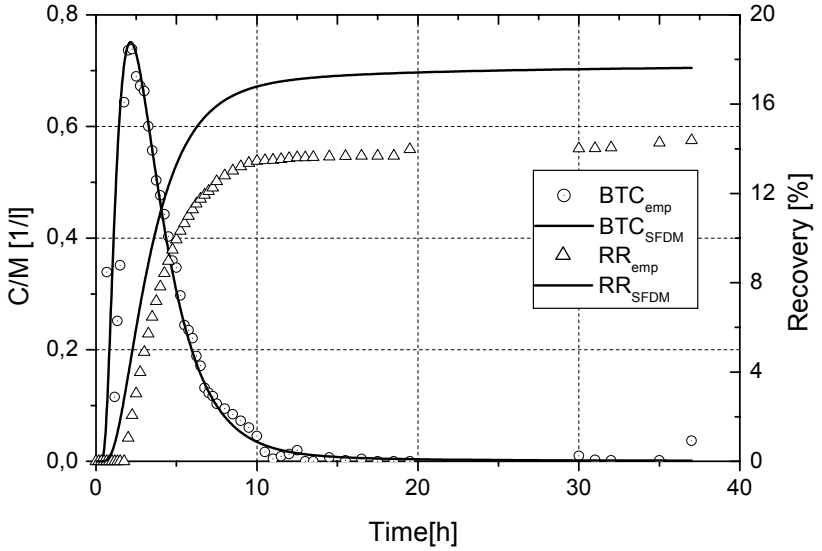

Fig. 7-7: Nitrate test 1, block A: residual breakthrough and recovery curves and fitted SFDM.

The calculation of the residual breakthrough curves is particularly important for calculating the whole theoretical curves (cumulative breakthrough curves Fig. 7-8 to 7-10) for each tracer test. Theoretically, the sum of all partial curves (residual BTC's) is equal to

the total or the whole theoretical curve (cumulative BTC). Finally, the cumulative BTC will be compared with the experimental tracer curve.

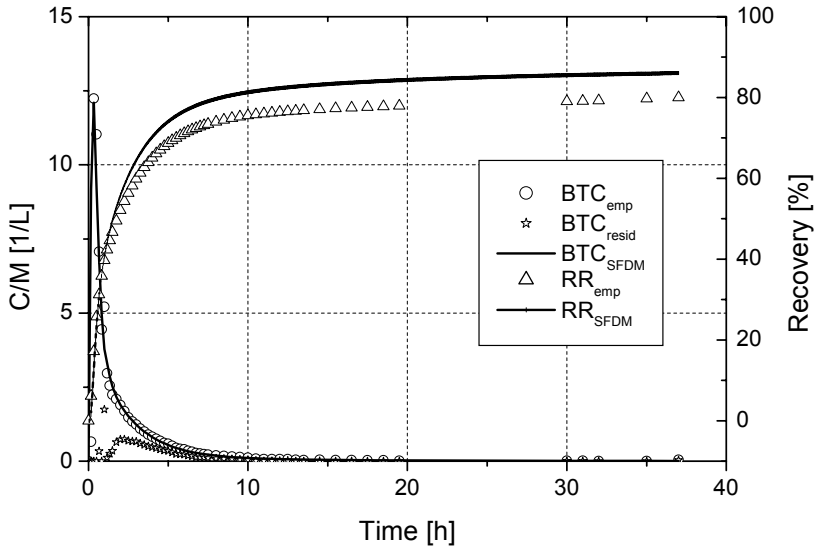

Fig. 7-8: Nitrate test 1, block A: cumulative breakthrough, recovery and residual curves and fitted SFDM.

The multi-channel SFDM assumes that the tracer is transported in several parallel flow paths, which conduct the flow from the inlet to the outlet without any mixing between them in the way. An instantaneous and complete mixing of the flow paths at the outlet is assumed. According to the multi-channel model, flow distances measured between the inlet and the outlet can be different for different flow paths and are not exactly known. Due to this reason the flow velocities and dispersivities of the different flow paths are calculated using the same lengths (0.17 m and 0.32 m) for block A and B respectively.

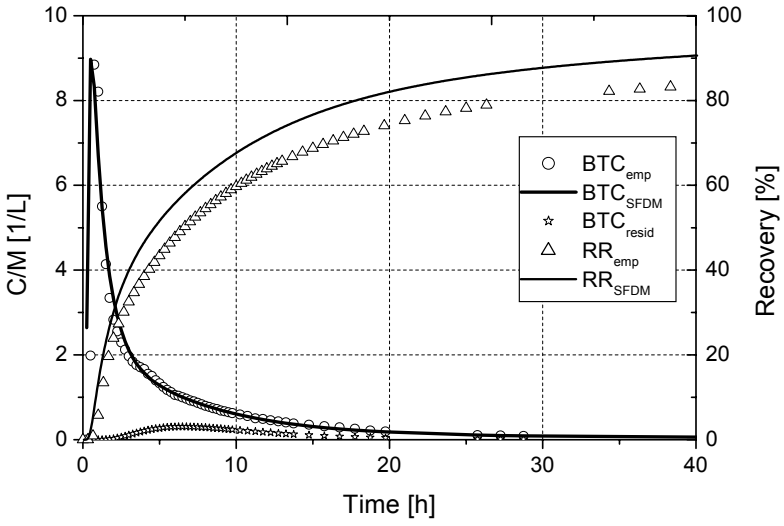

Fig. 7-9: Nitrate test 2, block A: cumulative breakthrough, recovery and residual curves and fitted SFDM.

Based on the multi-channel SFDM, it is assumed that the BTC of the tracer is a super-position of BTC's of at least two different flow paths (main and residual flow paths), which were separately fitted with the SFDM. Therefore, the simulation of the experimen-

tal data with the multi-channel SFDM enables the only reasonable fit of the BTC's and the recovery curves. Thus giving a reasonable affirmation that at least two flow channels might exist.

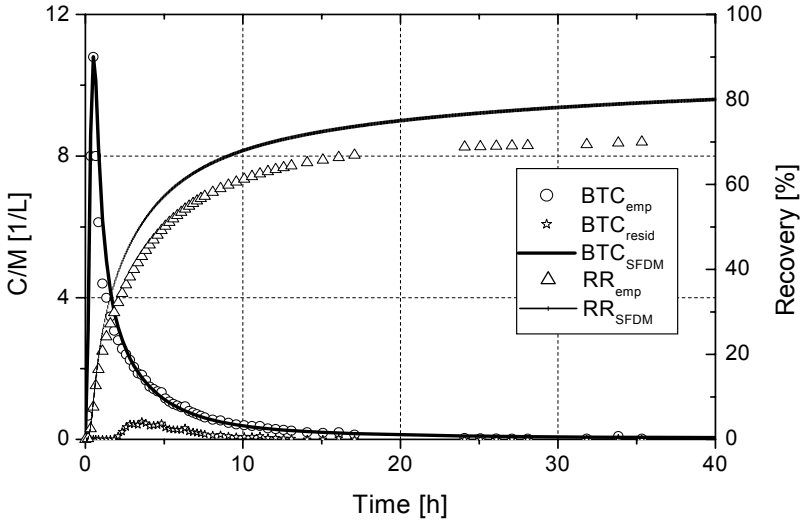

Fig. 7-10: Nitrate test 3, block A: cumulative breakthrough, recovery and residual curves and fitted SFDM.

Contrary to BTC's in the Fig. 7-6 to 7-10 the modelling of the BTC of nitrate tracer test 4 (Fig. 7-11) revealed only a single flow path. This might be due to an artifact of the tracer injection process. Especially taking into account that the three former tests yielded nearly reproducible transport parameters, thus supporting the existence of a second flow channel (Fig. 7-12). The result of this single test 4 should not be overestimated.

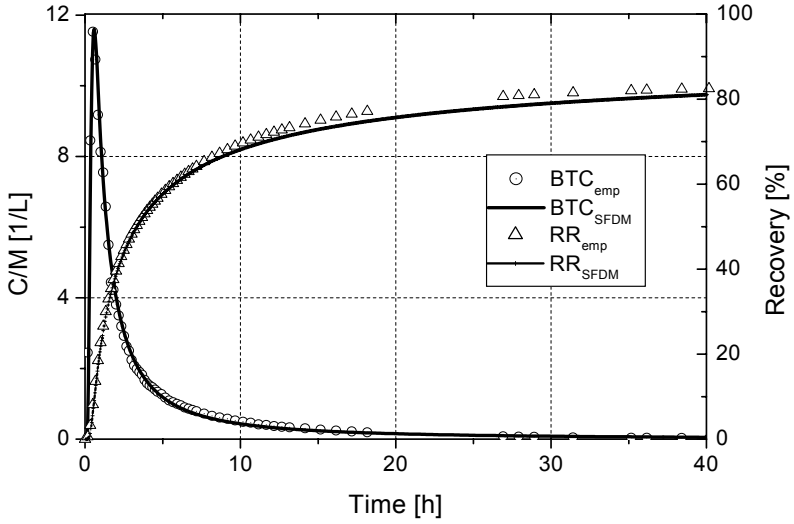

Fig. 7-11: Nitrate test 4, block A: experimental breakthrough and recovery curves and fitted SFDM.

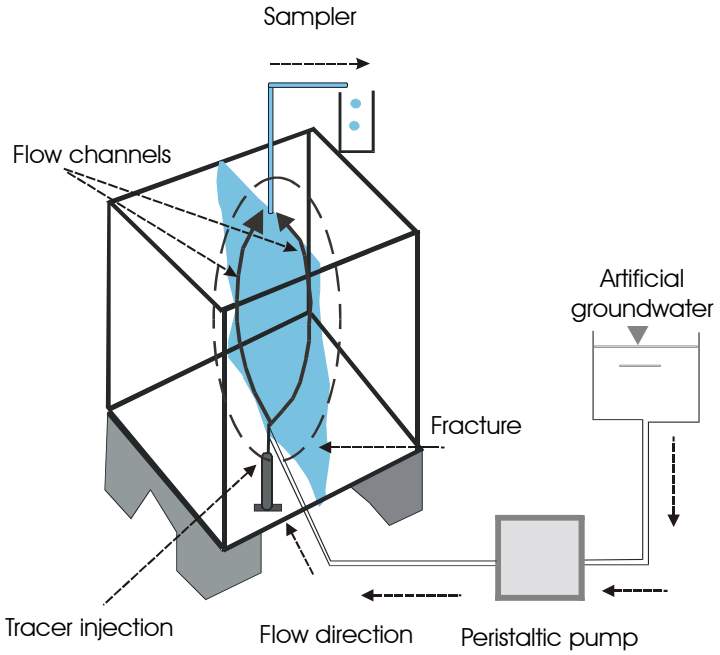

Fig. 7-12: Sketch of the fractured chalk block with different flow paths.

The fitting parameters of the SFDM and derived physical transport parameters obtained from the inverse modelling of the experimental data with the multi-channel SFDM are given in Tab.7-7 and 7-8. In general minor variations of the model parameters t_0 and Pe are observed from the simulation processes of test 1-3 (Tab. 7-7 and 7-8). The multi-channel SFDM fit gives Pe values for the main flow paths from 0.7 to 1.5 and from 4.0 to 6.0 for the second flow paths. Reversible sorption might contribute to the lower values of Pe. For the main flow path the derived values of the fracture aperture vary between 195 and 201 µm, which match quite well with values obtained from the Darcy experiments (197 µm). The derived effective diffusion coefficients vary between 3.96 E-10 m^2/s and 4.19 E-10 m^2/s, are in the same order of those determined in the laboratory diffusion experiments (4.16 E-10 m^2/s) (see Tab. 7-5).

Tab. 7-7: Nitrate tests, block A: fitting parameters of the SFDM and derived physical parameters (main flow path).

Parameter			Test 1	Test 2	Test 3	Test 4
fitted	a	[$s^{-1/2}$]	0.007	0.0072	0.007	0.0072
	t_0	[s]	1800	6550	6500	6000
	Pe	[-]	1.5	1.5	0.7	1.5
calculated	Q	[L/s]	1.30 E-5	8.57 E-6	8.06 E-6	8.17 E-6
	2b	[µm]	201	195	201	195
	α_l	[m]	11.3 E-2	11.3 E-2	24.3 E-2	11.3 E-2
	v_{SFDM}	[m/s]	9.4 E-5	2.6 E-5	2.6 E-5	2.8 E-5
	D_{hl}	[m^2/s]	1.1 E-5	2.9 E-6	6.4 E-6	3.2 E-6
	D_e	[m^2/s]	3.96 E-10	4.19 E-10	3.96 E-10	4.19 E-10

In general, a good reproducibility of the transport parameters except for test 4 can be observed (Tab. 7-7). Estimation of the fracture aperture 2b for the second flow paths is in the current model concept not included. Additional significant differences between the calculated and the measured diffusion coefficients (Tab. 7-8) exist. Although a satisfactory explanation cannot be given so far, the sensitivity of the BTC's to the fitting processes might be behind these discrepancies.

Tab. 7-8: Nitrate tests, block A: fitting parameters of the SFDM and derived physical parameters (second flow path).

Parameter			Test 1	Test 2	Test 3
fitted	a	[$s^{-1/2}$]	0.00017	0.000043	0.00009
	t_0	[s]	8500	25800	10000
	Pe	[-]	4.7	6	4
calculated	Q	[L/s]	2.80 E-6	1.43 E-6	9.40 E-7
	α_l	[m]	3.60 E-2	2.80 E-2	4.25 E-2
	v_{SFDM}	[m/s]	2.0 E-5	6.6 E-6	1.7 E-5
	D_{hl}	[m^2/s]	7.23 E-7	1.87 E-7	7.23 E-7
	D_e	[m^2/s]	2.34 E-13	1.5 E-14	6.55 E-14

A calculation of the flow rates of the main flow channels and the partial (residual) flow rates in the second flow paths is possible using Eq. (3-54) and the total flow rates (see Tab. 6-4) of the tests (Tab. 7-7 and 7-8). Nevertheless, the assumption of two flow channels as suggested by the applied multi-channel SFDM needs more data such as aperture measurements with NMR and MRI techniques. The applied model shows only a potential approach to describe BTC`s in case of channelling effects. Nevertheless several conclusions based on the clear inspection of the BTC's and from the SFDM fitting can be drawn. As a consequence of the simulation of the experimental data with the multi-channel SFDM, the tracer was transported in at least two flow paths, which support the presence of channelling effects within the fracture. Furthermore, tracers diffuse into the nearby stagnant water zones within the fracture and the matrix, thus causing a non complete mass recovery. The determined values of the effective diffusion coefficients and fracture apertures are in well agreement with values obtained from through-diffusion and Darcy experiments. The simulation processes of the experimental data with the multi-channel SFDM show high dispersion within the fracture. Velocity variations between the different flow paths along with spreading of solutes by possible diffusion into stagnant water zones in the matrix and in the fracture itself is responsible for the observed high dispersivity values.

7.3.3 Single-tracer test with uranin in the fractured chalk block A

A single-tracer test with uranin was conducted in the fractured chalk block A. The BTC is characterised by a narrow peak and a long tailing. The time of the first arrival and peak concentration time of uranin are 600 and 1200 seconds respectively (Fig. 7-13).

The tracer was almost completely (98 %) recovered after 90 hours from the injection. The mass recovery (cumulative curve) obtained from the simulation process with the multi-channel SFDM is 93 %. According to the multi-channel model most of the injected tracer was transported in the main channel with a flow rate of 8.32 E-6 L/s (92.5 %) and a partial (residual) flow rate in the second flow path of 6.78 E-7 L/s (7.5 %).

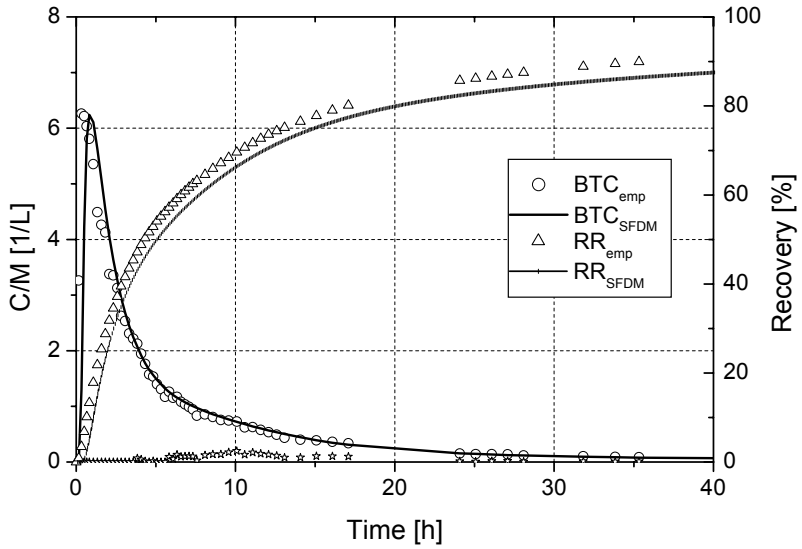

Fig. 7-13: Uranin test, block A: cumulative breakthrough, recovery and residual curves and fitted SFDM.

The results from the simulation process of the experimental data (main and second flow paths) with the multi-channel model are given in Tab. 7-9. The determined value of the fracture aperture (185 µm) agrees well with the value (197 µm) calculated from the Darcy experiments. The effective diffusion coefficient for uranin from the simulation process (3.42 E-10 m^2/s) is about four times higher than that obtained from the parallel diffusion experiments (9.75 E-11 m^2/s). The difference between the fitted and measured diffusion coefficients might be due to the increasing of the available surface area.

Tab. 7-9: Uranin test, block A: fitting parameters of the SFDM and derived physical parameters (main and second flow paths).

Parameter			main flow path	second flow path
fitted	a	[$s^{-1/2}$]	0.0065	0.000025
	t_0	[s]	8250	35000
	Pe	[-]	2.5	12
calculated	Q	[L/s]	8.32 E-6	6.78 E-7
	2b	[µm]	185	-
	α_l	[m]	6.8 E-2	1.42 E-2
	v_{SFDM}	[m/s]	2.06 E-5	4.9 E-6
	D_{hl}	[m^2/s]	1.40 E-6	6.9 E-8
	D_e	[m^2/s]	3.42 E-10	5.05 E-15

7.3.4 Single-tracer test with uranin in the fractured chalk block B

Two single-tracer tests with 10 µg and 12.67 µg uranin were performed in the fractured chalk block B (Fig. 7-14 to 7-17). All BTC's of uranin have relatively narrow peaks and long tailing. The time of the first arrival is between 1800 seconds and 3600 seconds and the time of peak concentrations are between 4500 seconds and 7200 seconds after injection. After 71 hours from the injection 79 % of the injected tracer mass was recovered in the 1st tracer test. After 30 hours the experimental mass recovery from the 2nd tracer test is 72 %. The BTC's of uranin (Fig. 7-14 and 7-17) show that the existence of a second flow path within the fracture can be assumed and more than one peak can be observed. Therefore, the attempt to describe the breakthrough curves with a simple SFDM results in huge deviations between the measured and the simulated curves (Fig. 7-14). Only the multi-channel SFDM gives reasonable results (Fig. 7-16).

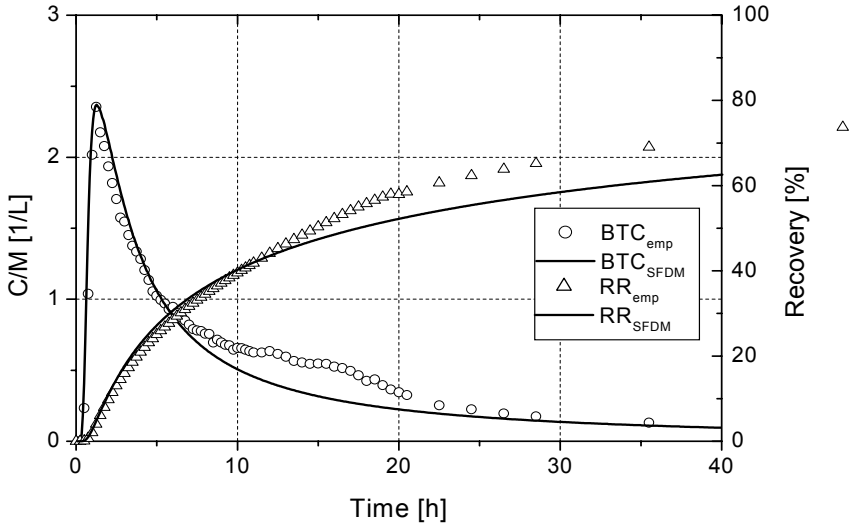

Fig. 7-14: Uranin test 1, block B: experimental breakthrough and recovery curves and fitted SFDM.

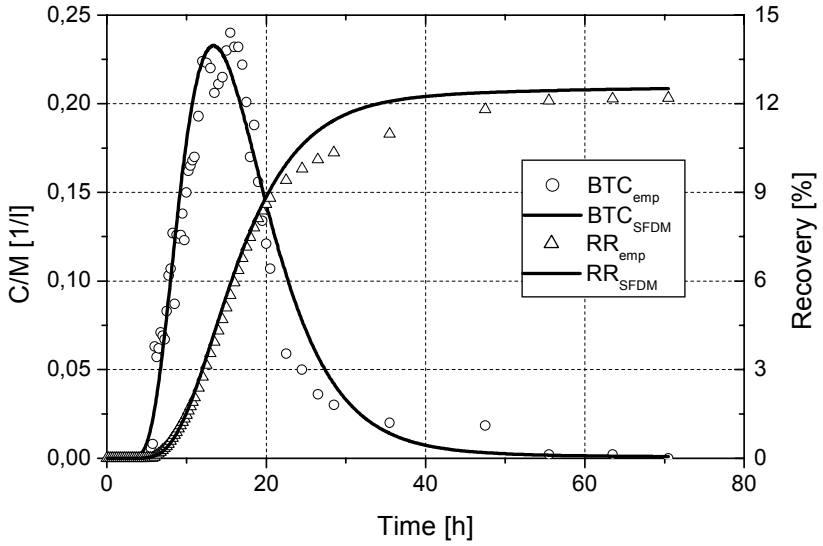

Fig. 7-15: Uranin test 1, block B: residual breakthrough and recovery curves and fitted SFDM.

The cumulative breakthrough curve (Fig. 7-16 and 7-17) for each tracer test was calculated according to the multi-channel SFDM approach. The simulation process of the experimental data with the multi-channel model indicated that uranin tracer is transported into at least two flow paths. Each of these flow paths has independent transport parameters (Tab. 7-10).

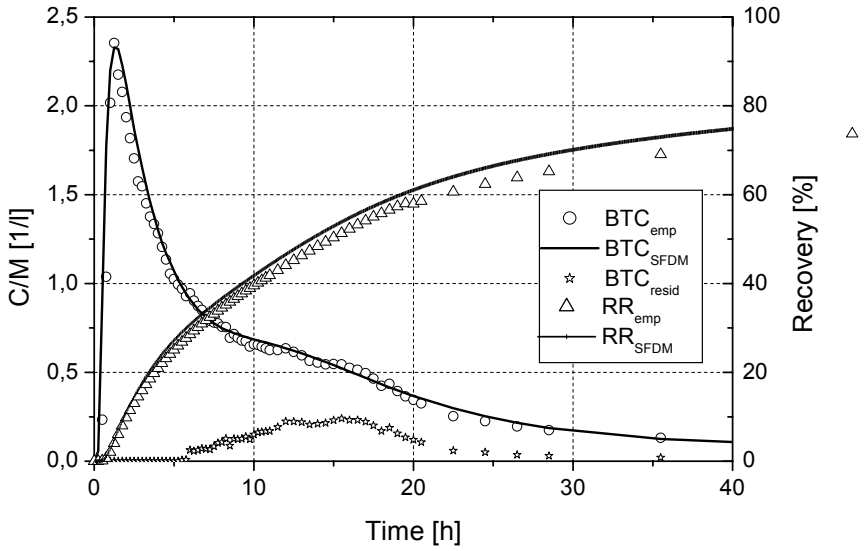

Fig. 7-16: Uranin test 1, block B: cumulative breakthrough, recovery and residual curves and fitted SFDM.

The high dispersivity value (Tab. 7-10) of uranin in the first test indicates that mixing by dispersion within the fracture is the dominant transport process. Pe numbers for the main flow paths are 1 and 3.5 for the second flow paths are 12 and 17. The determined values of the fracture aperture (225 and 194 µm) agree well with an aperture of 225 µm calculated from the Darcy experiments. The modelled values of the effective diffusion coefficients for uranin (Tab. 7-10) agree reasonably well with those measured from parallel diffusion experiments (9.75 E-11 m^2/s).

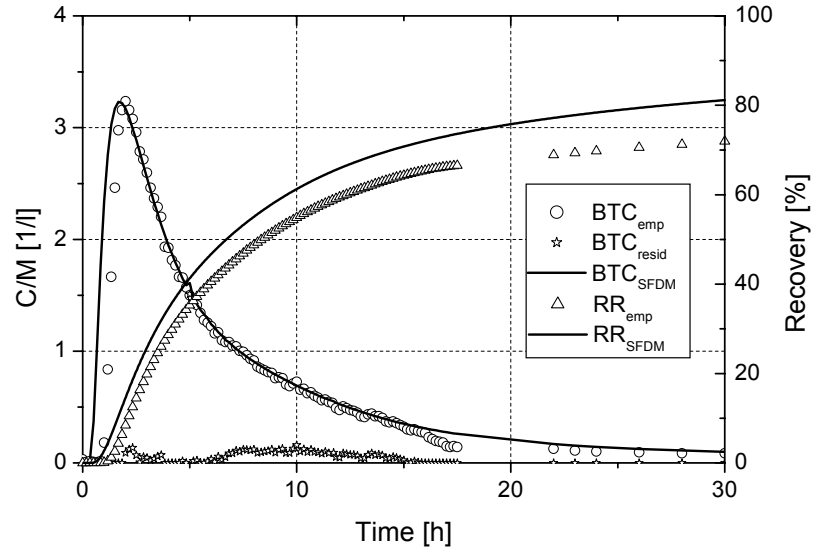

Fig. 7-17: Uranin test 2, block B: cumulative breakthrough, recovery and residual curves and fitted SFDM.

The fitting parameters of the SFDM and derived physical transport parameters obtained from the inverse modelling with the SFDM for both tracer tests are given in Tab. 7-10.

Tab. 7-10: Uranin tests, block B: fitting parameters of the SFDM and derived physical parameters (main and second flow paths).

			main flow path		second flow path	
Parameter			**test 1**	**test 2**	**test 1**	**test 2**
fitted	a	[$s^{-1/2}$]	0.0058	0.005	0.000028	0.000009
	t_0	[s]	27350	12000	50000	32500
	Pe	[-]	1	3.5	12	17
calculated	Q	[L/s]	8.45 E-6	1.02 E-5	1.55 E-6	6.73 E-7
	2b	[µm]	194	225	-	-
	α_l	[m]	32.0 E-2	9.14 E-2	2.67 E-2	1.88 E-2
	v_{SFDM}	[m/s]	1.17 E-5	2.67 E-5	6.4 E-6	9.8 E-6
	D_{hl}	[m^2/s]	3.74 E-6	2.44 E-6	1.7 E-7	1.85 E-7
	D_e	[m^2/s]	3.79 E-10	3.18 E-10	8.84 E-15	9.13 E-16

7.3.5 Multi-tracer tests performed in the fractured chalk block A

A multi-tracer test with nitrate (34 mg) and eosin (10 µg) injected simultaneously in the fractured block A was performed. Both BTC's (nitrate and esoin) have a relatively similar shape with narrow peaks and long tailings (Fig. 7-18 and 7-19). For nitrate and eosin, equal times of the first arrival and peak concentration are observed (600 seconds and 1200 seconds respectively). The relatively higher peak and higher mass recovery obtained for eosin than those for nitrate is probably a result of lower diffusion rate of eosin into the chalk matrix. This hypothesis is confirmed by parallel laboratory diffusion experiments and from the simulation value of the effective diffusion coefficient.

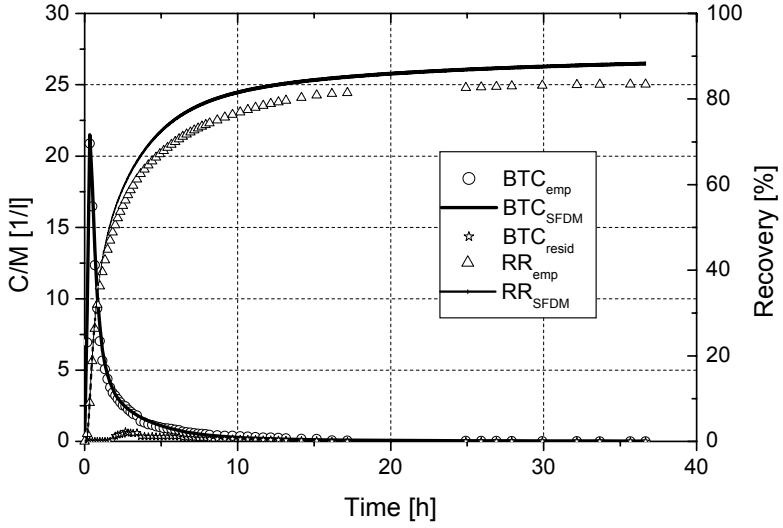

Fig. 7-18: Nitrate in the multi-tracer test 1, block A: cumulative breakthrough, recovery and residual curves and fitted SFDM.

The experimental mass recoveries for nitrate and eosin 37 hours after injection are 83 % and 89 % respectively. The simulated recovery rate is 88 % for both tracers. It is obvious from the simulation process with the multi-channel SFDM that nitrate and eosin are transported in at least two flow paths. From the simulation process with the SFDM model representative values for the transport parameters are determined (Tab. 7-11). The obvious variations of the model parameters a, t_0 and Pe for nitrate and eosin is caused by their different transport parameters.

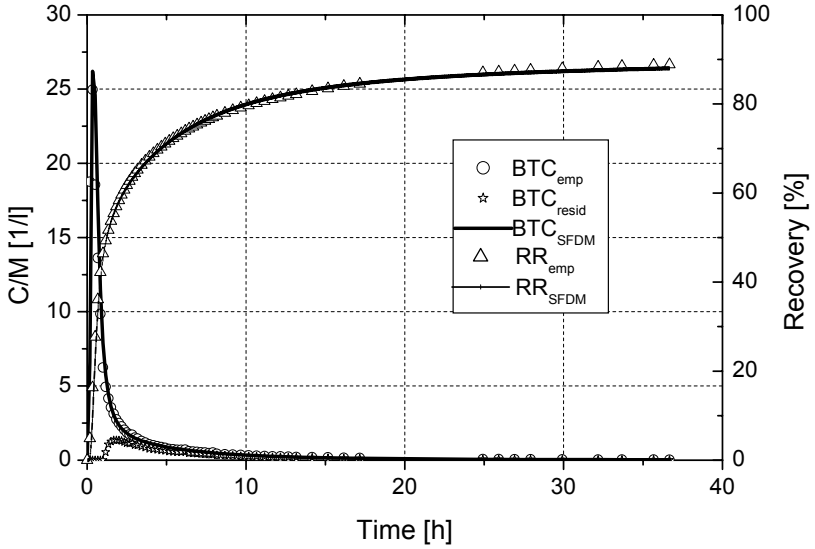

Fig. 7-19: Eosin in the multi-tracer test 1, block A: cumulative breakthrough, recovery and residual curves and fitted SFDM.

Comparing to eosin the values of retardation factor for the fracture surface R_f and for the matrix R_p for nitrate are found to be 1.86 and 1.68 respectively and the mean residence time and diffusion parameter of nitrate are higher than that of eosin. The differences in transport parameters between nitrate and eosin might be explained by the possible adsorption or degradation processes of nitrate within the fracture and the chalk matrix. The results from the simulation process (Tab. 7-11) indicated that nitrate shows a higher dispersivity value than that of eosin. The inverse modelling with SFDM yielded values of the effective diffusion coefficients for nitrate and eosin agree well with those (4.38 E-10 m^2/s and 1.1 E-10 m^2/s) determined from the through-diffusion experiments. The simulated values of the fracture aperture for the eosin BTC is 165 µm which is relatively small compared to 190 µm from the nitrate BTC and 197 µm from the Darcy experiments.

Tab. 7-11: Multi-tracer test 1, block A: fitting parameters of the SFDM and derived physical parameters for nitrate and eosin (main and second flow paths).

			main flow path		second flow path	
Parameter			**nitrate**	**eosin**	**nitrate**	**eosin**
fitted	a	[$s^{-1/2}$]	0.0074	0.0044	0.00007	0.00036
	t_0	[s]	2600	1400	12000	10000
	Pe	[-]	1.6	5	6	0.6
calculated	2b	[µm]	190	165	-	-
	α_l	[m]	10.63 E-2	3.40 E-2	2.83 E-2	28.33 E-2
	v_{SFDM}	[m/s]	6.54 E-5	1.21 E-4	1.42 E-5	1.70 E-5
	D_{hl}	[m^2/s]	6.95 E6	4.13 E-6	4.01 E-7	4.82 E-6
	D_e	[m^2/s]	4.43 E-10	1.57 E-10	3.96 E-14	1.05 E-12

A 2nd multi-tracer test was carried out into the fractured chalk block A. by simultaneously injecting a cocktail of 30 mg nitrate, 0.3 mg lithium and 0.017 mg uranin. Although the time of the first arrival is 600 seconds for all tracers the peak concentration differ significantly with 1200 seconds for uranin and lithium and 1800 seconds for nitrate (Fig. 7-20 to 7-22). 84 hours after the injection, the experimental mass recoveries for uranin and nitrate are 99 % and 75 %. The SFDM gives recoveries of 91 % and 79 %. The experimental mass recovery value from lithium (82 %) is much lower than the theoretically fitted value of 95 % (56 hours).

The relatively higher peak concentrations and the higher mass recoveries obtained for uranin and lithium compared with those for nitrate are a result of the lower diffusion rates of uranin and lithium in the chalk matrix. Possible reversible sorption and diffusion within stagnant water zones into the matrix and within the fracture itself might be contributing to the small mass recovery of nitrate. Furthermore possible reduction or degradation of nitrate within the fracture and within the chalk matrix might take place. Degradations of nitrate by micro organisms can only take place within the fracture. This is due to the small pore-size of chalk matrix compared with the size of the micro-organisms.

Again a channelling effect was clearly observed for all tracers used. Therefore additional fitting procedures using multi-channel SFDM model were carried out to improve the fitting process by calculating the cumulative tracer breakthrough and recovery curves (Fig. 7-20 to 7-22).

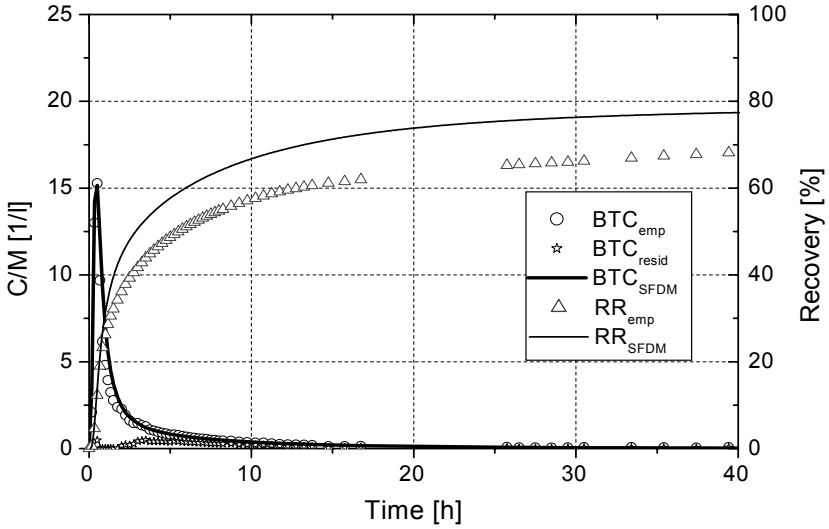

Fig. 7-20: Nitrate in the multi-tracer test 2, block A: cumulative breakthrough, recovery and residual curves and fitted SFDM.

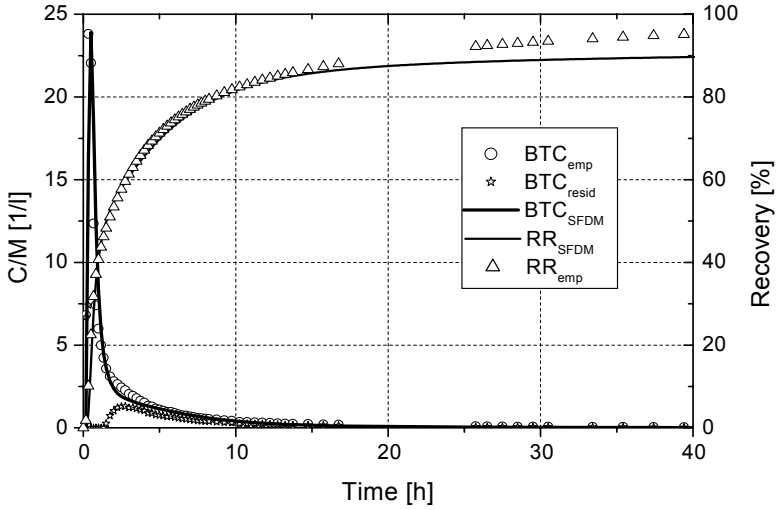

Fig. 7-21: Uranin in the multi-tracer test 2, block A: cumulative breakthrough, recovery and residual curves and fitted SFDM.

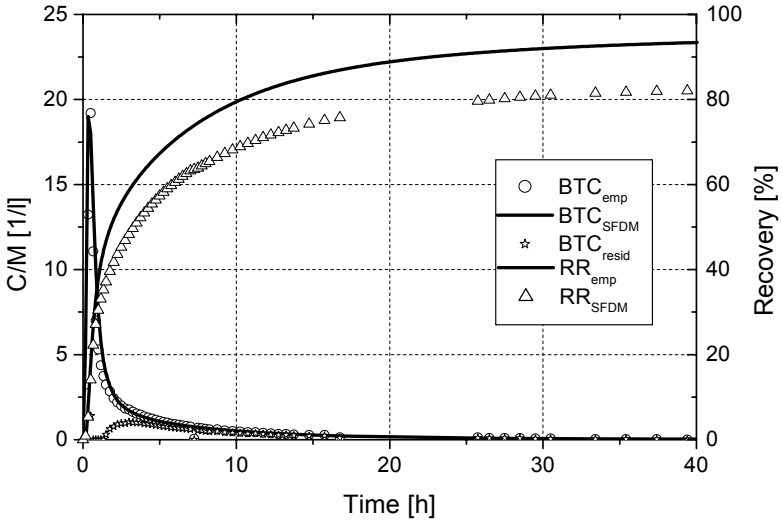

Fig. 7-22: Lithium in the multi-tracer test 2, block A: cumulative breakthrough, recovery and residual curves and fitted SFDM.

The fitting parameters of the SFDM and derived physical parameters obtained from the inverse modelling of the experimental data (main and residual channels) are given in Tab. 7-12. The mean residence time for nitrate in the fracture is higher than that of uranin and lithium and the differences in the values of diffusion parameters reflect the difference in the effective diffusion coefficient between the tracers. Comparing with uranin and lithium the values of the retardation factors for the fracture surface R_f and for the matrix R_p for nitrate are 1.17, 1.01 and 1.17, 1.27 respectively. Which means that nitrate is to some degree adsorbed or degraded within the fracture and the matrix. The calculated value of the fracture aperture from the nitrate BTC (189 µm) is identical with (197 µm) the value from the Darcy tests. For lithium and uranin the simulated values of the fracture aperture are 176 and 161 µm respectively which are relatively low compared to the values from the nitrate BTC and from the Darcy test. At all, the inverse modelling with SFDM yielded values of the effective diffusion coefficient for nitrate, uranin and lithium agree with those (4.38 E-10 m^2/s, 9.75 E-11 m^2/s and 2.3 E-10 m^2/s) determined in parallel laboratory diffusion experiments.

Tab. 7-12: Multi-tracer test 2, block A: fitting parameters of the SFDM and derived physical parameters for nitrate, uranin and lithium (main and second flow paths).

			main flow path			second flow path		
Parameter			nitrate	uranin	lithium	nitrate	uranin	lithium
fitted	a	[$s^{-1/2}$]	0.0075	0.0074	0.0059	0.00012	0.00019	0.00029
	t_0	[s]	1750	1500	1500	18000	15000	16500
	Pe	[-]	2	7.5	3	2	4	1
calculated	2b	[µm]	189	161	176	-	-	-
	α_l	[m]	8.50 E-2	2.30 E-2	5.70 E-2	8.50 E-2	4.30 E-2	17.00 E-2
	v_{SFDM}	[m/s]	9.70 E-5	1.10 E-4	1.10 E-4	9.40 E-6	1.10 E-5	1.00 E-5
	D_{hl}	[m^2/s]	8.30 E-6	2.60 E-6	6.40 E-6	8.0 E-7	4.80 E-7	1.80 E-6
	D_e	[m^2/s]	4.49 E-10	4.48 E-10	2.81 E-10	1.16 E-13	2.29 E-13	6.80 E-13

7.3.6 Multi-tracer test in the fractured chalk block B

A simultaneous injection of uranin and lithium (22 µg and 0.189 mg) was performed in the fractured block B. Both experimental curves have a similar shape with almost identical narrow peaks and long tailings (Fig. 7-23 and 7-24). The times of the first arrival are 1200 seconds and 2400 seconds after injection and the peak concentration times are 3600 seconds and 4800 seconds for uranin and lithium respectively. The experimental mass recoveries for lithium and uranin 49 hours after injection are 93 % and 72 % respectively, while the values from the simulation process are 96 % and 80 for lithium and uranin respectively.

Again the BTC's clearly show the existence of more than one flow path. The results from the simulation process with the multi-channel SFDM show, that the main residence

time and dispersivity for uranin within the fracture are higher than that of lithium, in consequence a higher transport velocity for lithium is calculated (Tab. 7-13).

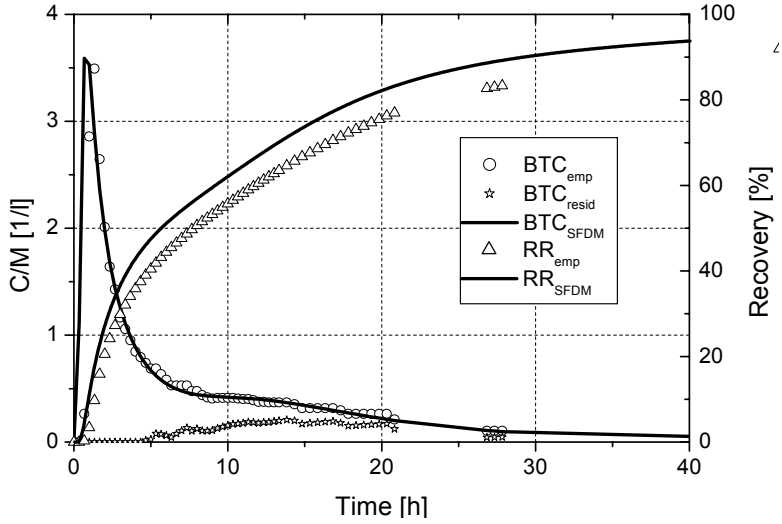

Fig. 7-23: lithium in the multi-tracer test 1, block B: cumulative breakthrough, recovery and residual curves and fitted SFDM.

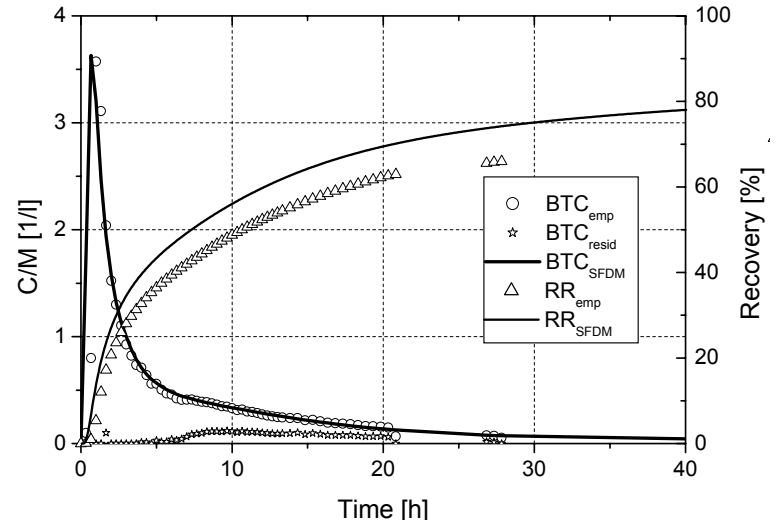

Fig. 7-24: Uranin in the multi-tracer test 1, block B: cumulative breakthrough, recovery and residual curves and fitted SFDM.

It is clear that the distribution of flow rate into different flow paths shows that the main flow paths carried most of the flowing water and the tracers arrived in very varying concentration in water flows to different flow paths. The values of the effective diffusion coefficient obtained from the simulation process match well with 9.8 E-11 m^2/s and 2.3 E-10 m^2/s obtained from the diffusion experiments. The calculated values of the fracture aperture are 225 µm and 226 µm for nitrate and lithium respectively and therefore identical with the 225 µm calculated from the Darcy experiments.

Tab. 7-13: Multi-tracer test 1, block B: fitting parameters of the SFDM and derived physical parameters for uranin and lithium (main and second flow paths).

			main flow path		second flow path	
Parameter			**uranin**	**lithium**	**uranin**	**lithium**
fitted	a	[$s^{-1/2}$]	0.005	0.0043	0.000024	0.000035
	t_0	[s]	22500	13500	40000	500000
	Pe	[-]	0.4	1	8	12
calculated	Q	[L/s]	1.45 E-5	1.27 E-5	2.18 E-6	3.89 E-6
	2b	[µm]	225	226	-	-
	α_l	[m]	80.0 E-2	32.0 E-2	4.0 E-2	2.67 E-2
	v_{SFDM}	[m/s]	1.42 E-5	2.37 E-5	8.0 E-7	6.4 E-7
	D_{hl}	[m^2/s]	1.14 E5	7.59 E-6	3.2 E-7	1.7 E-7
	D_e	[m^2/s]	2.82 E-10	2.08 E-10	5.5 E-15	1.38 E-14

8 SUMMARY AND CONCLUSION

Analysis of contaminant transport in a single fracture is an effective tool to understand the physical transport processes controlling solute migration, like dispersion, matrix diffusion and channelling in the fractured media. These aspects are particularly important in the assessment of landfills and water quality in fractured aquifers. Diffusion of contaminants from the mobile into the stagnant water zones in the matrix and/or in the fracture itself is considered as an important transport mechanism in fractured porous media. In double porosity media such as chalk which are characterized by low permeabilities but significant porosities, diffusion into the matrix adjacent to the fractures is one of the main factors effecting contaminant transport.

The sorption and diffusion properties of Danish chalk were evaluated by performing batch as well as through-diffusion experiments. Linear sorption isotherms (Henry-isotherms) were obtained by the batch tests. The generally low sorption capacity of Danish chalk, remarkable low for nitrate and uranin, is due to its high purity and its really low contents of clay minerals, organic carbon and iron oxides of the chalk. The results of through-diffusion experiments clearly showed that the diffusion coefficient of nitrate, chloride and lithium were nearly in the same range (1.54 E-10 m^2/s to 5.46 E-10 m^2/s), but higher than those of hydrogeological tracers such as uranin, pyranin and eosin. The observed variations of the effective diffusion coefficients can be explained by both the variations in molecular diffusion coefficients of the solutes and the porosity values of the chalk samples. The obtained rock capacity factors indicate a very small retardation in the Danish chalk as expected by the laboratory batch experiments. Assuming linear sorption isotherms and the whole porosity as transport porosity ($\varepsilon = \varepsilon_t$) the determined rock capacity factors can be used to calculate the distribution coefficient ($\alpha = \varepsilon + \rho K_d$). These coefficients were several times higher than those obtained from the batch experiments. The available surface area for sorption might be the reason behind these high values for the distribution coefficients. According to Archie's law, a chalk specific exponent m (Archie exponent) of 2.2 was derived. Based on this exponent, effective diffusion coefficients were predicted by taking into account the relative diffusivity and porosity of the chalk samples. Multi-tracer diffusion experiments showed a noticeable decrease in the relative diffusivities of tracers compared to those predicted from Archie's law. This might be due to interactions between the ionic tracers. The decreasing relative diffusivities are accompanied by an increasing chalk-specific m-value of 2.6 for Archie's law. Comparing to the reported values of Archie's exponent m in the literature, Archie's exponent m of 2.2 for the Maastrichtian chalk lies in the range of the reported values. According to the results of the batch and diffusion experiments, nitrate, uranin, eosin, pyranin and lithium showed low retardation in the chalk.

In order to investigate the possible effects of matrix diffusion process and flow channelling within the fracture, laboratory single- and multi-tracer tests with nitrate compared to

various hydrogeological tracers (uranin, eosin and lithium) have been carried out. These laboratory tracer tests were performed using two artificially fractured Danish chalk blocks A and B (17x15x14 cm^3 and 32x29x23 cm^3 respectively). Pulse injection tracer tests conducted within the fractured chalk blocks (steady-state flow field) showed BTC's with fast rise in concentration to reach an early peaks and long tails into late time values. The most common explanation for this skewed BTC's is that a fast transit of tracers through open channels occupying only a small percent of the fracture plane. Thus resulting in early and sharp peaks. Long tailings reflect the tracer dispersion and diffusion into the matrix and/or into stagnant water zones within the fracture. The simulation processes of the experimental data with the SFDM model clearly showed that, simulation of the BTC's with a simple dispersion model could not reasonably fit the specific shape of the BTC's. Thus the concept of a single flow system within the fracture is not satisfying at all, but distinct flow systems and the superposition of the simulated BTC's leads to the total simulated concentration. Applying the multi-channel SFDM leads to acceptable fits with reasonable transport parameters. Those simulations suggest that a fast advective transport component in pronounced channels, which occupy only a small percent of the fracture plane, is responsible for the high peak concentrations. Whereas, the transport in the remaining fracture area is characterised by dispersive and diffusive exchange with the matrix and with stagnant water zones leading to a distinct tailing.

Generally, high dispersion values are obtained from the simulation processes. Velocity variations in the channels, and those between the different flow channels as well as possible diffusion from mobile water into stagnant water zones (between these channels and/or into the chalk matrix) might be responsible for those high dispersivity values. Those results indicate that dispersion processes within the fracture had a large effect on tracer migration in those tracer tests. From the inverse modelling of the experimental data with the SFDM, the fracture apertures obtained from all BTC's vary from a minimum value of 161 µm for the uranin to a maximum of 201 µm for the nitrate in the fractured chalk block A. For tracer tests performed in fractured chalk block B the determined values for the fracture apertures varied between 194 µm to 226 µm. Those values agree well with the apertures (197 µm and 225 µm) calculated from Darcy experiments for block A and B, respectively. So far, no convincing explanation has been found for the variations between the simulated and measured values of the fracture aperture. Hence both the solute itself as well as the channelling within the fracture might be behind those deviations, further detailed researches are needed to explain this observed difference in fracture aperture estimates. Furthermore, the results indicate that the fitted values of the effective diffusion coefficient agree well with those obtained from the laboratory through-diffusion experiments.

From the results of the multi tracer tests, the differences in the transport parameters of nitrate and the non-reactive tracers uranin, lithium and eosin may indicate possible ad-

sorption or degradation of nitrate within the fracture and within the chalk matrix. But microbial degradations of nitrate can only take place within the fracture due to the small pore-size of chalk matrix compared with the size of the micro-organisms. Furthermore, the relatively low normalized concentrations (C/M) of nitrate compared to those for uranin, eosin and lithium might be due to the increased diffusion rate of nitrate into the matrix and possible reduction processes.

Though the assumption of two flow paths as suggested from the applied multi-channel model is still a theoretical suggestion, which needs more investigations, especially to quantify and measure the fracture aperture with different techniques such as NMR and MRI, it yields a very good fit in all tests. In this way the idea of a multi-flow system within the fracture seems to be applicable for transport processes in the fractured porous media. It must be emphasized that flow and contaminant transport within the fracture is strongly affected by channelling as a result of the roughness and available contact area within the fracture. This channelling cause a distinct diffusive exchange within both the fracture and the matrix. In summary, interpretation of the tracer tests in combination with geological information, hydraulic tests information and laboratory studies (e.g. batch and diffusion experiments) have resulted in a well improved understanding of the physical transport processes in a single fracture. Further experiments should be performed to justify those results.

The slow release of contaminant or mobile/immobile mass-transfer in such highly porous media is important for the prediction of contaminant transport and hence for the monitoring and remediation strategies. The higher the matrix porosity, the higher the transport rate from the fracture to the matrix that implies a large contaminant mass is likely to migrate into and be stored within the chalk matrix. This large mass is bound to lengthen any remediation efforts and reduce their effectiveness. Consequently, assessment and remediation of contaminant should take into account the matrix diffusion as a more important retardation factor, where the matrix acting as sink or source for the transported solutes in the fractures. Due to the high purity of Danish chalk, sorption processes play a minor role in the retardation processes.

The data and results presented here could be applied as a preliminary base for investigating solute transport in any kind of rock. Since the magnitude and extent of transport and retardation processes are essentially determined by the mineralogical composition of the rock varieties being tested. Therefore, it is necessary to take their changes of the mineralogical composition into account. Finally, the information derived from these small laboratory tracer tests can be transformed to the field tracer-test scale considering the complexity of the reality. However, in situ fracture pathways, fracture orientations as well as fracture apertures are always difficult to capture.

Based on the results of the research, it appears that, matrix diffusion processes play only a minor role in the determination of the fate of nitrate in the groundwater systems.

Since the fractures and macro-pores constitute zones of increased densities of bacteria associated with downward transport and accumulation of organic materials from natural vegetation and agricultural production, the most important key factor controlling the fate of nitrate is the redox process. Anaerobic reduction in the subsurface can limit the nitrate contamination within groundwater. More studies are required to evaluate the nitrate reduction capacity and rate, which is of particular importance for natural remediation process specifically caused by chemically/microbial reduction for the contaminated aquifers in agricultural areas.

A more general recommendation can be given to minimize the applications of N-fertilizers especially in the irrigated areas over fractured aquifers and near the recharging zones. This is due to the fact that, nitrate is highly water-soluble, mobile and can easily pass through agricultural soil to the groundwater and has low retardation properties. Furthermore, groundwater quality monitoring system should be established to determine progress of nitrate concentrations in groundwater under irrigated lands. The obtained results can provide the farmers and the responsible authorities with a set of guidelines to monitor and control groundwater contamination in fractured aquifers, which will be helpful to improve nitrate management strategies for water quality purposes.

9 SUGGESTIONS FOR FUTURE INVESTIGATIONS

Research can go further with the diffusion experiments to test whether the whole matrix really participates in the diffusion or the process is limited to the zone near the fracture surfaces (small depth into the matrix). The finding from this point can be used to aid in the remediation of contaminant in fractured media.

To improve the results from laboratory tracer tests it is necessary to develop laboratory techniques to determine the detailed fracture geometry without disturbing the fracture. Better ideas of the fracture parameters like fracture aperture which plays a major role in flow and transport in such media, fracture roughness and fracture width can be obtained by using NMR, MRI and resin casting techniques. Therefore, detailed studies are required especially to characterise the fracture aperture heterogeneity and its effects on the transport mechanisms that control the solute transport.

Additional research is also needed to investigate reduction or degradation of nitrate within the fracture. This could give further findings about the behaviour of nitrate as a contaminant and can help especially in the remediation for the contaminated aquifers in agricultural areas. We therefore need to devote more research to get a complete qualitative and quantitative understanding of dispersive and diffusive transport in fractured geologic media.

10 REFERENCES

Abdel-Dayem, S. and Abdel-Ghani, M. (1992): Concentrations of agricultural chemicals in drainage water. In: Drainage and Water Table Control. Proc. 6th Int. Drainage Sym., 13-15 Dec. 1992, Nashville, TN/St. Joseph, MI, pp. 353-360.

Abelin, H., Birgersson, L., Gidlund, J. and Neretnieks, I. (1991): A Large-Scale flow and tracer experiment in Granite. 1. Experimental design and flow distribution. Water Resour. Res. 27 (12): 31o7-3117.

Abelin, H., Birgersson, L., Moreno, L., Widen, H., Agren, T. and Neretnieks, I. (1991): A Large-Scale flow and tracer experiment in Granite. 2. Results and Interpretation. Water Resour. Res. 27 (12): 3119-3135.

Abelin, H., Neretnieks, I., Tunbrant, S., and Moreno, L. (1985): Final report of the migration in a single fracture- Experimental results and evaluation, Tech. Rep. 85-03, Stripa Proj., Stockholm.

Agrawal, G.D., Lunkad, S.K. and Malkhed, T. (1999): Diffuse agricultural nitrate pollution of groundwater in India. Wat. Sci. Tech. 39 (3): 67-75.

Ahmed, M., Sharma, M.L., Richards, Q.D. and Ahmad, A.R. (1994): Field scale nitrogen leaching. Application of model 'LEACHN'. Agricultural impacts on groundwater quality: Proceedings of an international workshop held in Kota Bharu, Kelantan, Malaysia, 24-27 October.

Andersen, L.J. and Kristiansen, H. (1984): Nitrate in groundwater and surface water related to land use in the Karup basin, Denmark. Environ. Geol. 5: 207-212.

Appelo, C. and Postma, D. (1994): Geochemistry, groundwater and pollution, Balkema pub. Rotterdam. Netherlands, 536 pp.

Archie, G.E. (1942): The electrical resistivity log as an aid in determining some reservoir characteristics. Trans. AIME. 146, 54-61.

Atkins, P.W. (1986): Physical Chemistry. Oxford University Press, 857 pp.

Baartman, J.C. and Christensen, O.B. (1975): Contribution to the interpretation of the Fennoscandian Border Zone. Geological Survey of Denmark. II Series102, 47pp.

Bansemer, K. (2000): Sorption und Diffusion in Geklüfteter Poröser Kreide. Diplom Thesis, Geological Institute, Bonn University, Bonn, Germany.

Barrett, J.H., Parslow, R.C., McKinney, P.A., Law, G.R. and Forman, D. (1998): Nitrate in drinking water and the incidence of gastric oesophageal and brain cancer in Yorkshire, England. Cancer Causes Control 9 (2): 153-159.

Bäumle, R. (2003): Geohydraulic Characterisation of Fractured Rock Flow Regimes. Regional Studies in Granite (Lindau, Black Forest, Germany) and Dolomite (Tsumeb Aquifers, Northern Namibia). PhD Thesis, Department of Applied Geology, Karlsruhe, Germany.

Bäumle, R., Hötzl, H. and Witthüser, K. (2000): Flow pattern and transport behaviour of granitic rock intersected by a highly permeable fault zone. in: Dassargues, A. (Ed.) 2000): Tracers and Modelling in Hydrogeology. IAHS Publication No. 262: 283 - 288; Wallingford, UK (IAHS Press).

Bear, J. (1972): Dynamics of Fluids in Porous Media. 764 pp. New York, London (Elsevier).

Bear, J., Tsang, C.F. and de Marsily, G. (Eds.) (1993): Flow and Contaminant Transport in Fractured Rock. 560 pp. New York (Academic Press Inc.).

Becker, M. W. and Coplen, T.B. (2001): Use of deuterated water as a conservative artificial groundwater tracer. Hydrogeology Journal 9: 512-516.

Becker, M. W. and Shapiro, A. M. (2000): Tracer transport in fractured crystalline rock: Evidence of nondiffusive breakthrough tailing. Water Resour. Res. 36 (7): 1677-1686.

Becker, M. W., Reimus, P. W. and Vilks, P (1999): Transport and attenuation of carboxylate-modified-latex microspheres in fractured rock laboratory and field tracer tests. Ground Water 37 (3): 387-395.

Behrens, H. and Teichmann, G. (1988): Lichtempfindlichkeit von Pyranin, Uranin und Eosin in Abhängigkeikt vom pH-Wert.- GSF-Jahresbericht 1988: 235-242; Neuherberg bei München.

Berkowitz, B. (2002): Characterizing flow and transport in fractured geological media: A review. Adv. Water Resour. 25: 861-884.

Blood, D.C., Radostits, O.M., Henderson, J.A., Arundel, J.H. and Gay, C.C. (1983): Veterinary medicine. Bailliere Tindell, London.

Blum, P. (2000): Sorptions- und Diffusionsverhalten organischer Verbindungen in israelischen und europäischen Kreidekalken.- 102 S.; Dipl. Arb. University of Karlsruhe, Germany.

Bodin, J., Delay, F. and de Marsily, G. (2003a): Solute transport in a single fracture with negligible matrix permeability: 1. fundamental mechanisms. Journal of Hydrogeology 11: 418-433.

Bodin, J., Delay, F. and de Marsily, G. (2003b): Solute transport in a single fracture with negligible matrix permeability: 2. mathematical formalism. Journal of Hydrogeology 11: 434-454.

Boving, T.B. and Grathwohl, P. (2001): Tracer diffusion coefficients in sedimentary rocks: correlation to porosity and hydraulic conductivity. Journal of contaminant Hydrology 53: 85-100.

Bradbury, M.H. and Green, A. (1985): Measurement of important parameters determining aqueous phase diffusion rates through crystalline rock matrices. Journal of Hydrology 82: 39-55.

Canter, L.W. (1997): Nitrates in groundwater, University of Oklahoma, Norman, Oklahoma, Lewis Publishers, Boca Raton.

Carrera, J., Sanchez-Vila, X., Benet, I., Medina, A., Galarza, G. and Guimera, J. (1998): On Matrix Diffusion: Formulations solution methods and qualitative effects.- Hydrogeology Journal 6 (1): 178-190.

Carslaw, H.S. and Jaeger, J.C. (1959): Conduction of heat in solids. 510 pp.; Oxford (Clarendon Press).

Cherry, J. A., Gillham, R. W., and Barker, J. F. (1984): Contaminants in groundwater: Chemical processes.- In: National research council (Ed.) studies in geophysics, groundwater contamination: 47-64; Washington (National Academic Press).

Council for Agricultural Science and Technology (CAST), (1985): Agriculture and groundwater quality, ISSN; 0194-4088; No. 103: 62pp.

Council for Agricultural Science and Technology (CAST), (1992): Water quality: Agriculture's role. Task Force Report 120, Ames, USA.

Craun, G.F. (1984): Health aspects of groundwater pollution. Groundwater pollution Microbiology, eds. G. Bitton and C. P. Gerber. New York, John Wiley, p.135-179.

Day, M.J. (1977): Analysis of movement and hydrochemistry of groundwater in the fractured clay and till deposits of the Winnipeg area. An unpublished M.Sc. Thesis, Dept. of Earth Sciences, Waterloo Uni., Waterloo, Ontario.

Derouane, J. and Dassargues, A. (1998): Delineation of groundwater protection zones based on tracer tests and transport modelling in alluvial sediments. Environmental Geology 36 (1-2): 27-36.

Domenico, P.A. and Schwartz, F.W. (1990): Physical and chemical hydrogeology. John Wiley and Sons, INC. 824 pp.

Downing, R.A., Price, M. and Jones, G.P. (1993): The making of an aquifer. In: The Hydrogeology of the Chalk of North-West Europe, Downing, R.A., Price, M. and Jones, G.P.- pp. 1-13. Oxford University Press Inc., New York.

Drever, I.J. (1997): The Geochemistry of Natural Waters Surface and Groundwater Environments. Prentice-Hall, Inc, 436pp.

Dykhuizen, R.C. (1992): Diffusive matrix fracture coupling including the effects of flow channeling. Water Resour. Res. 28 (9): 2447-2450.

Einsiedl, F., Maloszewski, P., Witthüser, K. and Wohnlich, S. (2000): Application of two new fluorescent dyes and fluorescent particles in a horizontal and vertical fracture. In: Dassargues, A. (Ed.) (2000): Tracers and Modelling in Hydrogeology.- IAHS Publication No. 262: 175-179; Wallingford, UK (IAHS Press).

Epstein, N. (1989): On tortuosity and the tortuosity factor in flow and diffusion through porous media. Chem. Eng. Sci. 44: 777-779.

Feenstra, S., Cherry, J.A., Sudicky, E.A. and Hag, Z. (1984): Matrix diffusion effects of contaminant migration from an injection well in fractured sandstone. Ground Water 22 (3): 307-316

Fetter, C.W.(1994): Applied Hydrogeolog. Macmillan College Publishing Company, Inc, 619pp.

Foster, S.D. (1975): The Chalk groundwater tritium anomaly. A possible explanation. J. Hydrol. 25: 159-165.

Foster, S.D. and Bath, A.H. (1983): Distribution of agricultural soil leaches in the unsaturated zone of the British chalk. Environ. Geol 5: 53-59.

Fourmentraux-Chevron, F., Darmendrail, D. and Defives, C. (1998): Biological de-nitrification by chalk-fixed biofilms: laboratory studies. Environ. Technol. 19: 203-211.

FRACFLOW FINAL REPORT (2001): Co-ordinators Summary Report. 113pp (unpublished).

FRACFLOW FIRST ANNUAL PROGRESS REPORT (1998): Co-ordinators Summary Report (01.12.1997–30.11.1998).50pp (unpublished).

FRACFLOW FIRST ANNUAL PROGRESS REPORT (1999): Co-ordinators Summary Report (unpublished).

FRACFLOW THIRD ANNUAL PROGRESS REPORT (2000): Co-ordinators Summary Report (01.12.1999–30.11.2000). 197pp (unpublished).

Fredericia, J., Knud, E.S., Knudsen, C. (1998): Introduction to the geological framework of the excursion area. In: Mass transport in fractured aquifers and aquitards.- 4-23.- GEUS, Excursion guide (May 14-16, 1998). Geological Institute, Copenhagen University, Denmark.

Freeze, R.A. and Cherry, J.A. (1979): Groundwater. Prentice-Hall, Englewood Cliffs, N.J, 604 pp.

Fryar, A.E, Mako, S.A., Mullican III, W.F., Romanak, K.D. and Bennett, P.C. (2000): Nitrate reduction during ground-water recharge, Southern High plains, Texas. Journal of contaminant Hydrology 40: 335-363.

Frykman, P. (1994): Variability in petrophysical properties in U. Maastrichtian Chalk outcrops at Stevns, Denmark.- DGU Service report 38, Copenhagen (Ministry of the Environment, Geological Survey of Denmark GEUS).

Frykman, P. (2001): Spatial variability in petrophysical properties in Upper Maastrichtian chalk outcrops at Stevns Klint, Denmak, Marine and Petroleum Geology 18: 1041–1062.

Gavrilenko, P. and Gueguen, Y. (1998): Flow in fractured media: A modified renormalization method. Water Resour. Res. 34 (2): 177-191.

Ge, S. (1997): A Governing Equation for Fluid Flow in Rough Fractures. Water Resour. Res. 33 (1): 53-61.

Gelhar, L.W. (1987): Application of stochastic models to solute transport in fractured rocks, SKB Technical Report 87-05.

Gelhar, L.W., Welty, C. and Rehfeldt, R. (1992): A critical review of data on field-scale dispersion in aquifers. Water Resour. Res. 28 (7): 1955–1974.

Gerik, A. (2003): Numerische Modellierung der Strömung in geklüfteten Gesteinen am Beispiel des Steinsbruchs Sigerslev, Dänemark. Diplom Thesis, Geological Institute, Bonn University, Germany.

Gjerde,J. and Fritz, J.S. (1987): Ion chromatography. Dr. Alfred Hüthig Verlag, Heidelberg, Germany.

Gooddy, D.C., Kinniburgh, D.G. and Barker, J.A. (1996): Development of a rapid method for determining apparent diffusion coefficients for chloride in Chalk.- British Geological Survey. Technical Report WD/95/66: 21 pp.

Gouy, J., Berge, P. and Labroue, L. (1984): Gallionella ferruginea, facteur de denitrification dans les eaux pauveres en matiere organique, C. R. Acad. Sci. Paris, 298: 153-156.

Grathwohl, P. (1990): Influence of organic matter from soils and sediments from various origins and the sorption of some chlorinated aliphatic hydrocarbons: Implications on KOC correlations. Environ Sci. Technol. 24 (11): 1687-1693.

Grathwohl, P. (1998): Diffusion in natural porous media: Contaminant transport, Sorption/Desorption and Dissolution Kinetics. - Boston, Dordrecht, London (Kluwer Academic Publishers). 207pp.

Grisak, G.E. and Pickens, J.F. (1980): Solute transport through fractured media. 1. The effect of matrix diffusion. Water Resour. Res. 16 (4): 719-730.

Grisak, G.E. and Pickens, J.F. (1981): An Analytical Solution for Transport Through Fractured Media with Matrix Diffusion.- J. Hydrol. 52: 47-57.

Grisak, G.E., Pickens, J.F. and Cherry, J.A. (1980): Solute transport through fractured media. 2. Column study of fractured till. Water Resour. Res. 16 (4): 731-739.

Haggerty, R. and Gorelick, S (1995): Multiple-rate mass transfer for modelling diffusion and surface reactions in media with pore-scale heterogeneity Water Resour. Res. 31: 2383-2400.

Haggerty, R. (2000): Development of late-time slopes on log-log breakthrough curves after a pulse-type injection of the case of infinite matrix block. In: Interpretations of tracer tests performed in the Culebra dolomite at the waste isolation Pilot Plant site. Lucy, C.M., Richard, L.B. and Toya, L.J..- pp. 305-307, G.P. Sandia National Laboratories.

Hakami, E. and Larsson, E. (1996): Aperture measurements and flow experiments on a single natural fracture. Int. J. Rock Mech. Min. Sci. & Geomech. Abstr. 33 (4): 395-404.

Hancock, J.M. (1993): The formation and diagenesis of chalk. In: The Hydrogeology of the Chalk of North-West Europe, Downing, R.A., Price, M. and Jones, G.P.- pp. 14-34, G.P. Oxford University Press Inc., New York.

Hem, J.D. (1985): Study and interpretation of the chemical characteristics of natural water. United States Geological Survey water-Supply Paper 2245: 1-263.

Hill, D. (1984): Diffusion coefficient of nitrate, chloride, sulfate and water in cracked and uncracked chalk. J. of Soil Sci. 35: 27-33.

Himmelsbach, T. and Wendland, E. (1998): Dreidimensionale Modellierung eines Laborversuches zum Stofftransport in einer Einzelkluft. In Workshop Kluft-Aquifere (1999). 59-71.

Himmelsbach, T. Hötzl, H. and Maloszewski, P. (1998): Solute Transport processes in a highly permeable fault zone of Lindau fractured rock test site, Germany. Ground Water 36 (5): 792-800.

Hines and Maddox (1985): Mass transfer fundamentals and applications. Prentice_Hall, INC. Englewood Cliffs, New Jersey 542 PP.

Hoff, J. D., Nelson, D.W. and Sutton, A. L., (1981): Ammonia volatilization from liquid swine manure to cropland. J. Environ. Qual. 10: 90-95.

Höhn, E., Eikenberg, J., Fierz, T. And Frick, U. (1994): Field experiments of radionuclide migration at the Grimsel Test Site (Swiss Alps), Transport and Reactive Processes in aquifers, Dracos and Stauffer (eds). Balkema, Rotterdam.

Hornsby, A.G.(1990): Pollution and public health problems related to irrigation. In: Steward, B.A. and Nielsen, D.R. ed. Irrigation of Agricultural crops. American Society of Agronomy, Madison, Wisconsin, USA. Agronomy Series, No. 30: 1176-1187.

Howard, K.W.F. (1984): Denitrtification in a major limestone aquifer. J. Hydrol. 76: 265-280

Hsieh, P.A., Shapiro, A.M., Barton, C.C., Haeni, F.P., Johnson, C.D., Martin, C.W., Paillet, F.L., Winter, T.C. and Wright, D.L. (1993): Methods of Characterizing Fluid Movement and Chemical Transport in Fractured Rock: Field trip guidebook for the Northeastern United States, Chapter R. Boston, USA.

Hudak, P.F. (2000): Regional trends in nitrate content of Texas groundwater. Journal of Hydrology 228: 37-47.

Huyakorn, P.S., and Pinder, G.F. (1983): Computational methods in subsurface flow, Academic Press, New York, 473pp.

Jakobsen, P.R. and Klitten, K. (1998): Fracture systems and groundwater flow in the Kobenhavn Limestone. Poster with abstract at Mass Transport in Fractured Aquifers and Aquitards.

Jardine, P.M., Sanford, W. E., Gwo, J.P., Reedy, O.C., Hicks, D.S., Riggs, J.S., and Bailey, W.B. (1999): Quantifying diffusive mass transfer in fractured shale bedrock, Water Resour. Res. 35 (7): 2015-2030

Jardine, P.M., Wilson, G.V. and Luxmoore, R.J. (1988): Modelling the transport of inorganic ions through undisturbed soil columns from two contrasting watersheds. J. of Soil Sci. Soc. Am. 52 (5): 1252-1259.

Job, C. and Zötl, J. (1969): Zur Frage der Herkunft des Gasteiner Thermalwassers?. Steir. Beitr. Hydrogeol.: 51-115. Graz.

Jorgensen, P. R., McKay, L. D. And Spliid, N. H. (1998): Evaluation of chloride and pesticide transport in a fractured clayey till using large undisturbed columns and numerical modelling. Water Resour. Res. 34 (4): 539-553.

Jorgensen, P. R., Urup, J., Helstrup, T., Jensen, M.B., Eiland, F. and Vinther, F.P. (2004): transport and reduction of nitrate in clayey till underneath forest and arable land. Journal of Contaminant Hydrology 73: 207-226.

Joung, C.P. (1983): Data acquisition and evaluation of groundwater pollution by nitrate, pesticides and disease-producing bacteria. Environ. Geol. 5: 11-18.

Kacaroglu, F., Gunay, G., (1997): Groundwater nitrate pollution in an alluvium aquifer, Eskisehir urban area and its vicinity, Turkey. Environmental Geology 31 (3/4): 178-184.

Karickhoff, S.W. (1981): Semi-empirical estimation of sorption of hydrophobic pollutants on natural sediments. Chemosphere. 10: 833-846.

Karickhoff, S.W., Brown, D.S. and Scott, T. A. (1979): Sorption of hydrophobic pollutants in sediment suspension. Water Research 13: 241-248.

Kasnavia, T., Vu, De, and Sabatini, D.A. (1999): Fluorescent dye and media properties affecting sorption and tracer selection. Ground Water 37 (3):376-381.

Käss, W. (1992): Geohydrologische Markierungstechnik.- Lehrbuch der Hydrogeologie, Band 9, 519p., Gebrüder Bornträger, Berlin-Stuttgart, Germany.

Käss, W. (1998): Tracing Technique in Geohydrology, Balkema pub. Rotterdam. Netherlands, 581 pp.

Kenaga, E.E. (1980): Predicted bioconcentration factors and soil sorption coefficients of pesticides and other chemicals. Ecotoxical. Environ. Saf., 4: 26-38.

Klingenberg, L.J. (1951): Analogy between diffusion and electrical conductivity in porous rocks. Bulletin of the Geological Society of America 62: 559-564.

Knudsen, C. (1996): De danske kalktyper og deres anvendelse. GEUS report 1996/7. 30pp.

Kölle, W., Strebel, O. and Böttcher, J. (1985): Formation of sulfate by microbial denitrification in a reducing aquifer. Water Supply 3: 35-40.

Kölle, W., Strebel, O. and Böttcher, J. (1987): Reduced sulfur compounds in sandy aquifers and their interactions with groundwater, paper presented at International Symposium on Groundwater Monitoring, Dresden, Germany.

Kölle, W., Werner, P., Strebel, O. and Böttcher, J. (1983): Denitrifikation in einem reduzierenden Grundwasserleiter. Wasser, 61: 125-147.

Kozai, N., Inada, K., Kozaki, T., Sato, S. Ohashi, H. and Banba, T. (2001): Apparent diffusion coefficients and chemical species of neptunium (V) in compacted Na-montmorillonite. Journal of Contaminant Hydrology 47: 149-158.

Kozaki, T., Inada, K., Sato, S., and Ohashi, H. (2001): Diffusion mechanism of chloride ions in sodium montmorillonite. Journal of Contaminant Hydrology 47: 159-170.

Kozaki, T., Satio, N., Fujishima, A., Sato, S. and Ohashi, H. (1998): Activation energy for diffusion of chloride ions in compacted sodium montmorillonite.. Journal of Contaminant Hydrology 35: 67-75.

Kozaki, T., Sato, H., Sato, S. and Ohashi, H. (1999): Diffusion mechanism of cesium ions in compacted montmorillonite. Engineering Geology 54: 223-230.

Lagerstedt; E., Jacks, G., Sefe, F., (1994): Nitrate in groundwater and N circulation in eastern Botswana. Environmental Geology 23 (1): 60-64.

Lapcevic, P.A., Novakowski, K.S. and Sudicky, E.A. (1999): Groundwater flow and solute transport in fractured media. In Handbook of Groundwater Engineering. CRC Press, 17-1-17-39.

Lapcevic, P.A., Novakowski, K.S. and Sudicky, E.A. (1999): The interpretation of tracer experiment conducted under conditions of natural groundwater flow. Water Resour. Res. 35: 2301-2312.

Lee, C. and Farmer, I. (1993): Fluid flow in discontinuous rocks (Chapman and Hall, 169 pp).

Lever, D.A., Bradbury, M.H. and Hemingway, S.J. (1985): The effect of dead-end porosity on rock-matrix diffusion. J. Hydrol. 80: 45-76.

Loeher, R.C., Reuss, J.O., and Pilbeam, T.E.,(1983):Resources conservation and utilization in animal waste management. EPA Res. Rept. 600/S2-83-024.

Lomize, G.M. (1951): Flow in fractured rocks (in Russian), 127 pp., Gosenergoizdat. Moscow

Louis, C. (1969): A study of groundwater flow in jointed rock and its influence on the stability of rock masses, Rock Mech. Res. Rep. 10, 90 pp., Imp. Coll., London.

Lyman, W.J., Reehl, W.F. and Rosenblatt, D.H.(1990): Handbook of chemical property estimation methods. Washington, Am. Chem. Soc.

Macko, S. A., Ostrom, N.E. (1994): Pollution studies using stable isotopes. In: Lajtha, K., Michener, R. (Eds.), Stab. Isotopes in Ecology. Blackwell, Oxford, pp 45-62.

Maloszewski, P. and Zuber, A. (1985): On the theory of tracer experiments in fissured rocks with a porous matrix. J. Hydrol. 79: 333-358.

Maloszewski, P. and Zuber, A. (1990): Mathematical modelling of tracer behaviour in short-term experiments in fissured rocks.- Water Resour. Res. 26 (7): 1517-1528.

Maloszewski, P. and Zuber, A. (1991): Influence of matrix diffusion and exchange reactions on radiocarbon ages in fissured carbonate aquifers.- Water Resour. Res. 27 (8): 1937-1945.

Maloszewski, P. and Zuber, A. (1993): Tracer experiments in fractured rock: matrix diffusion and the validity of models. Water Resour. Res. 29 (8): 2723-2735.

Maloszewski, P., Harum, T. and Benischke, R. (1992): Mathematical Modelling in tracer experiments in the Karst of Lurbach System. Steir. Beitr. Z. Hydrogeologie, 116-136, Graz.

Maloszewski, P., Herrmann, A. and Zuber, A. (1999): Interpretation of tracer test performed in fractured rock of the Lange Bramke basin, Germany. J Hydrol. 7: 209-218.

Maloszweski, P. (1994): Mathematical Modelling of Tracer Experiments in Fissured Rocks.- Freiburger Schriften zur Hydrologie 2: 107 S.; Freiburg i. Breisgau.

Margolin, G., Berkowitz, B. and Scher, H. (1998): Structure, flow, and generalized conductivity scaling in fractured networks. Water Resour. Res. 34: 2103-2121.

McGeehin MA,Reif J.S., Becher, J.C, Mangione E.J. (1993): Case-control study of bladder cancer and water disinfection methods in Colorado. Am J Epidemiol 138 (7): 492-501.

McKay, L. D., Cherry, J. A., Bales, R. C., Yahya, M. T. and Gerba, C. P. (1993): A field example of bacteriophage as tracers of fractured flow. Environ. Sci. Technol. 27: 1075-1079.

Means, J.C., Wood, S.G., Hasset, J.J. and Banwart, B.L. (1980): Sorption of polynuclear hydrocarbons by sediments and soils. Environ. Sci. Technol. 21: 1524-1528.

Mikulla, C., Einsiedl, F., Schlumprecht, Ch. and Wohnlich, S. (1997): Sorption of uranin and eosin on an aquifer material containing high organic carbon. In: Kranjc, A. (ed.), Tracer Hydrology 1997. Balkema: 77-83.

Moncaster; S.J., Bottrell, S.H., Tellam, J.H., Lloyd, J.W. and Konhauser, K.O (2000): Migration and attenuation of agrochemical pollutants: insights from isotopic analysis of groundwater sulphate. Journal of contaminant Hydrology 43: 147-163.

Morales-Suarez-Varela, M., Llopis-Gonzalez, A., Tejerizo-Perez, M.L., Ferrandiz-Ferragud, J. (1993): Concentration of nitrates in drinking water and its relationship with bladder cancer. J Environ Pathol Toxicol Oncol 12 (4): 229-236.

Moreno, L. and Tsang, C.F. (1994): Flow channelling in strongly heterogeneous porous media: A numerical study. Water Resour. Res. 30: 1421-1430.

Moreno, L., Gylling, B. and Neretnieks, I. (1997): Solute transport in fractured media-the important mechanisms for performance assessment. Journal of contaminant Hydrology 25: 283-298.

Moreno, L., Tsang, Y.W., Tsang, C.F., Hale, F.V. and Neretnieks, I. (1988): Flow and transport in a single fracture: a stochastic model and its relation to some field observations. Water Resour. Res. 24: 2033-2048.

Mortimore, R.N.(1990): Chalk or chalk?. In: Chalk, pp.15-45.Thomas Telford, London.

Mueller, D.K., Hamilton, P.A., Helsel, K.J. and Ruddy, B.C. (1995): Nutrients in groundwater and surface water of the United States- an analysis of data through 1992. USGS. Water Resources Investigations Report 95-4031, 74 pp.

Neretnieks, I. (1980): Diffusion in the Rock Matrix: An Important Factor in Radionuclide Retardation. J. of Geophysical Research 85 (B8): 4379-4397.

Neretnieks, I. (1980b): some difficulties in interpreting in-situ tracer tests, paper presented at the third international symposium on the scientific basis for nuclear waste management, Mater. Res. Soc., Boston, Nov. 16-20.

Neretnieks, I. (1983): A note on fracture flow mechanisms in the ground. Water Resour. Res. 19: 364–370.

Neretnieks, I. (1985): Transport in Fractured Rocks. Paper at IAH 17th Congress, Tucson, Arizona. XVII (2): 301–318.

Neretnieks, I. (1991): Large-Scale flow and tracer experiment in Granite. 2. Results and Interpretation. Water Resour. Res. 27 (12): 3119-3135.

Neretnieks, I. (2002): A stochastic multi-channel model for solute transport - analysis of tracer tests in fractured rocks. Journal of contaminant Hydrology 55: 175-211.

Neretnieks, I., Eriksen, T. and Tähtinen, P. (1982): Tracer movement in a single fracture in granitic rock: Some experimental results and their interpretation. Water Resour. Res. 18: 849-858.

Nicholl, M.J., Rajaram, H., Glass, R.J. and Detwiler, R. (1999): Saturated flow in a single fracture: Evaluation of the Reynolds equation in measured aperture field. Water Resour. Res. 35: 3361-3373.

Nuclear Waste Technical Review Board (1996): Disposal and storage of spent nuclear fuel-Finding the right balance, report to Congress and the Secretary of Energy, Arlington, Va.

Nygaard, E. (1993): Denmark. In: The Hydrogeology of the Chalk of North-West Europe, Downing, R.A., Price, M. and Jones, G.P. pp. 35-58. Oxford University Press Inc., New York.

Nygaard, E. (2002): Geological survey of Denmark and Greenland, Personal communication.

Oakes, D.B (1977): The movement of water and solutes through the unsaturated zone of the chalk in the United Kingdom, paper presented at the Third International Hydrology Symposium, Int. Ass. For Sci. Hydrol., Fort Collins, Colo.

Obermann, P. (1981): Hydrochemische/hydromechanische Untersuchungen zum Stoffgehalt von Grundwasser bei landwirtschaftlicher Nutzung. Besond. Mitt.Z-Deutsche Gewässerkundlichen Jahrbuch Nr.42, 217pp.

O'Connor, D.J. and Connolly, J.P. (1980): The effect of the concentration of adsorbing solids on the partition coefficient. Water Research 14: 1517 - 1523.

Ohlsson, Y. and Neretnieks, I. (1995): Literature survey of matrix diffusion theory and of experiments and data including natural analogues. Technical Report SKB 95-12. Stockholm, Sweden. 89pp.

Parker, J.M. and James, R.C. (1985): Autochthonous bacteria in the Chalk and their influence on groundwater quality in East Anglia. J. Appl. Bacteriol., Symp. Suppl. 15S-25S.

Pauwels, H., Foucher, J-C. and Kloppmann, W. (2000): Denitrification and mixing in a schist aquifer: influence on water chemistry and isotopes. Chemical Geology 168: 307-324.

Pauwels, H., Kloppmann, W., Foucher, J-C., Lachassagne, P. and Martelat, A. (1997): Tracer tests applied to nitrate transfer and denitrification studies in a shaly aquifer (Coet-dan basin, Brittany, France). In: Kranjc, A. (ed.), Tracer Hydrology 1997. Balkema: 327-330.

Pauwels, H., Kloppmann, W., Foucher, J-C., Martelat, A. and Fritsche, V. (1998): Field tracer test for denitrification in a pyrite-bearing schist aquifer. Appl. Geochem. 13 (6): 767-778.

Polak, A., Grader, A.S., Wallach, R. and Nativ, R. (2003): Chemical diffusion between a fracture and the surrounding matrix: Measurement by computed tomography and modelling. Water Resour. Res. 39 (4): 10-1 to 10-14.

Postma, D. (1990): Kinetics of nitrate reduction by detrital Fe(II)-silicates. Geochimica et Cosmochimica Acta 54: 903-908.

Postma, D., Boesen, C., Kristiansen, H. and Larsen, F. (1991): Nitrate reduction in an unconfined sandy aquifer: Water chemistry, reduction processes and geochemical modelling. Water Resour. Res. 27 (8): 2027-2045.

Price, M. (1987): Fluid flow in the chalk of England. In: Fluid flow in sedimentary basins and aquifers (ed. Goff, J.C. and Williams, B.P.J.), pp. 141-156. Sep. Pubn 34, Geol. Soc. London.

Price, M., Downing, R.A. and Edmunds, W.M. (1993): The Chalk as an aquifer. In: The Hydrogeology of the Chalk of North-West Europe, Downing, R.A., Price, M. and Jones, G.P. pp. 35-58. Oxford University Press Inc., New York.

Price, M., Morris, B.L. and Robertson, A.S. (1982): A study of intergranular and fissure permeability in chalk and Permian aquifers using double-packer injection testing. J. Hydrol. 54: 401-423.

Rasmuson, A. and Neretnieks, I. (1986): Radionuclide transport in fast channels in crystalline rock.- Water Resour. Res. 22 (8): 1247-1256.

Raven, K.G., Novakowski, K.S. and Lapcevic, P.A. (1988): Interpretation of field tests of a single fracture using a transient solute storage model. Water Resour. Res. 24 (12): 2019-2032.

Reedy, O.C., Jardine, P.M., Wilson, G.V. and Selim, H.M. (1996): Quantifying the diffusive mass transfer of nonreactive solutes in columns of fractured saprolite using flow interruption. Soil Sci. Soc. 60: 1376-1384.

Reichert, B. (1991): Anwendung natürlicher und künstlicher Tracer zur Abschätzung des Gefährdungspotentials bei der Wassergewinnung durch Uferfiltration. PhD Thesis, Department of Applied Geology, Karlsruhe, Germany.

Reichert, B. and Heotzl, H. (1992): Transport processes by bank filtration in heterogeonous porous media. Tracer hydrology 157-163.

Romm, E. S. (1966): Flow characteristics of fractured rocks (in Russain), 283 pp., Nerda, Moscow.

Ryden, J.C. and Pratt, P.F. (1980): Phosphorus removal from wastewater applied to land. Hilgardia 48: 1-36.

Sahimi, M. (1993): Flow, dispersion, displacement processes in porous media and fractured rocks: from continuum models to fractals, percolation, cellular automata and simulated annealing. Rev Model Phys 65 (4):1393-1534.

Sahimi, M. (1995): Flow and transport in porous media and fractured rock: from classical methods to modern approaches. VCH, Weinheim, Germany, 482 pp.

Shackelford, C.D. (1991): Laboratory diffusion testing for waste disposal – A review. Journal of contaminant Hydrology 7: 177-217.

Shamrukh, M., Corapcioglu, Y. and Hassona, A. (2001): Modeling the effect of chemical fertilizers on groundwater quality in the Nile Valley aquifer, Egypt. Ground Water 39: 59-67.

Shapiro, A.M. (2001): Effective matrix diffusion in kilometer-scale transport in fractured crystalline rock. Water Resour. Res. 37 (3): 507-522.

Skagius, K. and Neretnieks, I. (1986): Porosities and diffusivities of some nonsorbing species in crystalline rocks. Water Resour. Res. 22 (3): 389-398.

Skjernaa, L. (1998): Steven Klint at Hojerup. In: Mass transport in fractured aquifers and aquitards.58-61.- GEUS, Excursion guide (May 14-16, 1998). Geological Institute, Copenhagen University, Denmark.

Spitz, K. and Moreno, J. (1996): A practical guide to groundwater and solute transport modelling. John Wiley and Sons, INC. 471 pp.

Stagnitti, F., Allinson, G., Mortia, M., Nishikawa, M., Il, H. and Hirata, T. (2000): Temporal moments analysis of preferential solute transport in soils. Env. Mod. and Asses. 5: 229-236.

Steger, H. (1998). Vergleichende Untersuchungen zum Diffusionsverhalten konservativer und kationischer Tracer in unterschiedlichen Festgesteinen. Diploma Thesis, Karlsruhe University. Part I, 196pp.

Steindorf, K., Schlehofer, B., Becher, H., Hornig, G. and Wahrendorf, J. (1994): Nitrate in drinking water. A case-control study on primary brain tumours with an embedded drinking water survey in Germany. Int. J. Epidemiol. 23 (3): 451-457.

Stenestad, E. (1972):Traek af det danske Bassins udvikling i Ovre kridt. Dansk Geol. Foren., Arsskrift for 1971, 63-69. (in Danish).

Strebel, O., Böttcher, J. and Kölle, W. (1985): Stoffbilanzen im Grundwasser eines Einzugesgebietes als Hilfsmittel bei Klärung und Prognose von Grundwasserqualitätsproblemen (Beispiel Fuhrberger feld). Z. Dt. Geol. Ges., 136: 533-541.

Stumm, W. and Morgan, J.J. (1996): Aquatic Chemistry, 3rd ed. Wiley-Interscience, New York. 1022 pp.

Sudicky, E.A. and Frind, E.O. (1982): Contaminant transport in fractured porous media: Analytical solution for a system of parallel fractures. Water Resour. Res. 18 (6): 1634-1642.

Sudicky, E.A. and Frind, E.O. (1984): Contaminant transport in fractured porous media: Analytical solution for a two-member decay chain in a single fracture. Water Resour. Res. 20 (7): 1021-1029.

Tang, D.H., Frind, E.O. and Sudicky, E.A. (1981): Contaminant transport in fractured porous media: Analytical solution for a single fracture. Water Resour. Res. 17 (3): 555-564.

Thein, J., Veerhoff, M and Klinger, C. (1997): Geochemische Barrieren bei Versatzbergwerken im Fels. In: Matschullat, J., Tobschall, H.J. and Voigt, H.J. [Hrsg.]: Geochemie und Umwelt. XXIII S. 186 Abb. 116 Tab.; Berlin, Heidelberg, New York (Springer-Verlag).

Thompson, S.T. (2001): Nitrate Concentrations in Private Rural Drinking Water Supplies in Saskatchewan, Canada. Bull. Environ. Contam. Toxicol. 66: 64-70.

Thorbjarnarson, K.W. and Mackay, D.M. (1997): A field test of tracer transport and organic contaminant elution in a stratified aquifer at the Rocky Mountain Arsenal. Denver, Colorado, USA. Journal of contaminant Hydrology 24: 287-312.

Trauth, R. and Xanthopoulos C. (1997): Non-Point pollution of groundwater in urban areas. Wat. Res. 31. (11): 2711-2718.

Tsang C.F and Neretnieks, I. (1998): Flow channelling in heterogeneous fractured rocks. Rev. Geophys. 36: 275-298.

Tsang C.F. (1993): Tracer Transport in Fractured Systems.- in: Bear, J., Tsang, C.-F. & de Marsily, G. (Eds.) (1993): Flow and Contaminant Transport in Fractured Rock: 237 - 266; New York (Academic Press Inc.).

Tsang, C.F. (1991): Coupled hydromechanical-thermochemical processes in rock fractures, Rev. Geophys., 29 (4): 537-551.

Tsang, Y.W. (1995): Study of alternative tracer tests in characterizing transport in fractured rocks, Geophys. Res. Lett., 22 (11): 1421-1424.

Tsang, Y.W. and Tsang, C.F. (1987): Channel model of flow through fractured media. Water Resour. Res. 23: 467-479.

Tsang, Y.W. and Tsang, C.F. (1989): Flow Channelling in a Single Fracture as a two-dimensional strongly heterogeneous permeable medium. Water Resour. Res. 25 (9): 2077-2080.

Tsang, Y.W. and Tsang, C.F. (2001): A particle-tracking method for advective transport in fractures with diffusion into finite matrix block. Water Resour. Res. 37 (3): 831-835.

Tsang, Y.W. and Tsang, C.F., Neretnieks, I., Moreno, L. (1988): Flow and tracer transport in fractured media: a variable aperture channel model and its properties. Water Resour. Res. 24 :2049-2060.

Tsang, Y.W., Tsang, C.F. and Hale, F. (1991): tracer transport in fractures: analysis of field data based on a variable-aperture channel model. Water Resour. Res. 27: 3095-3106.

Ullmann's Encyclopedia of industrial chemistry (1988): 5 Ed., A15: 630 p. Weinheim: Verlag Chemie.

Van Beek, C.G.E., Boukes, H., van Rijsbergen, D. and Straatman, R. (1988): The threat of the Netherlands waterworks by nitrate in the abstracted groundwater, as demonstrated on the well field Vierlingsbeek. Water Supply. 6: 313-318.

Van Loon, A.J., Botterweck, A.A., Goldbohm, R.A., Brants, H.A., van Klaveren, J.D., van den Brandt, P.A. (1998): Intake of nitrate and nitrite and the risk of gastric cancer: a prospective cohort study. Br J Cancer 78 (1): 129-135.

Wang, J.S.Y. and Narasimhan, T.N. (1988): Aperture Correlation of a Fractal Fracture. J. of Geophysical Research 93 (B3):2216-2224.

Weber, W. J.J., McGinley, P.M. and Katz, L.E. (1991): Sorption phenomena in subsurface system: concepts, models and effects on contaminant fate and transport. Water Res. 25 (5): 499-528.

Wellings, S.R. and Bell, J.P. (1980): Movement of water and nitrate in the unsaturated zone of upper chalk near Winchester, Hants., England. Journal of hydrology 48: 119-136.

Wichmann, F. (1995). Hydrogeologi pa det centrale Stevns. Unpublished Thesis. Copenhagen University.

Wilson, J.T., Miller, G.D., Ghiorse, W.C. and Leach, F.R. (1986): Relationship between the ATP content of subsurface material and the rate of biodegradation of alkylbenzenes and chlorobenzene. J. Contam. Hydrol. 1: 163-170.

Witherspoon, P.A., Amick, C.H., Gale, I.E and Iwai, K. (1979): Observation of a potential size effect in experimental determination of the hydraulic properties of fractures. Water Resour. Res. 15: 1142-1146.

Witherspoon, P.A., Wang, J.S.y., Iwai, K. and Gale, I.E. (1980): Validity of cubic law for fluid flow in a deformable rock fracture. Water Resour. Res. 16 (6): 1016-1024.

Witthüser, K., Hötzl, H., Reichert, B., Stichler, W. and Nativ, R. (2000): Laboratory experiments for diffusion transport processes in fractured chalk. in: Dassargues, A. (Ed.): Tracers and modelling in Hydrogeology. Proc. of Tram' 2000, the int. Conf. On Tracers and Modelling in Hydrogeology held Liege, Belgium, in May 2000, IAHS Publication no.262, Wallingford, UK: 303-308.

Witthüser, K., Reichert, B, and Hötzl, H. (2003): Contaminant transport in fractured chalk: Laboratory and field experiments. Ground water 41 (6): 806-815.

Witthüser, K.T. (2001): Untersuchung zum Stofftransport in geklüfteten Festgesteinen unter besonderer Berücksichtigung der Matrixdiffusion. Ph.D Thesis, Department of Applied Geology, University of Karlsruhe, Germany.

Witthüser, K.T. (2003): Geology department, Pretoria University, South Africa, Personal communication.

World Health Organization (WHO) (1998b): Guidelines for drinking water quality. Second edition. Addendum to Volume 2. Health criteria and supporting information. WHO, Geneva. 283pp.

Xu, G., Song, P., Reed, P.J. (1992): The relationship between gastric mucosal changes and nitrate intake via drinking water in a high-risk population for gastric cancer in Moping county, China. Eur J Cancer Prev 1 (6): 437-443.

Xu, S. and Wörman, A. (1999): Implications of sorption kinetics to radionuclide migration in fractured rock. Water Resour. Res. 11 (35): 4329-3440.

Xu, S., Wörman, A. and Dverstorp, B. (2001): Heterogeneous matrix diffusion in crystalline rock-implications for geosphere retardation of migration radionuclides. Journal of contaminant Hydrology 47: 365-378.

Young, C.P., Oakes, D.B. and Wilkinson, W.B. (1976): Prediction of future nitrate concentration in groundwater. Ground Water 14 (6): 426-438.

Zhang, W.L., Tian, Z.X. and Li, X.Q. (1996): Nitrate pollution in groundwater in northern China. Agri. Ecos. and Env. 59 (3): 223-231.

INFORMATION ABOUT THE AUTHOR

Fathy Ahmed Abdalla Ahmed was born on 28 of April 1969 in Nag Elmoghera, Qena in Egypt. Between 1975 and 1981 he visited the primary school in Elkawaled and from 1981 to 1984 he visited the preparatory school in Aboushosha. From 1984 till 1987 he visited the Secondary school at Aboutesht. After four years and in 1991 he got his B.Sc. in Geology from the Faculty of Science at Qena. Assiut University. From 1992 to 1995 he got his M.Sc. in the field of geophysics from the Faculty of Science at Qena, South Valley University. From the period of1996 to 1999 he worked as assistant lecturer in the Geology department, Faculty of Science at Qena, South Valley University. From the period of 2000 to 2004 he is a PhD student in the Geological Institute, Bonn University, Germany. During this period he attainted many courses in hydrogeology and groundwater modelling.

The address of the author is:
Geology Department
Faculty of Science
South Valley University
Qena, Egypt
Email address: fathyhyd@yahoo.com.